

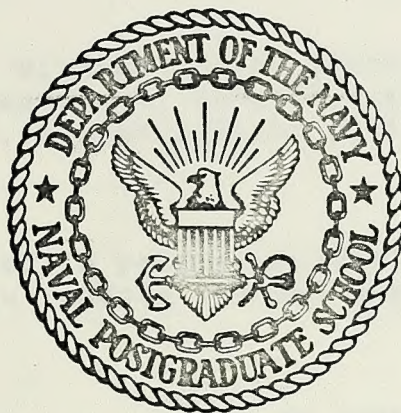
ESTIMATING BOUNDARY LAYER FLUXES FROM
SHIPBOARD MEASUREMENTS OF DISSIPATIONS OF
TURBULENT KINETIC ENERGY AND TEMPERATURE
VARIANCE

William Edward Johnston

Library
Naval Postgraduate School
Monterey, California 93940

NAVAL POSTGRADUATE SCHOOL

Monterey, California



THESIS

Estimating Boundary Layer Fluxes from
Shipboard Measurements of Dissipations of Turbulent
Kinetic Energy and Temperature Variance

by

William Edward Johnston

Thesis Advisor:

K. L. Davidson

March 1974

T158869

Approved for public release; distribution unlimited.

Estimating Boundary Layer Fluxes from
Shipboard Measurements of Dissipations of Turbulent
Kinetic Energy and Temperature Variance

by

William Edward Johnston
Lieutenant, United States Navy
B.S., Edinboro State College, 1965

Submitted in partial fulfillment of the
requirements for the degree of

MASTER OF SCIENCE IN METEOROLOGY

from the

NAVAL POSTGRADUATE SCHOOL
March 1974

ABSTRACT

Velocity and temperature fluctuation measurements were made over the open ocean from instruments mounted on the R/V ACANIA. These data were examined to determine the validity of present formulations and prediction techniques.

Values of momentum flux, u_*^2 , were inferred from the rate of dissipation of turbulent kinetic energy, ϵ . Dissipation values were obtained from spectral estimates and inner scale estimates. Values of u_* were examined for representativeness on the basis of the constant-flux assumption and by comparisons with other studies. The vertical variation of the dissipation rate was examined for possible effects of stability and wind-wave coupling.

The momentum flux, computed from spectra, supported the constant-flux assumption for neutral conditions. For periods of instability, the stability corrections applied to the vertical variation of ϵ resulted in the proper adjustments toward the predicted slope. The reductions in momentum transfer during periods of stable stratifications were consistent with wind-wave coupling effects described by Davidson. The shape of a spectrum of temperature fluctuations was in agreement with predictions.

TABLE OF CONTENTS

I.	INTRODUCTION - - - - -	9
II.	OBSERVATIONAL AND THEORETICAL CONSIDERATIONS -	13
	A. GENERAL BACKGROUND - - - - -	13
	B. TURBULENT BALANCE EXPRESSIONS- - - - -	14
	C. SIMILARITY EXPRESSIONS - - - - -	18
	D. FURTHER THEORETICAL CONSIDERATIONS - - - -	22
III.	OBSERVATIONS - - - - -	25
	A. THE EXPERIMENT - - - - -	25
	B. DESCRIPTION OF EQUIPMENT AND MEASUREMENTS-	25
	1. Velocity Measurements- - - - -	25
	2. Temperature Measurements - - - - -	32
	3. Parallel Measurements- - - - -	32
	C. SIGNAL PROCESSING AND RECORDING- - - - -	35
	1. Analog Recording - - - - -	35
	2. Real Time Analysis - - - - -	36
IV.	DATA REDUCTION AND ANALYSIS- - - - -	37
	A. PRELIMINARY ANALYSIS - - - - -	37
	B. ANALOG-TO-DIGITAL CONVERSION - - - - -	39
	C. SEVEN-TRACK TO NINE-TRACK CONVERSION - - -	39
	D. DIGITAL ANALYSES PROGRAMS- - - - -	42
V.	RESULTS- - - - -	47
	A. ONE POINT SPECTRAL METHOD- - - - -	47
	B. INTERCEPT METHOD - - - - -	54
	C. COMPARISON OF METHODS- - - - -	57

D.	EVALUATION OF THE VARIATION OF W_* WITH HEIGHT - - - - -	64
E.	THE VARIATION OF ϵ WITH HEIGHT- - - - -	65
F.	VARIATION OF TEMPERATURE FLUCTUATIONS - - -	83
VI.	CONCLUSIONS AND RECOMMENDATIONS - - - - -	86
A.	CONCLUSIONS - - - - -	86
B.	RECOMMENDATIONS FOR FUTURE EXPERIMENTS- - -	87
APPENDIX A	- ANEMOMETER SCHEMATICS- - - - -	88
APPENDIX B	- CALIBRATION AND SCALING PROCEDURES - - -	90
APPENDIX C	- TEMPERATURE MODULE SCHEMATICS- - - - -	99
APPENDIX D	- ANALOG RECORDING PROCEDURES- - - - -	100
APPENDIX E	- REAL TIME ANALYSIS PROCEDURES- - - - -	101
APPENDIX F	- DIGITAL TAPE OPERATIONS- - - - -	104
APPENDIX G	- SPECTRAL ANALYSIS PROGRAMS - - - - -	110
APPENDIX H	- DISSIPATION ANALYSIS PROGRAM - - - - -	124
LIST OF REFERENCES-	- - - - -	127
INITIAL DISTRIBUTION LIST	- - - - -	129
FORM DD 1473-	- - - - -	131

LIST OF TABLES

I.	Results of Momentum-Flux Calculations - - - -	17
II.	Data Periods Considered in this Study - - - -	26
III.	Momentum Flux Calculations for 1103-1138 20 Sept 73 using the One Point Spectral Method- - - - -	48
IV.	Momentum Flux Calculations for 2008-2018 20 Sept 73 using the One Point Spectral Method- - - - -	49
V.	Momentum Flux Calculations for 2023-2053 20 Sept 73 using the One Point Spectral Method- - - - -	50
VI.	Momentum Flux Calculations for 2323-2341 20 Sept 73 using the One Point Spectral Method- - - - -	51
VII.	Momentum Flux Calculations for 0637-0652 21 Sept 73 using the One Point Spectral Method- - - - -	52
VIII.	Momentum Flux Calculations for 1103-1138 20 Sept 73 using the Zero Intercept Method- -	59
IX.	Momentum Flux Calculations for 2008-2018 20 Sept 73 using the Zero Intercept Method- -	60
X.	Momentum Flux Calculations for 2023-2053 20 Sept 73 using the Zero Intercept Method- -	61
XI.	Momentum Flux Calculations for 2323-2341 20 Sept 73 using the Zero Intercept Method- -	62
XII.	Momentum Flux Calculations for 0637-0652 21 Sept 73 using the Zero Intercept Method- -	63
XIII.	A Comparison of Dissipation Obtained by Spectra (ϵ) and Dissipation Obtained from the Inner Scale (ϵ_o)- - - - -	73
XIV.	Flux-Profile Relationships Describing the Stability Function, ϕ_m - - - - -	77

LIST OF FIGURES

1.	The R/V ACANIA is operated by the Department of Oceanography - - - - -	10
2.	San Nicolas Island and ACANIA's Anchorage - - -	11
3.	Measured Values of ϵ vs z , the Height Above the Mean Sea Surface (after Stegen, et al)- - -	19
4.	A Schematic Drawing Showing Spectral Transfer and Illustrating (A) Energy Containing Region (B) Inertial Subrange (C) Dissipation Range and (D) Universal Equilibrium Range - - - - -	20
5.	An Illustration of a Possible Effect of Stability on the Variation of ϵ with Height - -	24
6.	ACANIA's Track in SNI Area- - - - -	28
7.	The San Nicolas Island Region - - - - -	29
8.	Mounting Arrangements - - - - -	30
9.	Probe Calibrator- - - - -	33
10.	Vertical Probe Mounting with TSI Calibrator - -	34
11.	Inadequate Temperature Signals Showing (A) Insufficient Signal Strength and (B) DC Drift -	38
12.	Typical Velocity Signal - - - - -	40
13.	A-D Conversion Procedures - - - - -	41
14.	FTOR Output - - - - -	43
15.	SCOR Spectral Statistics- - - - -	45
16.	SCOR Spectral Plot- - - - -	46
17.	Velocity Spectrum Showing Deviation from -5/3 Slope- - - - -	53
18.	Ten Minute Intercept Plot for 1103-1138 20 Sept 73- - - - -	55
19.	Three Minute Intercept Plot for 2023-2053 20 Sept 73- - - - -	56

20.	One Minute Intercept Plot for 2323-2341 20 Sept 73- - - - -	58
21.	Measured Values of ϵ vs Height for 1103-1138 20 Sept 73. For Scaling Purposes a Factor of 5.0 was Subtracted from the x-Values - - - -	66
22.	Measured Values of ϵ vs Height for 2008-2018 20 Sept 73. For Scaling Purposes a Factor of 5.0 and 1.4 were Subtracted from the X and Y Values, Respectively- - - - -	67
23.	Measured Values of ϵ vs Height for 2023-2053 20 Sept 73. For Scaling Purposes a Factor of 5.0 and 2.0 were Subtracted from the X and Y Values, Respectively- - - - -	68
24.	Measured Values of ϵ vs Height for 0637-0652 21 Sept 73. For Scaling Purposes a Factor of 6.0 was Subtracted from the X Values - - - -	69
25.	Measured Values of ϵ vs Height for 2323-2341 20 Sept 73. For Scaling Purposes a Factor of 5.0 and 1.4 were Subtracted from the X and Y Values, Respectively- - - - -	70
26.	Twenty Minute Velocity Spectrum for 2023- 2053 20 Sept 73 - - - - -	72
27.	Variation of β with R_i (after Haltiner and Martin) - - - - -	75
28.	Effect of Stability Correction for 2008- 2018 20 Sept 73 - - - - -	78
29.	Effect of Stability Correction for 2023- 2053 20 Sept 73 - - - - -	79
30.	Effect of Stability Correction for 0637- 0652 21 Sept 73 - - - - -	81
31.	Non-dimensional Dissipation Rate as a Function of z/L (after Garratt) - - - - -	82
32.	Ten Minute Temperature Spectrum for 2323- 2341 20 Sept 73 - - - - -	84
33.	Ten Minute Temperature Spectrum for 2008- 2018 20 Sept 73 - - - - -	85

ACKNOWLEDGEMENTS

Special thanks are extended to Dr. Kenneth L. Davidson for invaluable advice, suggestions and encouragement during all aspects of this research. The author is indebted to Dr. Thomas Houlihan for advice and assistance offered in setting up the experiment and for helpful comments in preparing this manuscript.

The author wishes to express his appreciation to Mr. Robert Smith and Mr. Steve Rinard for assistance in equipment and experiment preparations. For assistance while preparing and analyzing data, the author thanks Mr. Robert Limes for advice on the Hybrid Computer System, and Ms. Sharon Raney for assistance in IBM tape utilization procedures. Thanks also go to the crew of the R/V ACANIA for assistance in collecting the data.

This investigation was performed with support from the Naval Ordnance Systems Command under Contract No. WR-4-5737.

To my wife, Linda, and children, Karlyn and Derek, whose patient understanding made this endeavor possible, thank you.

I. INTRODUCTION

The structure of turbulence in the marine boundary layer has become of increasing importance in naval systems design. To gain a better understanding of turbulence statistics, such as the spectral distribution of wind fluctuations, the effects of wind-wave coupling and the accuracy of present prediction expressions, personnel at the Naval Postgraduate School, Monterey, California have undertaken a study to obtain the shipboard observational data necessary for an accurate examination of these problems. The group consists of personnel from several departments; Meteorology, Mechanical Engineering, Oceanography and Physics, whose primary objective is to obtain observational data and then to evaluate and improve existing prediction techniques.

Several observational experiments have been conducted and were followed by data reduction and analyses periods. The second observational experiment is the one considered in this study and was conducted from 18 September 1973 to 22 September 1973. Meteorological measurements were made from the oceanographic research ship, the R/V ACANIA shown in Figure 1, in the vicinity of San Nicolas Island. Figure 2 illustrates the "near" ocean environment and the ACANIA's anchorage where the majority of measurements were taken.

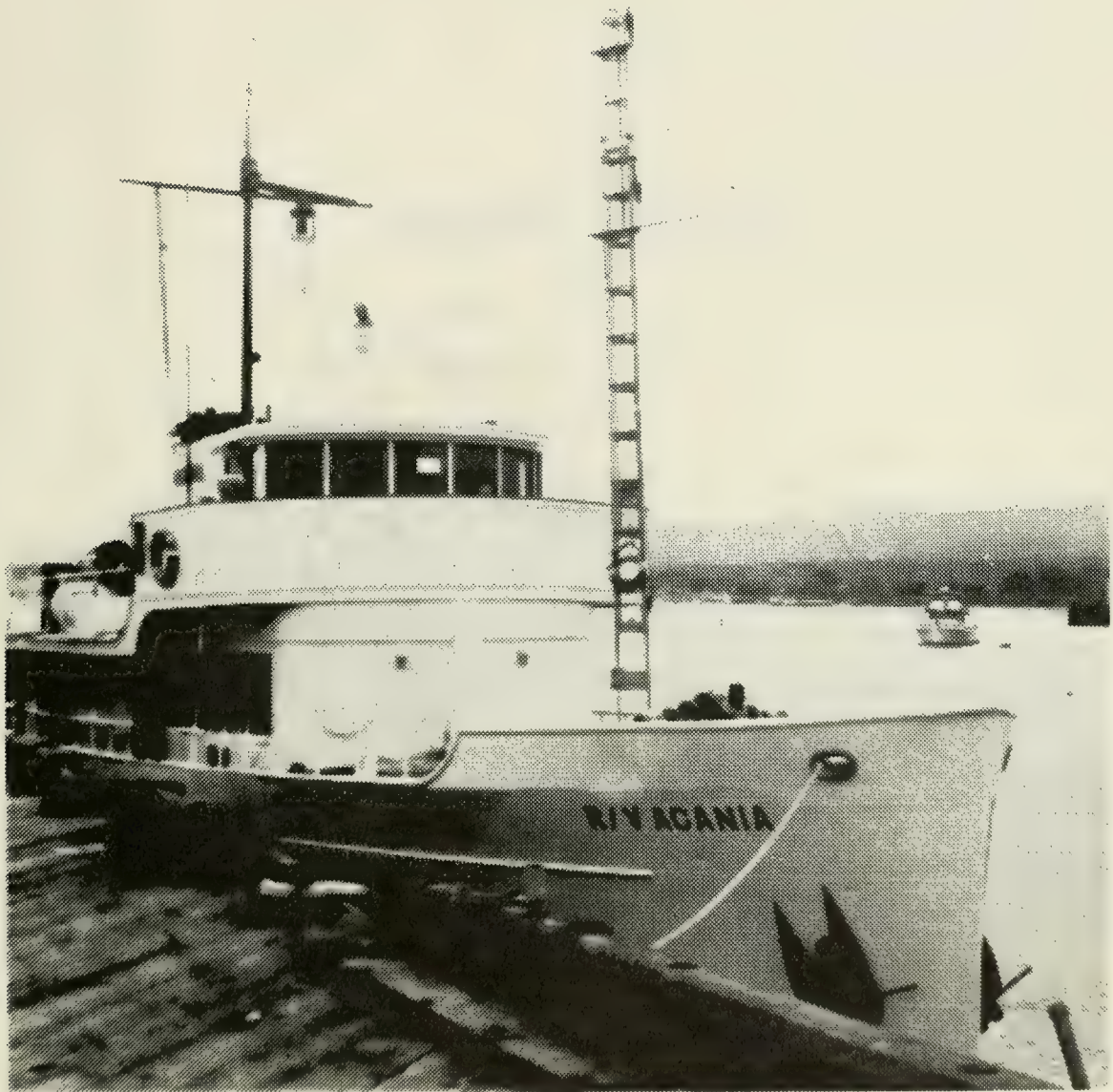


Figure 1. The R/V ACANIA is operated by the Department of Oceanography, NPS.

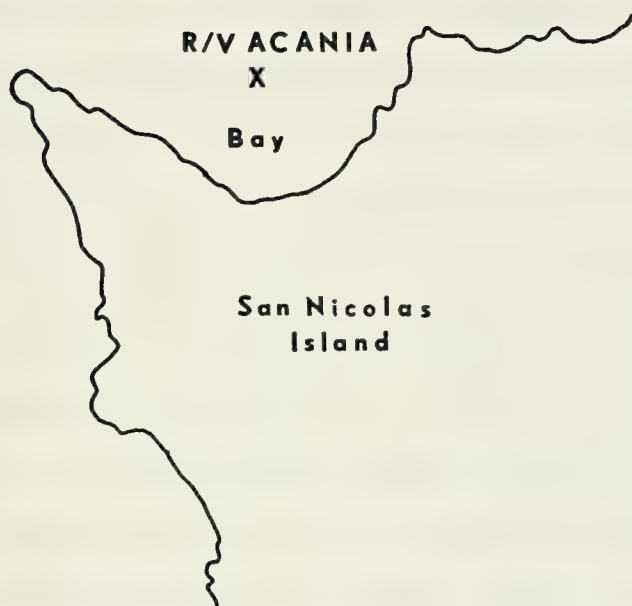


Figure 2. San Nicolas Island and ACANIA's Anchorage.

The meteorological measurements were of three different types. Two of these pertained to different scales of measurements and the third was of the influence of the moving platform on mean and turbulent measurements. The scales considered were the turbulent scale and that which is associated with the mean wind and thermal stratification.

The scope of this study is confined to turbulent fluctuations of velocity and temperature, although reference will be made to mean wind and thermal stratification measurements. The latter are important since they are required to relate to results from other experiments or for extrapolating to regions or conditions where turbulence measurements are not made. A nearly unique problem facing the Navy is that present expressions for the turbulent processes are empirical in nature and have only been previously validated, or at least tested, overland.

The purpose of this investigation is to test several expressions in the "near" ocean environment, interpret the results and evaluate existing turbulence expressions. To accomplish this, it was decided to concentrate the study on specific formulations. The formulations include (1) an evaluation of the constant flux layer (2) the variations of ϵ (the viscous dissipation of turbulent kinetic energy) with height and, where data permitted, (3) the variation of temperature fluctuations.

II. OBSERVATIONAL AND THEORETICAL CONSIDERATIONS

A. GENERAL BACKGROUND

This study represents one of the first attempts to make simultaneous, multiple-level observations over water from a ship. Previous measurements have been primarily overland or over water from near stable platforms. A study which closely approximates this experiment was described by Stegen, et al (1973). The measurements reported in that study were made from the Scripps Floating Instrument Platform (FLIP) during the Barbados Oceanographic and Meteorological Experiment (BOMEX). From FLIP, velocity and temperature measurements were made with a roving probe which cycled continuously between measurement stations located 2, 4, 7 and 12 meters above mean sea level. Results in the present study will be compared to those obtained by Stegen, et al, as well as to other contemporary studies.

The following paragraphs will provide a review of the theoretical considerations needed to interpret the data. From these considerations, the friction velocity (u_*) will be estimated from values of the dissipation of turbulent kinetic energy (ϵ) and ϵ will be obtained from spectra. For this reason we must examine both the turbulent kinetic energy balance expression and Kolmogorov's hypotheses.

B. TURBULENT BALANCE EXPRESSIONS

A general expression for the turbulent kinetic energy balance has the form

$$\begin{aligned} \frac{\partial}{\partial t} \left(\frac{\overline{v_i^2}}{2} \right) = & -\overline{v_i v_j} \frac{\partial \bar{u}_i}{\partial x_j} + \frac{g}{T_0} \overline{v_i \theta} \delta_{i3} - \epsilon + \frac{\partial}{\partial x_j} \left[\overline{v_j \left(-\frac{p}{\rho} - \frac{v_i v_i}{2} \right)} \right] \\ & - \frac{\partial}{\partial x_j} \left[\bar{u}_j \frac{\overline{v_i v_i}}{2} \right] \quad (1) \end{aligned}$$

If all eddy transports except those along the vertical are neglected, the turbulent kinetic energy balance can be expressed as

$$\begin{aligned} \frac{\partial}{\partial t} \left(\frac{\overline{v_i^2}}{2} \right) = & -\overline{v_3 v_i} \frac{\partial \bar{u}_i}{\partial x_3} + \frac{g}{T_0} \overline{v_i \theta} \delta_{i3} - \epsilon - \frac{\partial}{\partial x_3} \left[\overline{v_3 \left[\left(\frac{v_i v_i}{2} \right) + \frac{p}{\rho} \right]} \right] \quad (2) \end{aligned}$$

The time variation of turbulent kinetic energy is thus seen to depend on four processes represented by the four terms on the right hand side of Equation (2). The first represents production of turbulent kinetic energy by the interaction of the Reynolds stress with the mean shear flow. The second represents turbulent kinetic energy released or gained due to the work of vertical motions against the effects of buoyancy. The third represents viscous dissipation of turbulent kinetic energy. The final term represents both pressure work and the flux divergence of turbulent kinetic energy due to transfer by turbulent motion.

To obtain those expressions normally used for estimating the shear stress or eddy flux ($-\overline{v_1 v_3} = u_*^2$) on the basis of turbulent kinetic energy balance, the following assumptions and definitions are made:

- i) assume that the turbulent kinetic energy is in a statistically steady state

$$\frac{\partial}{\partial t} \left(\frac{\overline{v_i^2}}{2} \right) = 0$$

- ii) conditions are horizontally homogeneous for the irregularity fields (i.e., spatial variations of mean fluctuations are taken to be negligible over distances comparable to the largest scales of interest in the analysis).

$$\frac{\partial}{\partial x_1} () = \frac{\partial}{\partial x_2} () = 0$$

- iii) conditions are near neutral

$$\frac{g}{T_0} \overline{v_3 \theta} \approx 0$$

- iv) define the coordinate system so

$$\bar{u}_2 = \bar{u}_3 = 0$$

The above assumptions and definitions lead to the following turbulent energy balance expression

$$-\overline{v_1 v_3} \frac{\partial \bar{u}_1}{\partial x_3} = \epsilon + \frac{\partial}{\partial x_3} \left[\overline{v_3 \left\{ \frac{v_1^2 + v_2^2 + v_3^2}{2} + \frac{p}{\rho} \right\}} \right] \quad (3)$$

Furthermore, if the divergence terms are negligible, Equation (3) becomes

$$-\overline{v_1 v_3} \frac{\partial \bar{u}_1}{\partial x_3} = \epsilon \quad (4)$$

which states that mechanical production of turbulent kinetic energy equals dissipation of turbulent kinetic energy.

Equation (4) can be rewritten as

$$u_*^2 \frac{\partial \bar{u}}{\partial x_3} = \epsilon \quad (5)$$

where $u_*^2 = -\overline{v_1 v_3}$. For neutral conditions in a constant-stress boundary layer the following is an accepted expression for the wind shear

$$\frac{\partial \bar{u}}{\partial x_3} = \frac{u_*}{kz} \quad (6)$$

where k is Von Karman's constant and z is the height.

Combining Equations (5) and (6) yields the following estimate for u_* based on measurements of ϵ at known height z .

$$u_* = (\epsilon z k)^{1/3} \quad (7)$$

Equation (7) can be used to both estimate the value of the momentum flux, u_*^2 , and to examine if it is constant with respect to height, the constant-flux assumption.

Table I provides the momentum flux calculations presented by Stegen, et al with ϵ values derived from time derivatives of the velocity fluctuations. These values will be compared to those obtained from shipboard measurements to establish the validity of the expressions and assumptions used in this study.

TABLE I
Results of Momentum-Flux Calculations.¹

Height (m)	$kz\varepsilon$ (cm ³ sec ⁻³)	u_* (cm sec ⁻¹)	u_* (corrected) (cm sec ⁻¹)
11.69	4.02×10^3	15.9	14.0
6.70	6.86×10^3	19.0	17.3
3.89	6.36×10^3	18.5	17.4
2.39	6.03×10^3	18.2	17.4

¹Results taken from Stegen, et al (1973)

Equation (7) can be rewritten as

$$\ln \epsilon = -\ln z + \ln u_*^3/k \quad (8)$$

Therefore a plot of $\ln z$ versus $\ln \epsilon$ should yield a straight line with -1 slope. The intercept of this line with the $\ln z$ axis, $z = 1$, will yield the estimate of u_* . A plot of this shown by Stegen, et al appears in Figure 3. Deviations from this particular relation could be interpreted for possible deviation from the constant-flux assumption or for influence of wind-wave coupling or non-neutral stratifications.

C. SIMILARITY EXPRESSIONS

The parameter ϵ can be estimated on the basis of similarity expressions for the inertial subrange. According to Kolmogorov's second hypothesis, the inertial subrange is a region (in wave number space) where there is negligible dissipation of energy and where inertial energy transfer to higher wave numbers is the dominate feature.

Figure 4 from Lumley and Panofsky (1964) depicts the inertial subrange considering spectral energy transfers.

Based on a dimensional analysis Kolmogorov's second hypothesis yields the following functional relation

$$E(k) = c\epsilon^{2/3}k^{-5/3}$$

where $E(k)$ represents the three-dimensional energy density, k is the wave number and c is an empirical constant.

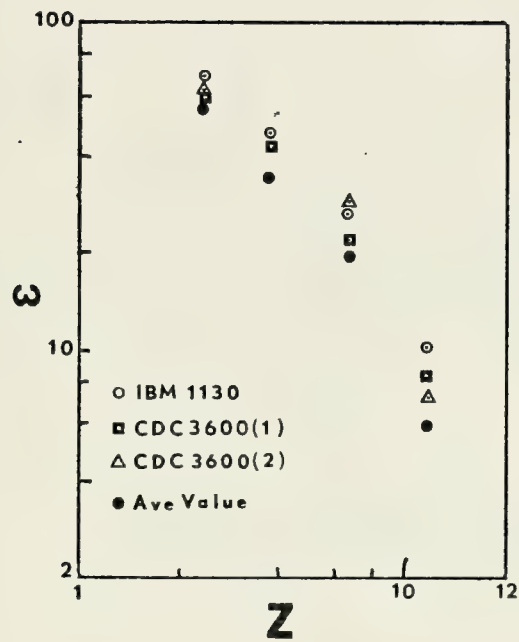


Figure 3. Measured Values of ϵ vs z , the Height Above the Mean Sea Surface (after Stegen, et al).

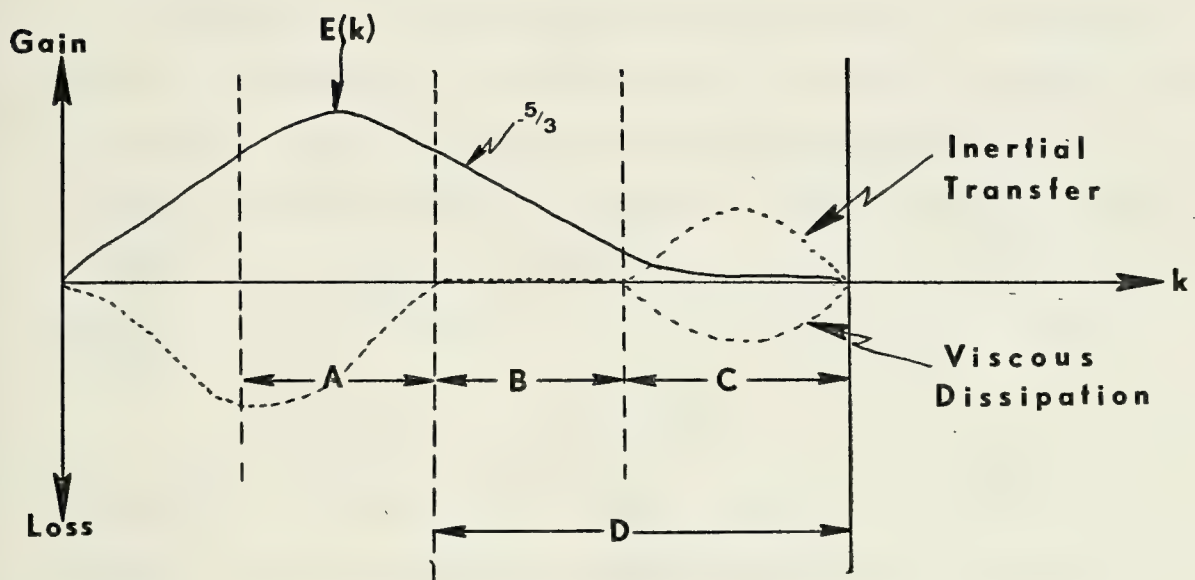


Figure 4. A Schematic Drawing Showing Spectral Transfer and Illustrating (A) Energy Containing Region (B) Inertial Subrange (C) Dissipation Range and (D) Universal Equilibrium Range.

Unfortunately, $E(k)$ is impossible to measure. It can be shown, however, that the one-dimensional energy density, $\phi_{11}(k)$, which can be measured, also has the form

$$\phi_{11}(k) = \alpha \varepsilon^{2/3} k^{-5/3} \quad (9)$$

where $\alpha = \text{constant}$.

Furthermore, measurements at the scales of interest have to be made at a fixed point in the flow and the spectra therefore are obtained for temporal frequency, f . In order to use Equation (9), time and space scales must be related using Taylor's (1938) "frozen turbulence" hypothesis

$$k = 2\pi f / \bar{U}$$

where \bar{U} is the mean wind speed, measured by a cup anemometer. The term "frozen turbulence" implies that the turbulence remains unchanged during the time required for it to sweep past the probe.

The following form of Equation (9) is often utilized and will be here,

$$f\phi_{11}(f) = k\phi_{11}(k) = \alpha \varepsilon^{2/3} k^{-2/3} \quad (10)$$

The parameter ε will be obtained from the spectra using Equation (10). The ε values obtained from simultaneous, multiple level measurements will then be used to estimate the value of the momentum flux, u_*^2 , from Equation (7).

There is another way of estimating ϵ based on the scale associated with the upper limit of the inertial subrange. If the spectrum is in statistical equilibrium it is independent of the source of the turbulence and depends only on ϵ , γ and k . A dimensional analysis yields the following expression for the inner scale, l_o

$$l_o = (\gamma^3/\epsilon)^{1/4} \quad (11)$$

where $k_s (= 2\pi l_o/\bar{u})$ is the dissipation wave number and γ is the kinematic viscosity of air. The dissipation wave number can be obtained from spectra which show scale separation between pure inertial transfer ($-5/3$ regions) and the viscous dissipation region. Dissipation of turbulent kinetic energy can then be obtained from Equation (11) and compared to those obtained from Equation (10) to establish greater confidence in the spectral estimate.

D. FURTHER THEORETICAL CONSIDERATIONS

Although the expressions previously described are based on accepted and consistent theories, there are several serious assumptions which must be considered in applying them to observational data. In many instances the theory is empirical and the formulating analyses were based on overland data. A recent effort in turbulence theory has been to prove or disprove the validity of overland formulations for non-neutral conditions or over water regimes where the wave influence may be important. The latter has been described by Davidson (1974).

In developing the turbulent kinetic energy balance, given by Equation (3), the existence of neutral conditions was a critical assumption. For non-neutral stratifications, Equation (7) would include a buoyancy term and be of the form

$$\epsilon = \frac{u_*^3}{kz} \left[\phi_1 \left(\frac{z}{L} \right) - \frac{z}{L} \right] \quad (12)$$

or

$$\epsilon = \frac{u_*^3}{kz} \phi_2(Ri)$$

where $L = -\bar{T}u_*^3/gk\bar{V}_3\bar{\theta} = \text{Monin-Obuhkov Length}$; $\bar{V}_3\bar{\theta} = \text{heat flux}$,

$Ri = \text{Richardson Number}$,

$\phi_1 = \text{empirical function of } \frac{z}{L}$,

$\phi_2 = \text{empirical function of } Ri$.

For the non-neutral case, the expression corresponding to Equation (8) becomes

$$\ln \epsilon = -\ln z + \ln \phi_2(Ri) + \ln \frac{u_*^3}{k} \quad (13)$$

Possible deviations from the constant flux assumption or wind wave coupling influence exhibited by spectral results could be examined by testing overland expressions for $\phi_2(Ri)$. A stability correction could then be applied for periods of non-neutral stratifications. A possible effect of the instability on the predicted plots of $\ln \epsilon$ versus $\ln z$ is illustrated in Figure 5.

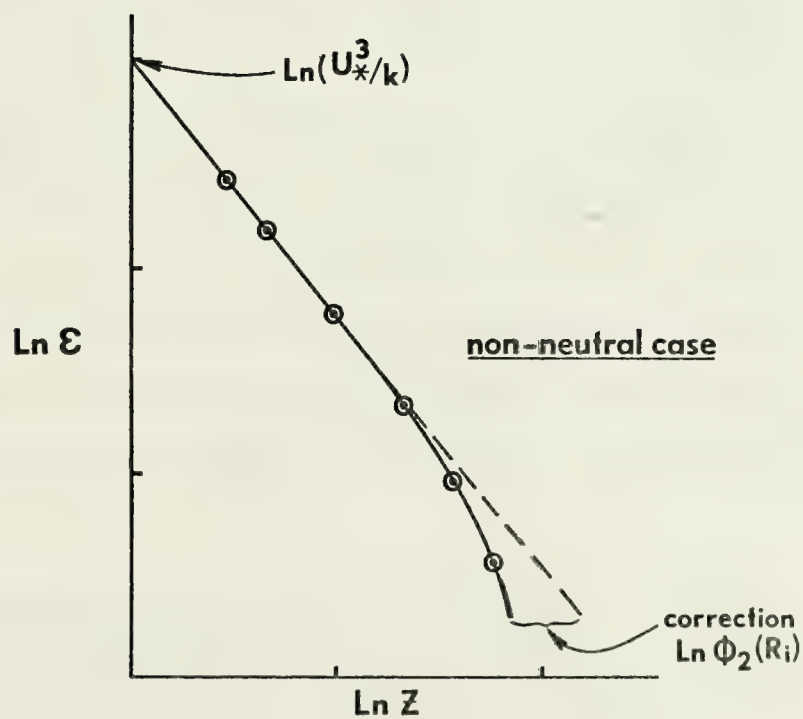
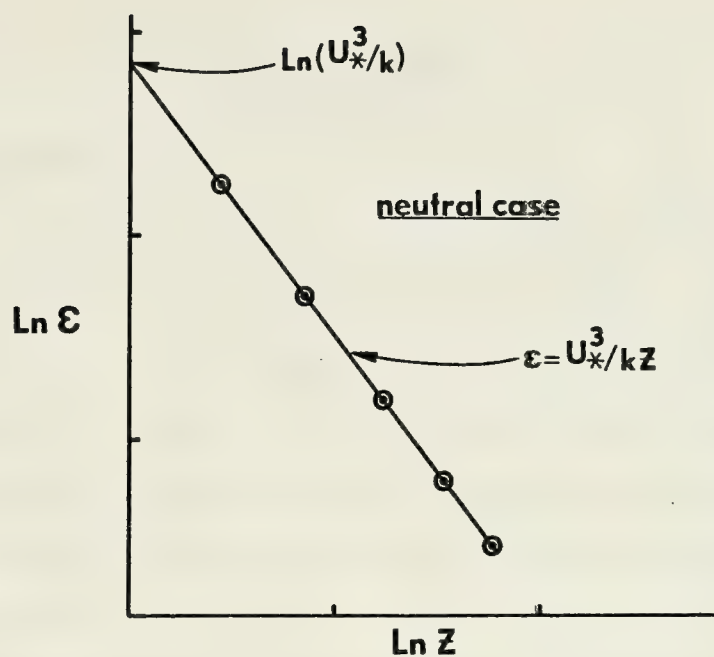


Figure 5. An Illustration of a Possible Effect of Stability on the Variation of ϵ with Height.

III. OBSERVATIONS

A. THE EXPERIMENT

The data considered in this study were obtained from measurements made aboard the R/V ACANIA, which is operated by the Department of Oceanography of the United States Naval Postgraduate School. As previously stated, San Nicolas Island was the experimental site and the majority of data were collected while the ship was at anchorage near the northwest tip of the island. Additional data were collected while the ship was enroute between Monterey and San Nicolas Island and also while the ship was transiting to the west side of the island. Since the data collected from anchorage comprise the largest percentage of successful runs and represents all stability conditions, data runs selected for analysis in this study are primarily anchorage data. Table II is a listing of the various data runs examined. Figure 6 shows the ship's track in the vicinity of San Nicolas Island and Figure 7 shows the route to and from the island.

B. DESCRIPTION OF EQUIPMENT AND MEASUREMENTS

Figure 8 shows the sensor placement at various levels along with the variables measured at each level.

1. Velocity Measurements

Velocity fluctuation measurements were made at three levels on the forward mast and one level on a single bow

TABLE II

Data Periods Considered in This Study

Date	Time	Digital Channel	Parameter
20 Sept. 73	1103-1138	1	u'_1 ¹
		2	u'_2
		3	u'_3
		4	u'_4
20 Sept. 73	2008-2018	1	u'_1
		2	u'_3
		3	u'_4
		4	T'_4
		5	T'_B
		6	upper level lateral accelera- tion
		7	upper level ver- tical acceleration
		8	upper level ver- tical acceleration (integrated)
20 Sept. 73	2023-2053	1	T'_4
		2	u'_3
		3	u'_4
		4	u'_1

¹The subscript refers to the level at which the measurement was made. Level 1 is the uppermost level.

TABLE II (continued)

Date	Time	Digital Channel	Parameter
20 Sept. 73	2323-2341	1	u'_1
		2	u'_2
		3	u'_3
		4	upper level fore-aft acceleration
		5	upper level lateral acceleration
		6	T'_4
		7	upper level vertical acceleration (integrated)
		8	upper level vertical acceleration
21 Sept. 73	0637-0652	1	upper level fore-aft acceleration
		2	u'_3
		3	u'_1
		4	T'_4
		5	T'_B
		6	upper level vertical acceleration
		7	upper level lateral acceleration
		8	upper level lateral acceleration (integrated)

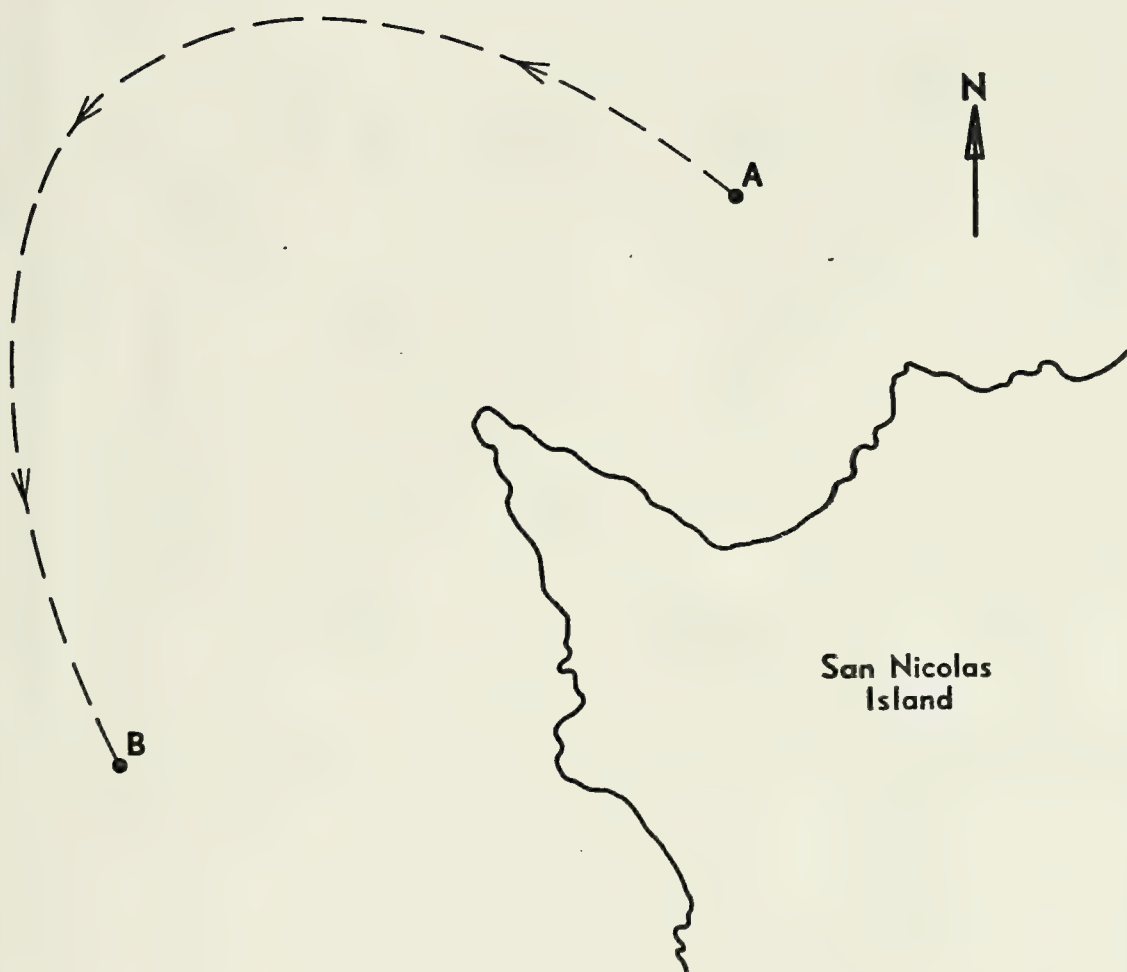


Figure 6. ACANIA's Track in SNI Area.

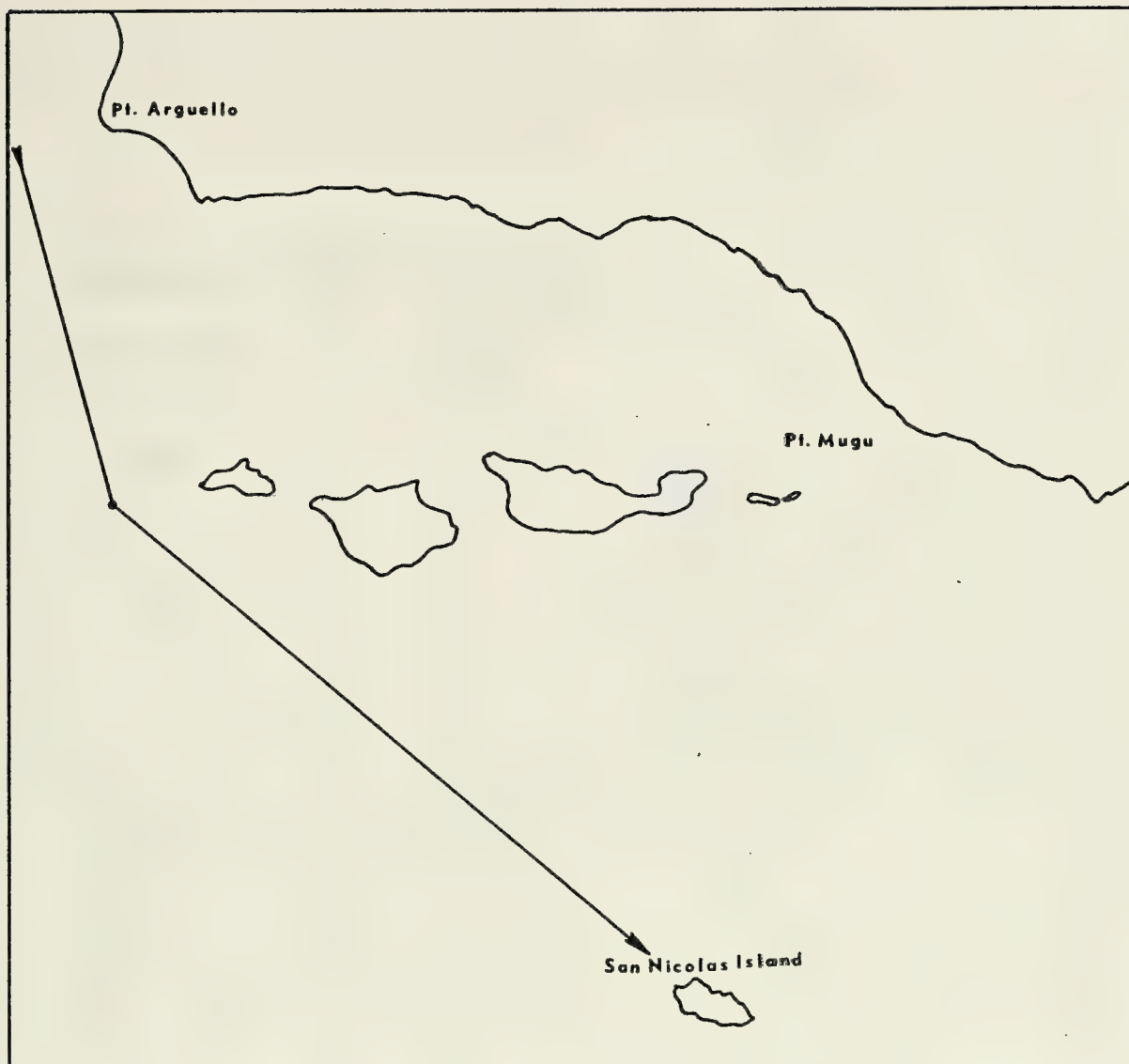


Figure 7. The San Nicolas Island Region.

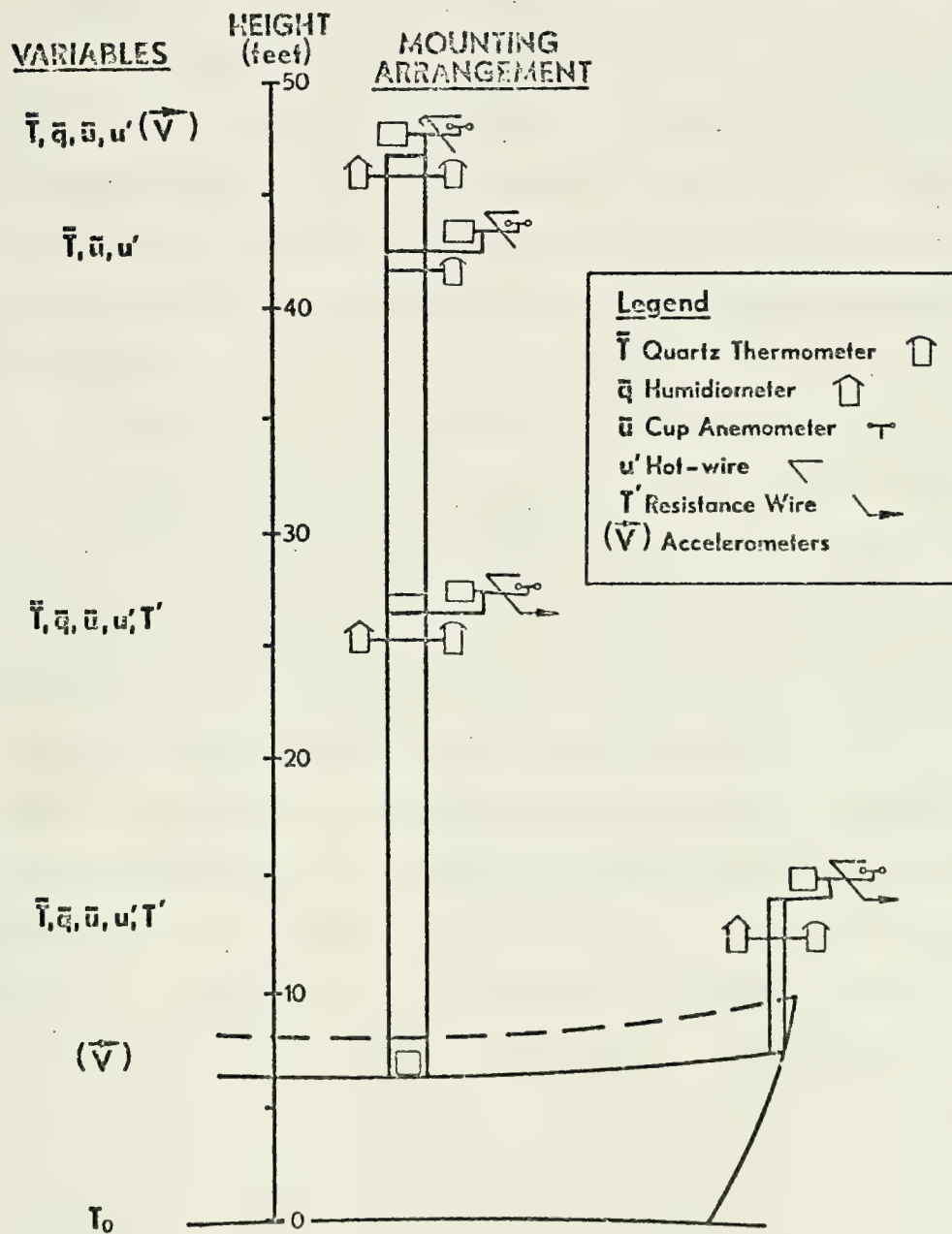


Figure 8. Mounting Arrangements

most as shown in Figure 8. Thermo-Systems (TSI) Model 1210 probes with sliding support shields were selected for these measurements. The sensor consisted of a platinum coated tungsten wire 0.00015 inches in diameter and 0.060 inches long, small enough to resolve the viscous dissipation scale without needing to apply wire length corrections. The wire was fitted with plated ends for isolating the sensing area and thereby minimizing flow disturbance.

Electronics associated with each probe were a TSI Model 1054B Linearized Anemometer, a TSI Model 1056 Variable Decade Module and a Model 1057 Signal Conditioner. Schematics of the anemometer circuits appear in Appendix A. The anemometer had a linear frequency response from DC to 10 KHz and the variable decade module operated with a 0-60 ohm range. The signal conditioner had a linear frequency response from DC to 400 KHz and permitted voltage suppression in one volt steps from 0-29 volts. The voltage output from the conditioner was recorded on magnetic tape.

Sensor placement required 200 foot cables instead of the usual 15 foot cables. This resulted in a decrease in system frequency response but the decrease had little effect in the frequency band of interest. Ten probes were available for the experiment and they were placed into four groups. Each group of probes was calibrated with separate cables and electronics which permitted a complete system calibration for each of the four sensing levels.

The calibration was completed with a manometer and a TSI Model 1125 Calibrator shown in Figures 9 and 10. Empirical relations used in interpreting the hot wire signals are presented in Appendix B along with the computer code used to evaluate these measurements and resultant calibration curves for each probe.

The performance of the hot-wire system was excellent throughout the experiment. Only one probe failure was experienced despite continued probe exposure during the data gathering period.

2. Temperature Measurements

Temperature fluctuation measurements were made at two levels on the forward mast of R/V ACANIA as shown in Figure 8. Electronics used were TSI Model 1044 Temperature Modules. The unit power supply consisted of six volt batteries. It can be utilized to make both temperature and ΔT measurements. The temperature module is designed for measurements of temperature variations down to 0.001°C at frequencies up to 1 KHz. The schematics for the Model 1044 Temperature Module are shown in Appendix C.

Probe failure occurred at the beginning of the first data run and to permit temperature measurements to continue the probe unit was fitted with a 60 ohm platinum wire sensor.

3. Parallel Measurements

Mean measurements of the wind speed, temperature and relative humidity have been described by Cavanaugh

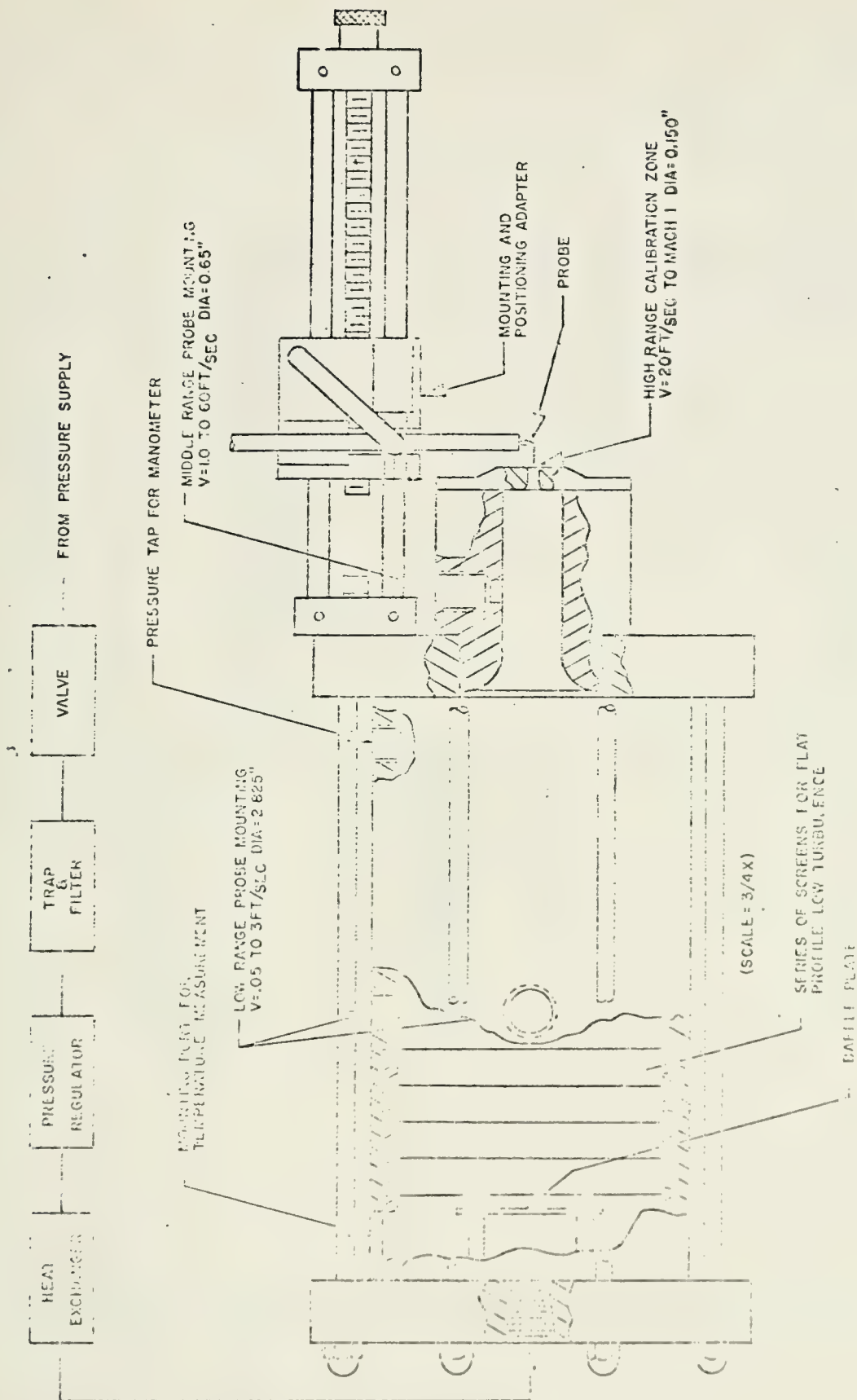


Figure 9. Probe Calibrator

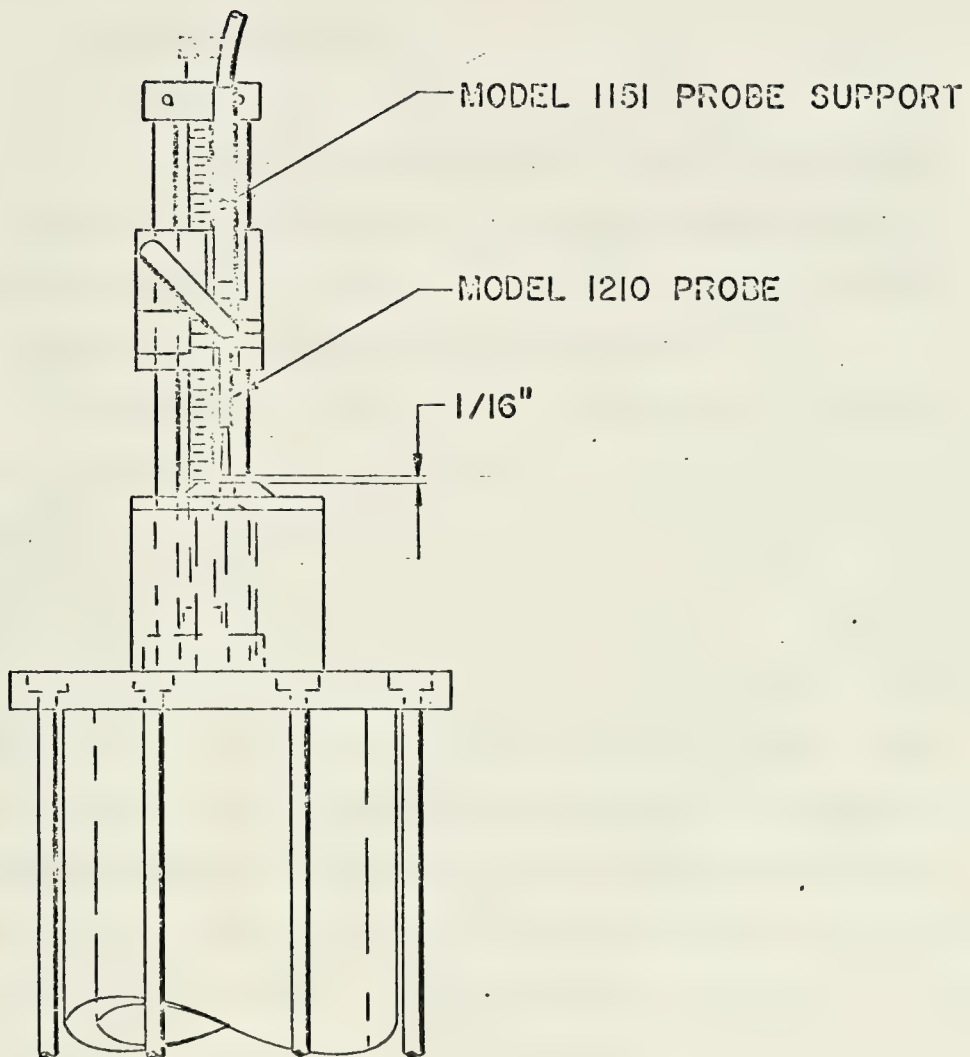


Figure 10. Vertical Probe Mounting with TSI Calibrator.

(1974). Measurements of ship's motion have been described by Welsh (1974).

C. SIGNAL PROCESSING AND RECORDING

1. Analog Recording

All data were recorded simultaneously in analog form with a 14 channel Sangamo Model 3562 FM Recorder. All recordings were made at a recording speed of 7 1/2 inches per second. At this recording speed the recorder had a frequency range from DC to 25 KHz.

A schematic diagram of the complete recording system is shown in Appendix D. The amplifier and suppressor combination in series with the sensor electronics and recorder channels were necessary to improve the signal to noise ratio of the inputs. The hot-wire signals were high pass filtered at 2 Hz during the majority of the runs. Two data runs were made without the filter to permit low frequency correlation between the velocity signal and ship's motion. The results of this correlation are discussed by Welsh (1974). The temperature signals were low pass filtered at 500 Hz. In addition to the signal recordings, a voice track was utilized to record observations pertinent to the data runs. Constant monitoring of amplified and preamplified signals was performed with an oscilloscope to evaluate the signals and to insure that the signal would not exceed amplifier or recorder input limits.

2. Real Time Analysis

Real time analysis was accomplished using a Spectral Dynamics Corporation (SD) Model SD301C Real Time Analyzer. This unit was used in conjunction with a Model SD309 Ensemble Averager, a Model 13116-2A X-Y Display Oscilloscope and an X-Y plotter to provide an instantaneous evaluation of the hot wire and temperature signals. The equipment allowed positive determination that measurements were sufficient to define the inertial subrange. A system operation diagram is provided in Appendix E along with several of the X-Y plots obtained from the real time analysis.

IV. DATA REDUCTION AND ANALYSIS

A. PRELIMINARY ANALYSIS

The analog tapes were played on a strip chart recorder to permit initial evaluations of the data. From this, data periods were chosen for subsequent reduction and analyses. This preliminary analysis disclosed a recording problem that had previously gone unnoticed. A periodic tape transport vibration had occurred due to the 7 1/2 ips gear drive and this obliterated the recorded signal. Fortunately, there were sufficient time intervals between vibrations to permit 20 minute data records to be obtained. It was from these data sections that the periods listed in Table II were obtained.

The difficulties encountered in making the temperature fluctuation measurements, as described in Section III, were evident in the strip chart recordings. The temperature data either failed to show sufficient signal strength or displayed a DC drift which rendered them impossible to digitize. An example of the two cases is shown in Figure 11.

The paucity of temperature data led to a focusing of attention on the velocity fluctuation measurements. The criteria for selection of subsequent data periods for inclusion in the reduction and analysis phase consisted of: (1) signal strength (2) averaging time (3) DC drift rate

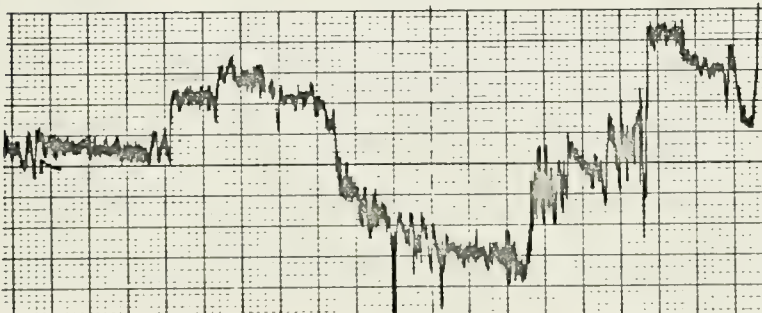
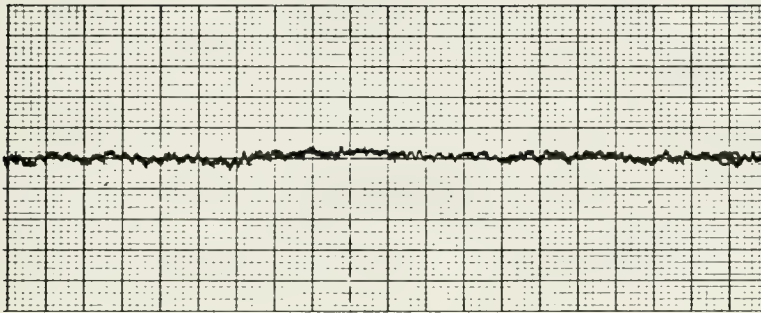


Figure 11. Inadequate Temperature Signals Showing (A) Insufficient Signal Strength and (B) DC Drift.

and (4) availability of mean profiles. Sufficient signal levels were required to minimize amplification during the analog-to-digital conversion process. Twenty minute data runs proved sufficient to permit ample averaging time for Fast Fourier Transform (FFT) calculations. DC drift was kept at a minimum to permit ease in digitization and to allow greater confidence in the data samples. Finally, data periods were selected to correspond to times when mean wind information was available. A typical signal meeting the above mentioned criteria is shown in Figure 12.

B. ANALOG-TO-DIGITAL CONVERSION

Analog-to-digital conversion was performed on a hybrid computer system located on the fifth floor of Spanagel Hall at NPS. The hybrid system consists of an analog computer, COMCOR Ci 5000, interfaced electrically with a digital computer, XDS 9300. A detailed discussion of the operation of this computer facility was given by McKendrick (1972) which should be referred to for additional information. A block diagram, provided in Figure 13, illustrates the analog-to-digital conversion sequence followed in this study.

C. SEVEN-TRACK TO NINE-TRACK CONVERSION

The analog-to-digital conversion process generated seven-track octal base data samples written on digital tape. The computer used to analyze the digital data was an IBM

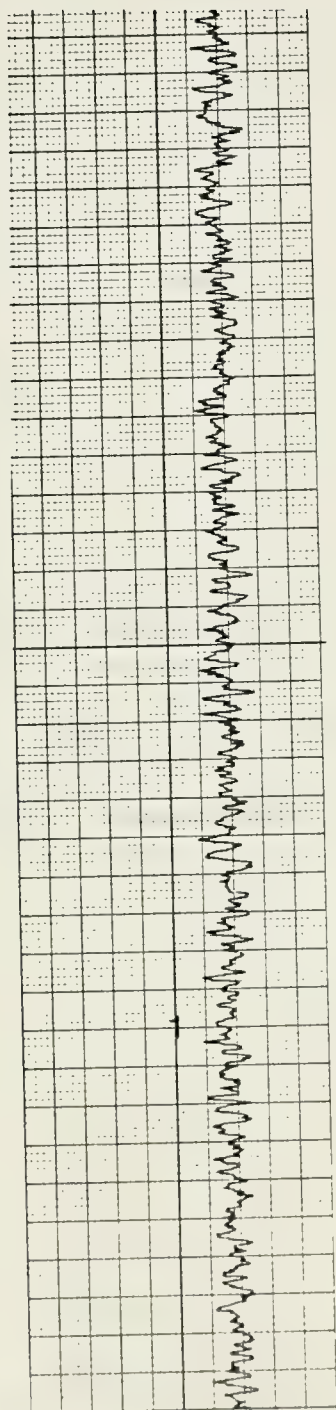


Figure 12. Typical Velocity Signal.

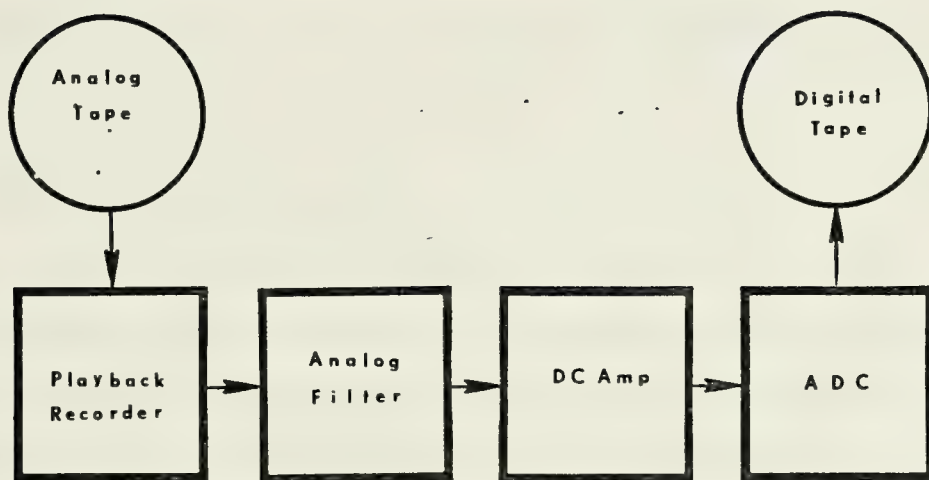


Figure 13. A-D Conversion Procedures.

360/67 computer. This computer utilizes nine-track hexadecimal based digital samples so a conversion between the seven-track and nine-track systems was necessary. A discussion of the procedures necessary for making the proper conversion to the nine-track hexadecimal based system are described in Naval Postgraduate School Computer Center Technical Note #0211-08. The two primary programs involved in this conversion are the TAPEOUT and CONVERT programs. These programs along with a description of digital tape operations are discussed in Appendix F.

D. DIGITAL ANALYSES PROGRAMS

Fast Fourier Transform (FTOR) and spectral analysis (SCOR) programs were available in the IBM 360/67 subroutine library. The following description of the FFT program package was taken from McKendrick. The programs were written by J. F. Garrett and J. R. Wilson while students at the Institute of Oceanography at the University of British Columbia. The "OCEAN" subroutines of the UBCFTOR program instructs the IBM 360 to read the input tape, one block at a time, compute the FFT of the data block and then store the resulting Fourier coefficients on the output tape. The computer printout for the FTOR program is a listing of each digital channel and the Fourier coefficients produced. An example of this output is shown in Figure 14.

With these coefficients, the UBCSCOR program is used to compute the spectrum for a given channel, or the cross

SUMMARY COEFFICIENTS FOR 2413 1TH BLOCK OF 256 SAMPLES									
IN THIS BLOCK PARITY ERRORS ON TAPE = 0, ALL ONES NOT FOUND IN CHANNEL 1 0 TIMES									
LAST HARM	K	CHANNEL		T U U	LEVEL LEVEL LEVEL LEVEL	NAME	CHANNEL 2		CAL. FACTOR
		REAL	IMAG				REAL	IMAG	
0	1	0.31E	0.04E	1.40E	1.40E	0.88E	0.05E	0.06E	1.00E
4	2	1.54E	0.03E	2.44E	2.44E	3.56E	0.05E	3.27E	1.00E
8	3	4.31E	0.03E	1.59E	1.59E	5.08E	0.04E	5.18E	1.00E
12	4	9.35E	0.04E	2.30E	2.30E	5.02E	0.04E	5.84E	1.00E
16	1	6.22E	0.03E	9.32E	9.32E	2.00E	0.03E	1.58E	1.00E
20	2	4.79E	0.03E	3.39E	3.39E	9.99E	0.04E	8.66E	1.00E
24	3	1.62E	0.02E	1.10E	1.10E	5.55E	0.04E	1.06E	1.00E
28	4	1.72E	0.03E	5.22E	5.22E	7.77E	0.03E	1.81E	1.00E
32	1	3.07E	0.03E	8.37E	8.37E	2.12E	0.04E	1.33E	1.00E
36	2	1.13E	0.02E	2.81E	2.81E	8.94E	0.04E	1.23E	1.00E
40	3	2.76E	0.03E	3.08E	3.08E	1.07E	0.03E	1.47E	1.00E
44	4	0.88E	0.03E	2.29E	2.29E	2.25E	0.04E	1.45E	1.00E
48	1	6.08E	0.03E	4.45E	4.45E	1.41E	0.04E	1.80E	1.00E
52	2	2.88E	0.03E	1.69E	1.69E	2.21E	0.04E	2.25E	1.00E
56	3	4.49E	0.02E	3.48E	3.48E	5.98E	0.03E	1.39E	1.00E
60	4	1.62E	0.02E	5.32E	5.32E	7.06E	0.04E	3.94E	1.00E
64	1	8.91E	0.03E	7.82E	7.82E	2.08E	0.03E	1.13E	1.00E
68	2	2.59E	0.03E	1.55E	1.55E	9.66E	0.04E	1.61E	1.00E
72	3	4.62E	0.02E	3.29E	3.29E	1.14E	0.03E	1.46E	1.00E
76	4	1.91E	0.03E	2.23E	2.23E	1.58E	0.03E	1.37E	1.00E
80	1	8.59E	0.02E	5.27E	5.27E	3.30E	0.04E	2.30E	1.00E
84	2	2.94E	0.03E	1.33E	1.33E	2.00E	0.03E	1.59E	1.00E
88	3	1.73E	0.03E	3.77E	3.77E	1.21E	0.03E	1.32E	1.00E
92	4	1.81E	0.03E	5.00E	5.00E	1.39E	0.04E	1.95E	1.00E
96	1	2.44E	0.03E	1.53E	1.53E	3.69E	0.03E	1.81E	1.00E
100	2	1.17E	0.03E	2.71E	2.71E	1.20E	0.04E	1.71E	1.00E
104	3	6.21E	0.02E	2.59E	2.59E	7.53E	0.02E	5.61E	1.00E

Figure 14. FTOR Output.

spectrum between a pair of channels, depending on what is selected by the user. The output of the SCOR program consists of a tabular computer printout, as shown in Figure 15, and a graphical plot of the spectrum versus frequency as shown in Figure 16. Appendix G of this thesis contains the preface comments of the FTOR and SCOR programs along with additional information for more efficient utilization of the spectral analysis package. Several difficulties were encountered during utilization of the analyses programs and consideration of these difficulties is the primary reason for inclusion of Appendix G.

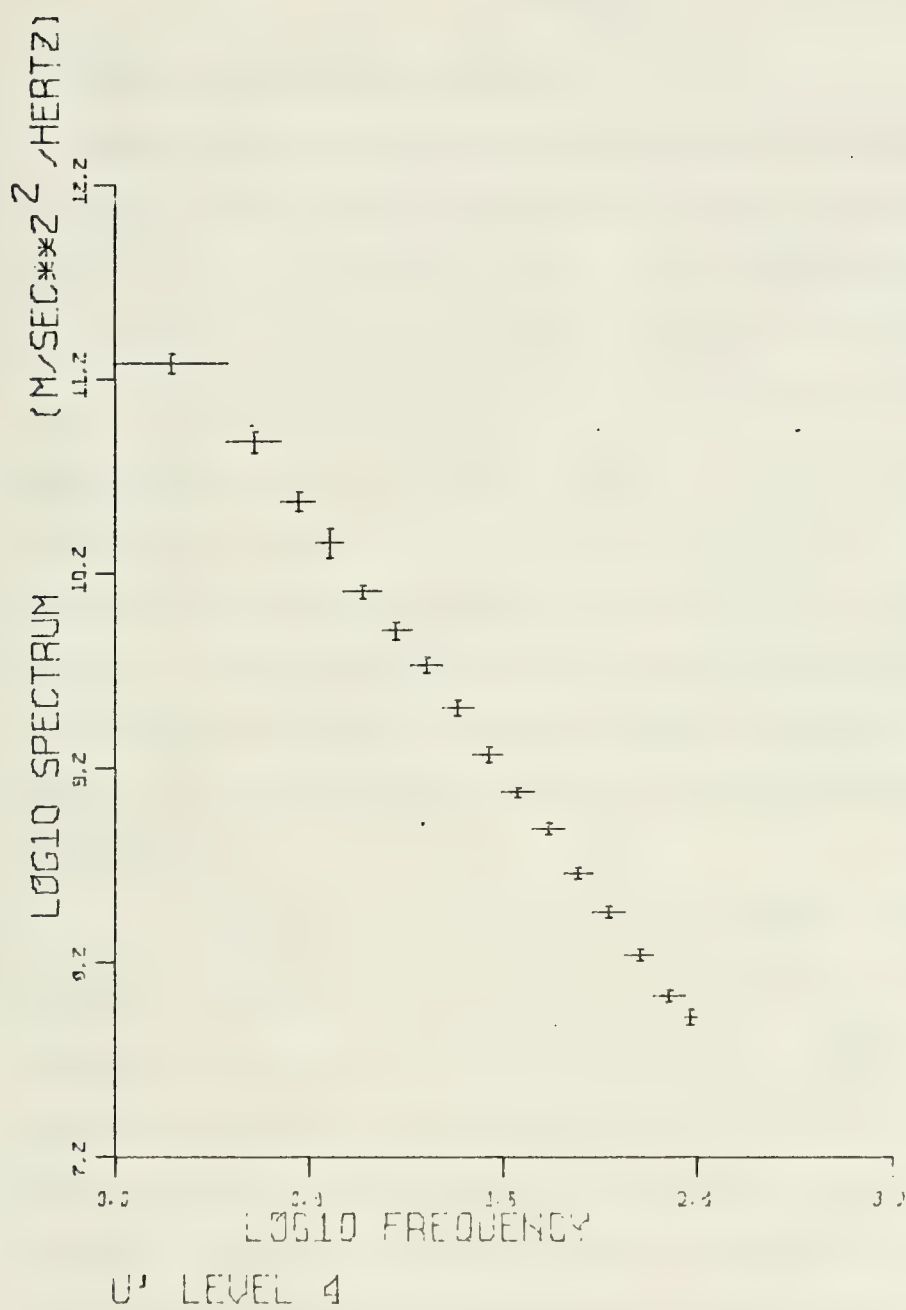


Figure 16. SCOR Spectral Plot.

V. RESULTS

A. ONE POINT SPECTRAL METHOD

The procedure first selected for estimating ϵ , and hence u_* , was to use single point values from the spectra, similar to that in Figure 16. A $-5/3$ slope was approximated for the spectrum and the frequency and spectral density, for a spectral value coincident with the line, were taken from computer output similar to that illustrated in Figure 15. Equation 10 was then used to obtain ϵ from values of frequency, spectral density, wind speed and probe height. The computed value of ϵ was then used in Equation 7 to obtain a value for the friction velocity (u_*). The computer program used for these calculations appears in Appendix H.

U_* values were obtained by this method for all data periods and tabulated results for one minute and 10 minute averages are listed in Tables III-VII. This method appeared successful for spectra such as those shown in Figure 16, which had a definite $-5/3$ slope for a majority of points. However, the single point spectral method is quite subjective when used with spectra such as the one shown in Figure 17. It is easily seen that selections of unrepresentative spectral estimates could result in values of ϵ which would differ significantly. Because of the subjective manner in which $-5/3$ slope lines could be drawn and

TABLE III

Momentum Flux Calculations for 1103-1138 20 Sept 1973
using the One Point Spectral Method

Height (m)	Time Average (min)	ϵ (cm ² sec ⁻³)	u_* (cm sec ⁻¹)
14.41	1	1.078	8.727
	10	1.319	9.129
13.20	1	1.010	8.532
	10	1.389	9.109
8.39	1	2.973	9.871
	10	2.075	8.865
4.52	1	2.418	7.602
	10	2.636	7.812

TABLE IV

Momentum Flux Calculations for 2008-2018 20 Sept 1973
using the One Point Spectral Method

Height (m)	Time Average (min)	ϵ (cm ² sec ⁻³)	u_* (cm sec ⁻¹)
14.41	1	9.742	17.674
	10	8.937	17.272
8.39	1	16.211	18.291
	10	11.679	15.769
4.52	1	20.806	15.643
	10	16.128	14.287

TABLE V

Momentum Flux Calculations for 2023-2053 20 Sept 1973
using the One Point Spectral Method

Height (m)	Time Average (min)	ϵ (cm ² sec ⁻³)	u_* (cm sec ⁻¹)
14.41	1	9.304	17.505
	10	9.556	17.662
8.39	1	14.042	16.768
	10	14.519	16.956
4.52	1	21.934	15.829
	10	22.634	15.996

TABLE VI

Momentum Flux Calculations for 2323-2341 20 Sept 1973
using the One Point Spectral Method

Height (m)	Time Average (min)	ϵ (cm ² sec ⁻³)	u_* (cm sec ⁻¹)
14.41	1	4.069	14.925
	10	3.543	12.688
13.20	1	3.316	12.973
	10	2.576	11.082
8.39	1	7.965	13.859
	10	6.265	12.813

TABLE VII

Momentum Flux Calculations for 0637-0652 21 Sept 1973
using the One Point Spectral Method

Height (m)	Time Average (min)	ϵ ($\text{cm}^2 \text{sec}^{-3}$)	u_* (cm sec^{-1})
14.41	1	1.923	10.146
	10	1.114	8.625
8.39	1	7.830	13.991
	10	5.660	12.386

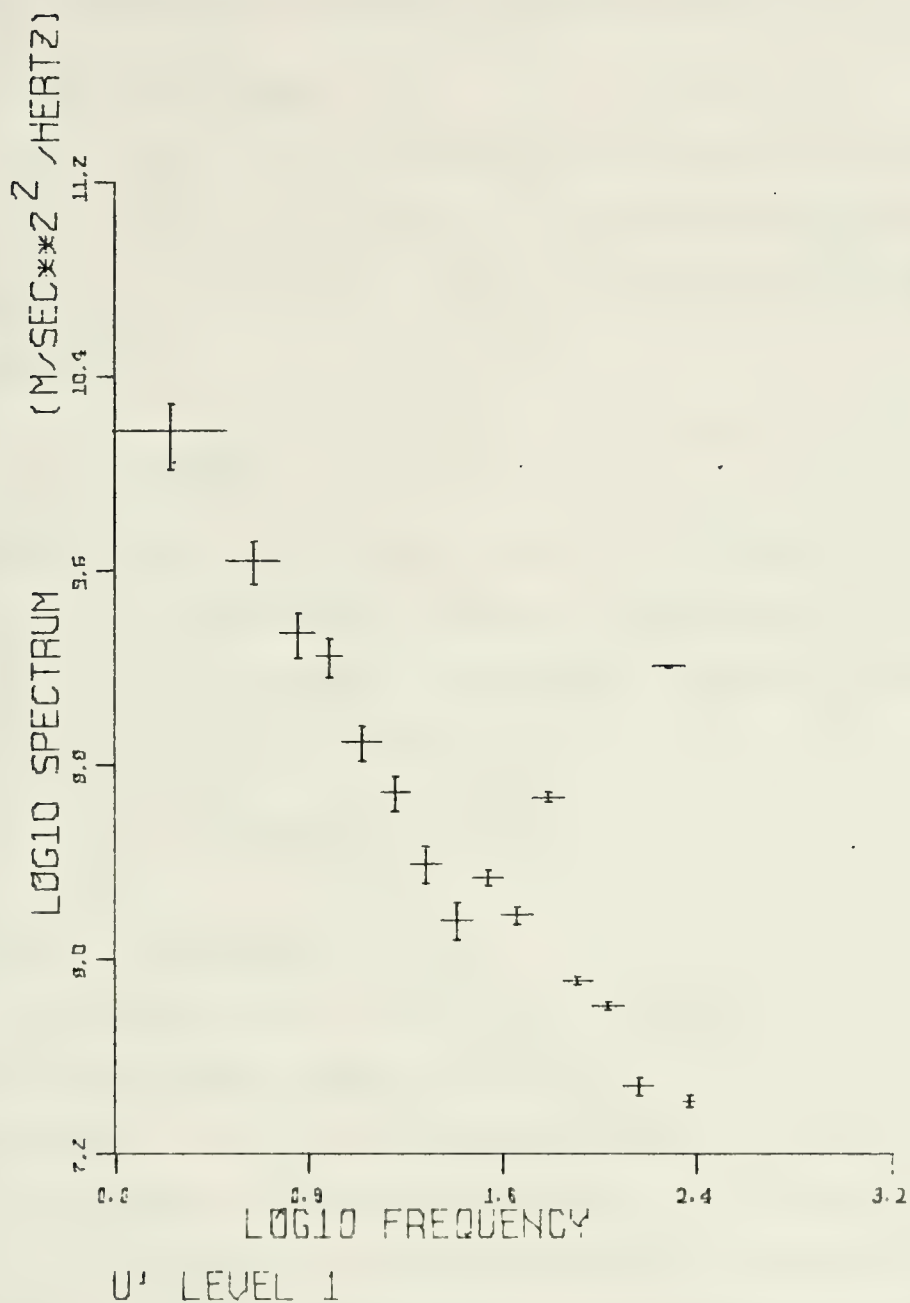


Figure 17. Velocity Spectrum Showing Deviation from -5/3 Slope.

a coincident spectral value selected, there was some doubt expressed in results from other than ideal spectra.

B. INTERCEPT METHOD

To avoid the subjectiveness of estimates of ϵ based on single spectral estimates, a second method was utilized. This method is based on Equation 10 rewritten in the following form

$$\text{Ln } k\phi(k) = -2/3 \text{ Ln } k + \text{Ln } \alpha\epsilon^{2/3} \quad (14)$$

For this expression a plot of $\text{Ln } k\phi(k)$ versus $\text{Ln } k$ would result in a curve with a slope of one and an intercept value equal to $\text{Ln } \alpha\epsilon^{2/3}$. From this intercept, the value of ϵ can be obtained from

$$\left[\frac{\text{Exp } b}{\alpha}\right]^{3/2} = \epsilon$$

where b = intercept value.

The advantage in using the intercept method versus the single point spectral method is that the intercept is determined from an average of the points along a line defined by the $-2/3$ slope. Figure 18 is an example of most curves obtained from the application of Equation 14 to spectral results. Difficulty in approximating the slope was encountered in a few cases such as that illustrated in Figure 19 but in most instances the forcing of a $+1$ slope permitted easier detection of spectral harmonics

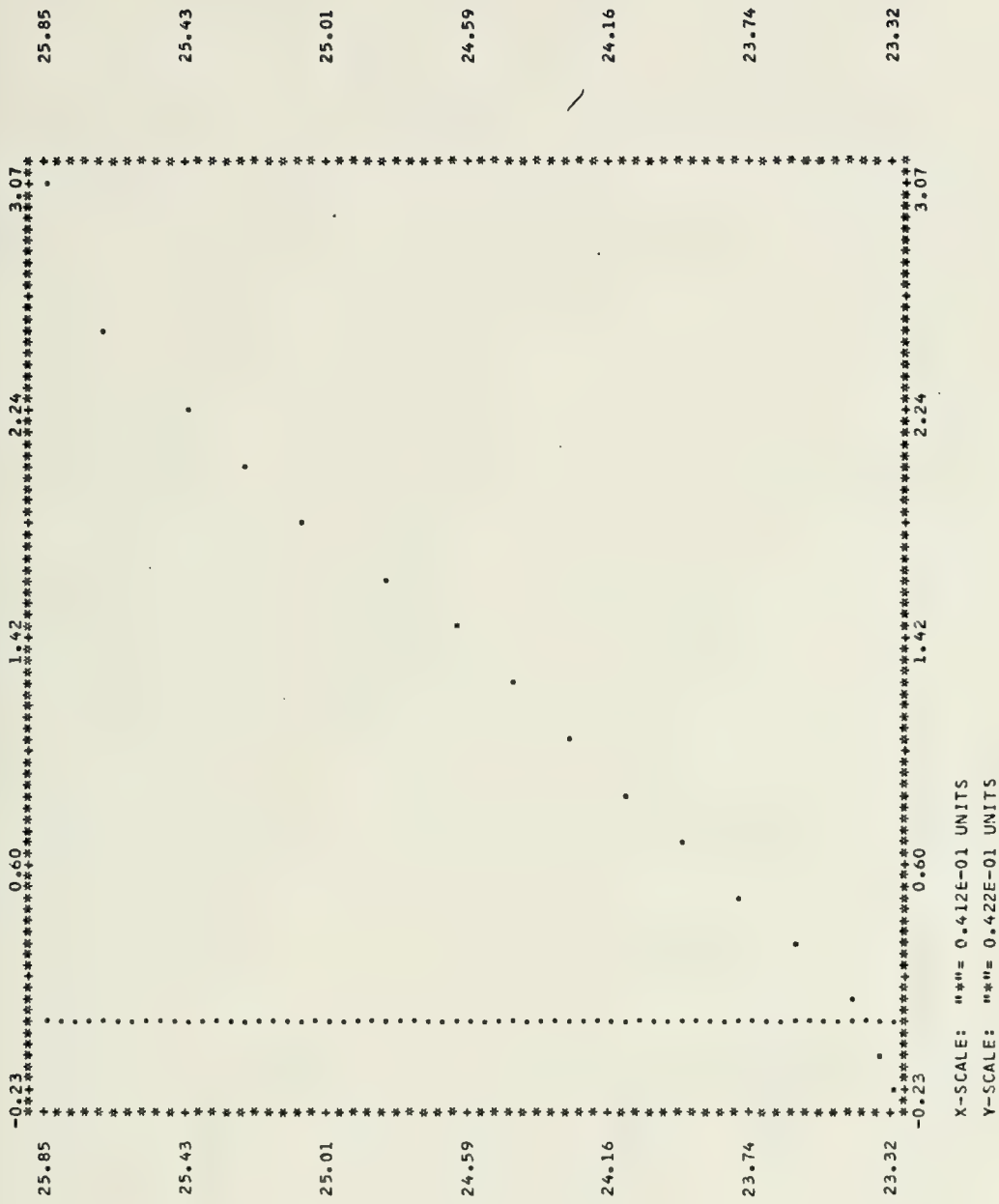
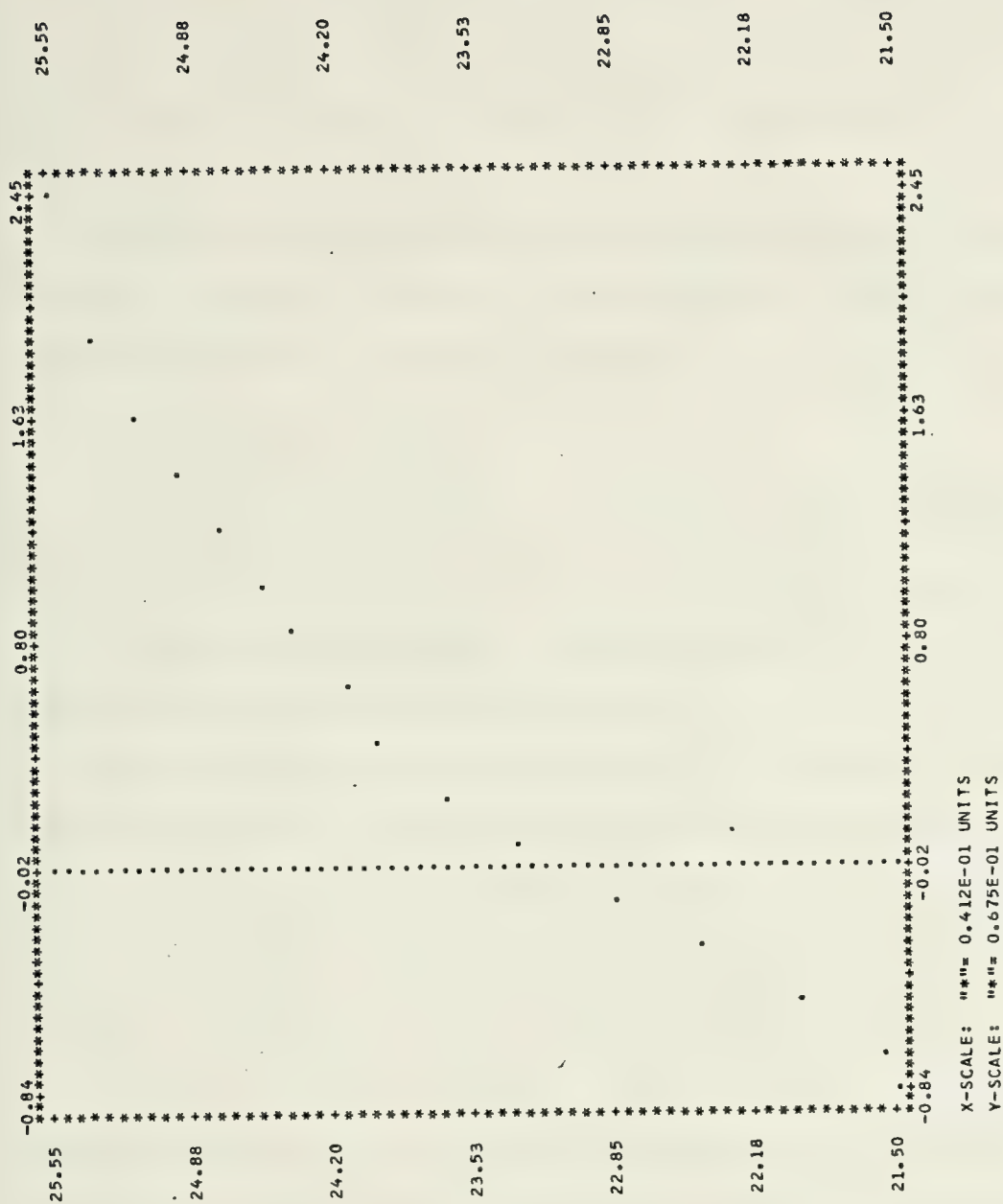


Figure 18. Ten Minute Intercept Plot for 1103-1138 20 Sept 73.



which did not fit the $-5/3$ criteria. Table XI does not indicate a one minute spectral average since the curves for that time average were similar to Figure 20. It is clear that fitting a $+1$ slope to this scattering of points would be difficult.

The intercept method was used to calculate ϵ and u_* for all five data periods. The results of these calculations are listed in Tables VIII-XII.

C. COMPARISON OF METHODS

A comparison of Tables III-VII and Tables VIII-XII indicates that somewhat higher u_* values were obtained with the intercept method. The apparent validity of the higher values will be examined later.

Considering the intercept method, a majority of cases yielded larger u_* values for longer time averages. The importance of resultant higher u_* values will be apparent when comparisons are made between shipboard results and results from other studies. The subjective nature of selecting spectral estimates in the one point spectral method is manifested by larger deviations in u_* values associated with periods when spectra were not "near-perfect."

The one point spectral method was compared with the intercept method because of interests in designing procedures for quick estimates of u_* during measurements. If valid values of ϵ could be obtained from single spectral

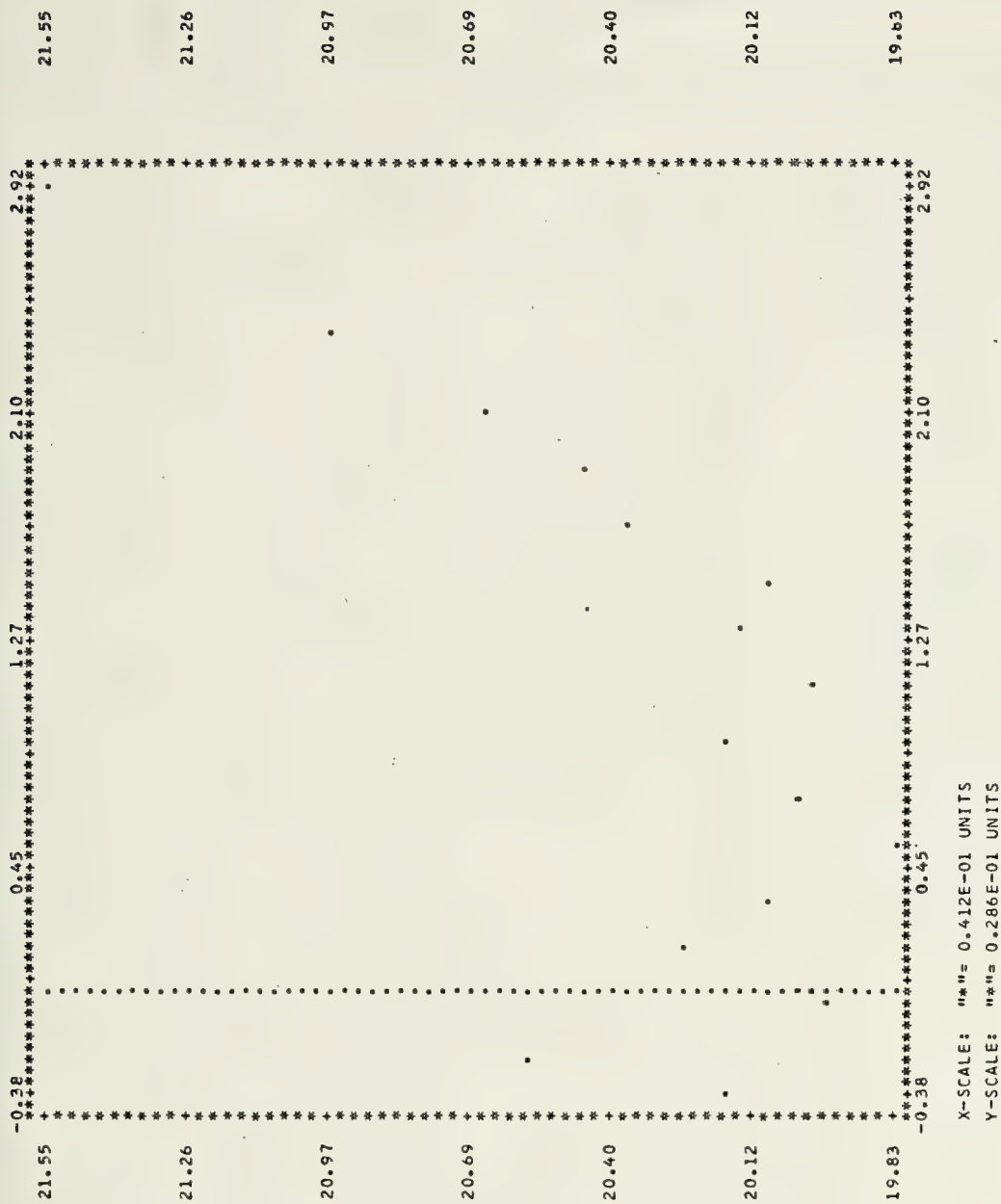


Figure 20. One Minute Intercept Plot for 2323-2341 20 Sept 73.

TABLE VIII

Momentum Flux Calculations for 1103-1138 20 Sept 1973
using the Zero Intercept Method

Height (m)	Time Average (min)	ϵ ($\text{cm}^2 \text{ sec}^{-3}$)	u_* (cm sec^{-1})
14.41	1	1.329	9.151
	4	1.378	9.330
	10	1.235	9.012
	20	1.372	9.248
13.20	1	1.445	9.139
	4	1.379	8.998
	20	1.503	9.260
8.39	1	2.635	9.600
	4	2.337	9.224
	20	2.622	9.584
4.52	1	3.086	8.233
	4	3.148	8.288
	20	3.689	8.738

TABLE IX

Momentum Flux Calculations for 2008-2018 20 Sept 1973
using the Zero Intercept Method

Height (m)	Time Average (min)	ϵ (cm ² sec ⁻³)	u_* (cm sec ⁻¹)
14.41	1	10.288	18.012
	3	8.285	17.135
	10	10.935	18.474
8.39	1	13.226	16.437
	3	11.828	15.988
	10	13.678	16.622
4.52	1	17.765	14.731
	3	14.677	13.846
	10	18.127	14.855

TABLE X

Momentum Flux Calculations for 2023-2053 20 Sept 1973
using the Zero Intercept Method

Height (m)	Time Average (min)	ϵ (cm ² sec ⁻³)	u_* (cm sec ⁻¹)
14.41	1	12.071	19.093
	3	11.825	18.985
	20	11.540	18.809
8.39	1	16.723	17.774
	3	16.496	17.694
	20	16.243	17.603
4.52	1	25.023	16.541
	3	24.492	16.432
	20	24.149	16.346

TABLE XI

Momentum Flux Calculations for 2323-2341 20 Sept 1973
using the Zero Intercept Method

Height (m)	Time Average (min)	ϵ (cm ² sec ⁻³)	u_* (cm sec ⁻¹)
14.41	3	12.925	19.533
	10	13.564	19.849
13.20	3	13.471	19.235
	10	14.009	19.488
8.39	3	14.418	16.917
	10	15.025	17.151

TABLE XII

Momentum Flux Calculations for 0637-0652 21 Sept 1973
using the Zero Intercept Method

Height (m)	Time Average (min)	ϵ (cm ² sec ⁻³)	u_* (cm sec ⁻¹)
14.41	1	1.209	8.868
	4	1.955	10.407
	10	1.570	9.675
8.39	1	5.316	12.131
	4	8.451	14.158
	10	7.643	13.691

estimates then the structure function measured may be valid. The latter has been shown to be a poor approach on the basis of these results.

D. EVALUATION OF THE VARIATION OF U_* WITH HEIGHT

A long accepted concept in turbulence theory has been the existence of a constant-stress layer. This concept is often used to evaluate the representativeness of accumulated data (e.g., Stegen, et al) and will be applied to test the validity of assumptions and expressions used in the present study.

Table I was compiled by Stegen, et al for conditions when the measured mean wind speed was 5.12 m sec^{-1} . This mean speed corresponds to the wind conditions for the values tabulated in Tables VII and XII. A comparison of results in Table I and Tables VII and XII reveals lower values of u_* in the present study. As previously mentioned, the constant, (α) , in Equation 10 is empirically derived and several values have been suggested in the literature. A value of $\alpha = 0.60$ was used in compiling the results in Table I while a value of 0.48, suggested by Pond, et al (1966), was used in the present study.

U_* results listed in Table VIII support a constant-flux assumption as well as the validity of Equation 7 for u_* calculations, for neutral or near neutral conditions. The anomalously low value of u_* at 4.52 meters could be the result of acceleration due to the ship's bow. It is

seen that as the spectral averaging time increases the value of the flux increases. This would be consistent with an interpretation that increased averaging time would reduce the observed acceleration effects.

Tables IX-XI correspond to periods of stable stratifications while Table XII reflects a period of unstable stratification. It is seen from Equation 12 that neglecting diabatic effects would introduce a bias into the data. A stability correction could be applied to adjust the flux values for the more general case of stratified flow.

E. THE VARIATION OF ϵ WITH HEIGHT

Figures 21-25 show the plots of $\ln \epsilon$ versus $\ln z$ for the periods listed in Tables VIII-XII. On the basis of Equation 8, a plot of $\ln \epsilon$ vs $\ln z$ should yield a -1 slope for neutral conditions. Results from Stegen, et al, Figure 3, were in agreement with this prediction.

In Figures 22 and 23 the slopes are less than -1 while in Figure 24 the slope is greater than -1. An initial concern when these results became known was whether possible attenuation of the sensors at lower levels was a factor. Such a concern is logical since the sensors near the surface would be likely to lose sensitivity more rapidly as a result of increased salt loading at lower levels.

The data period which occurred last is the one which shows the greatest slope which indicates that sensor deterioration at lower levels was not responsible for the

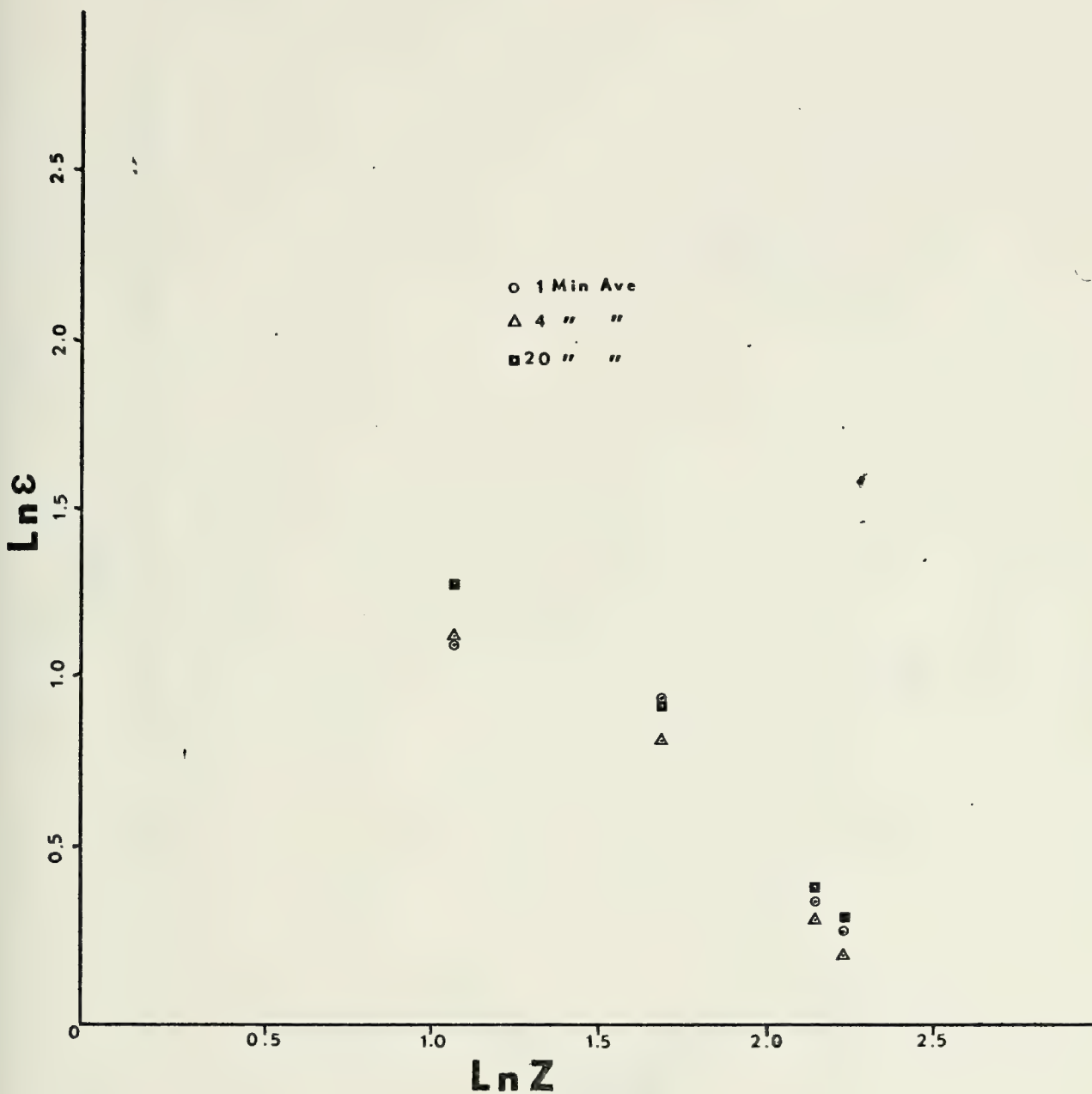


Figure 21. Measured Values of ϵ vs Height for 1103-1138 20 Sept 73. For Scaling Purposes a Factor of 5.0 was Subtracted from the x-Values.

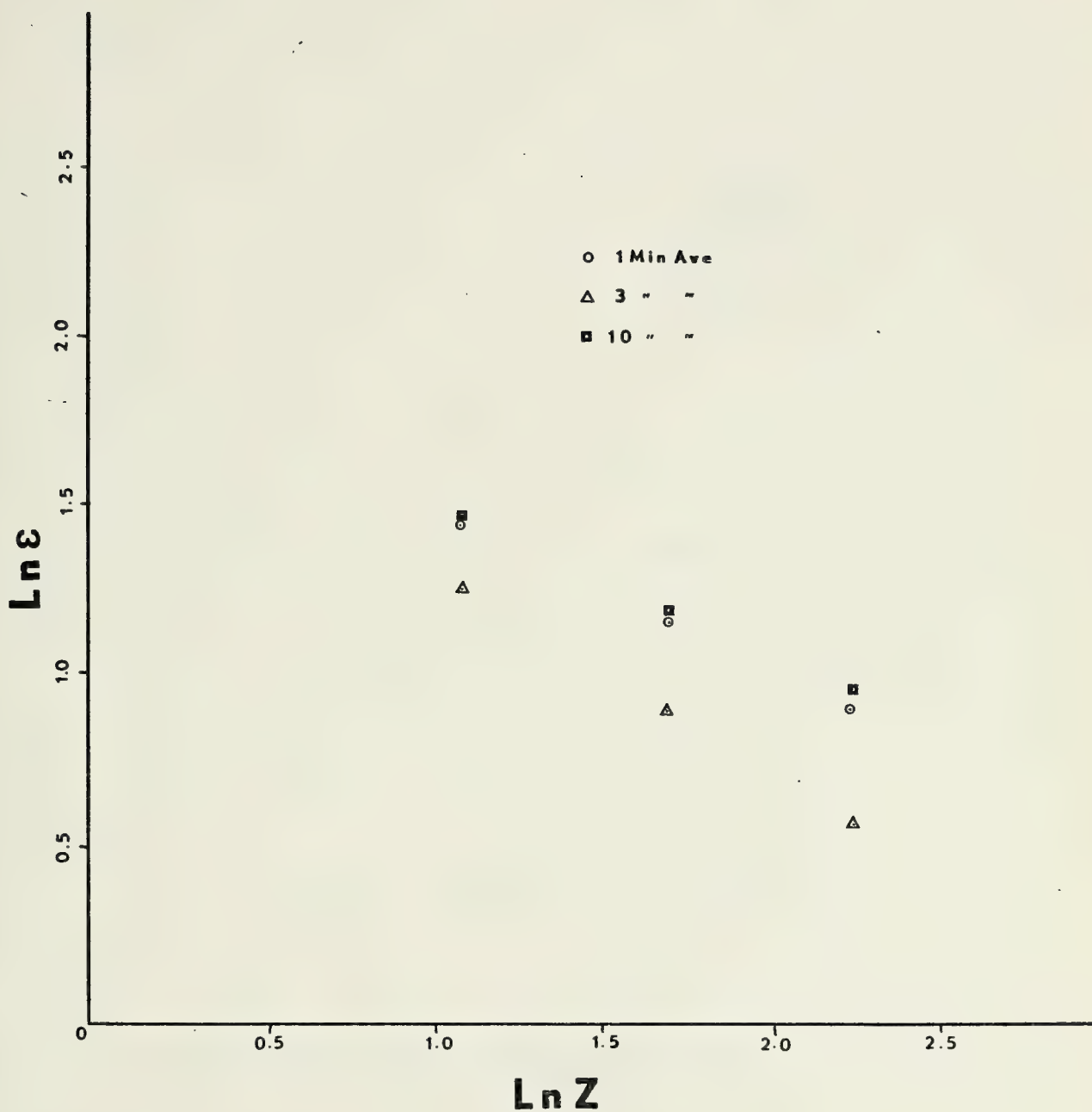


Figure 22. Measured Values of ϵ vs Height for 2008-2018 20 Sept 73. For Scaling Purposes a Factor of 5.0 and 1.4 were Subtracted from the X and Y Values, Respectively.

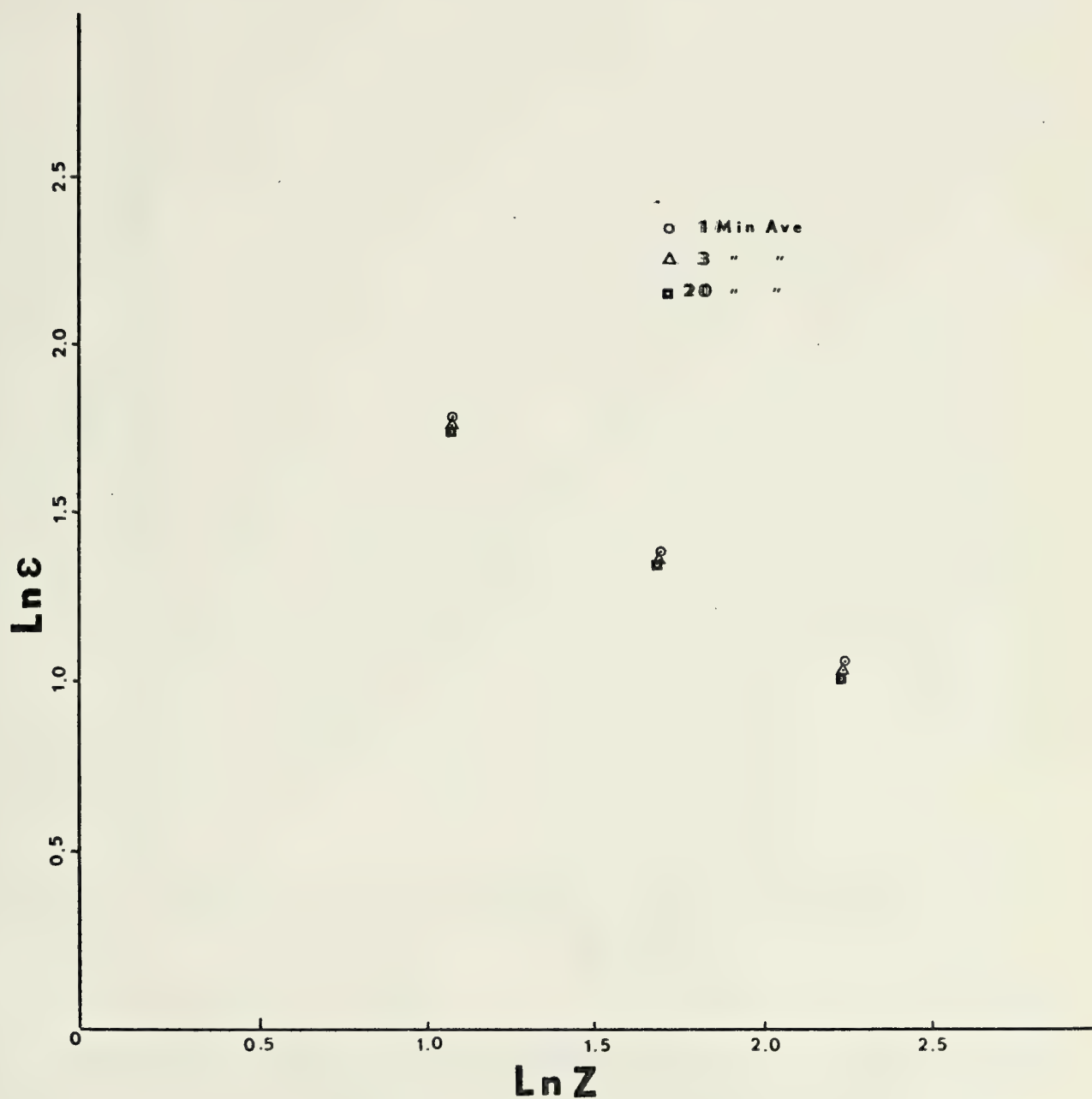


Figure 23. Measured Values of ϵ vs Height for 2023-2053 20 Sept 73. For Scaling Purposes a Factor of 5.0 and 2.0 were Subtracted from the X and Y Values, Respectively.

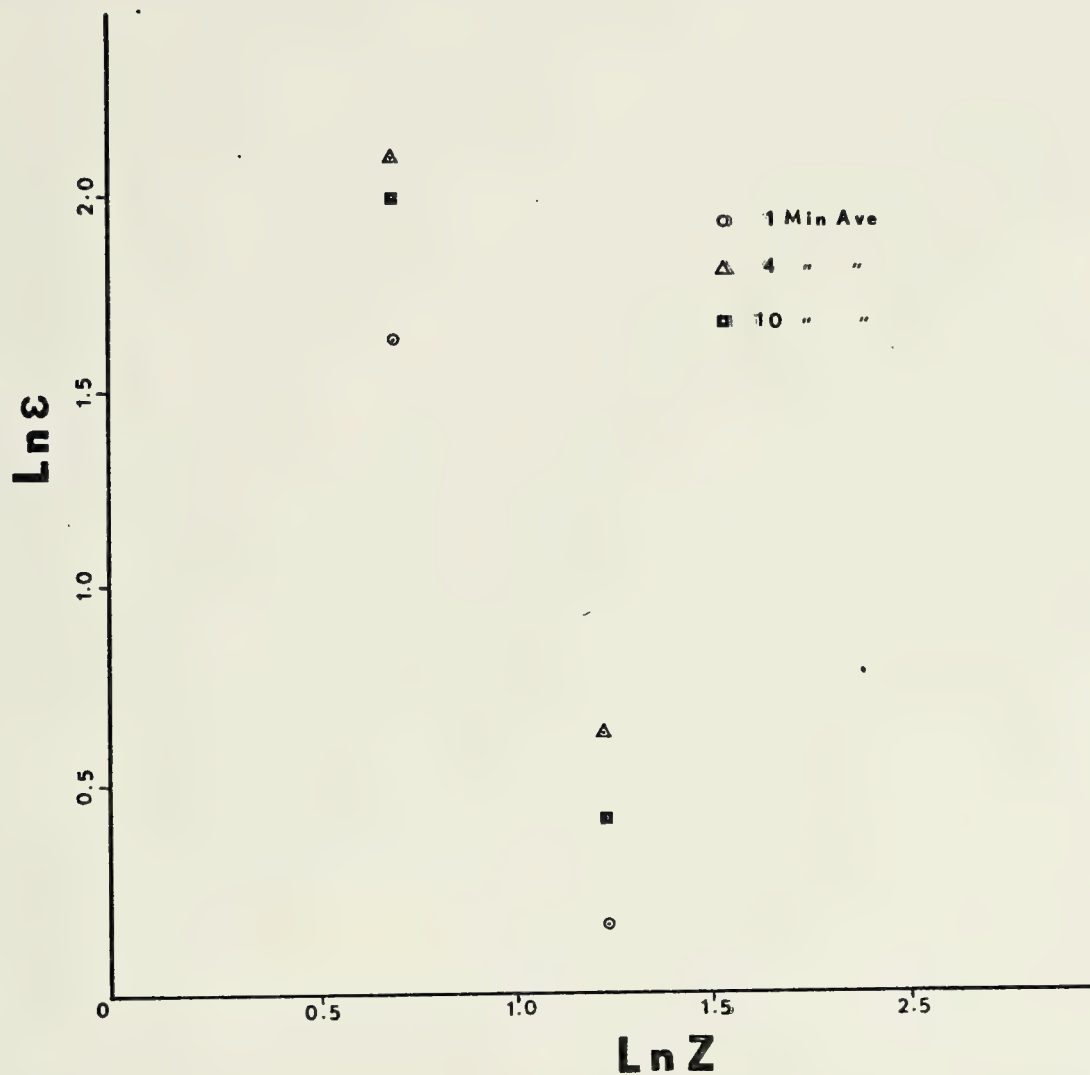


Figure 24. Measured Values of ϵ vs Height for 0637-0652 21 Sept 73. For Scaling Purposes a Factor of 6.0 was Subtracted from the X Values.

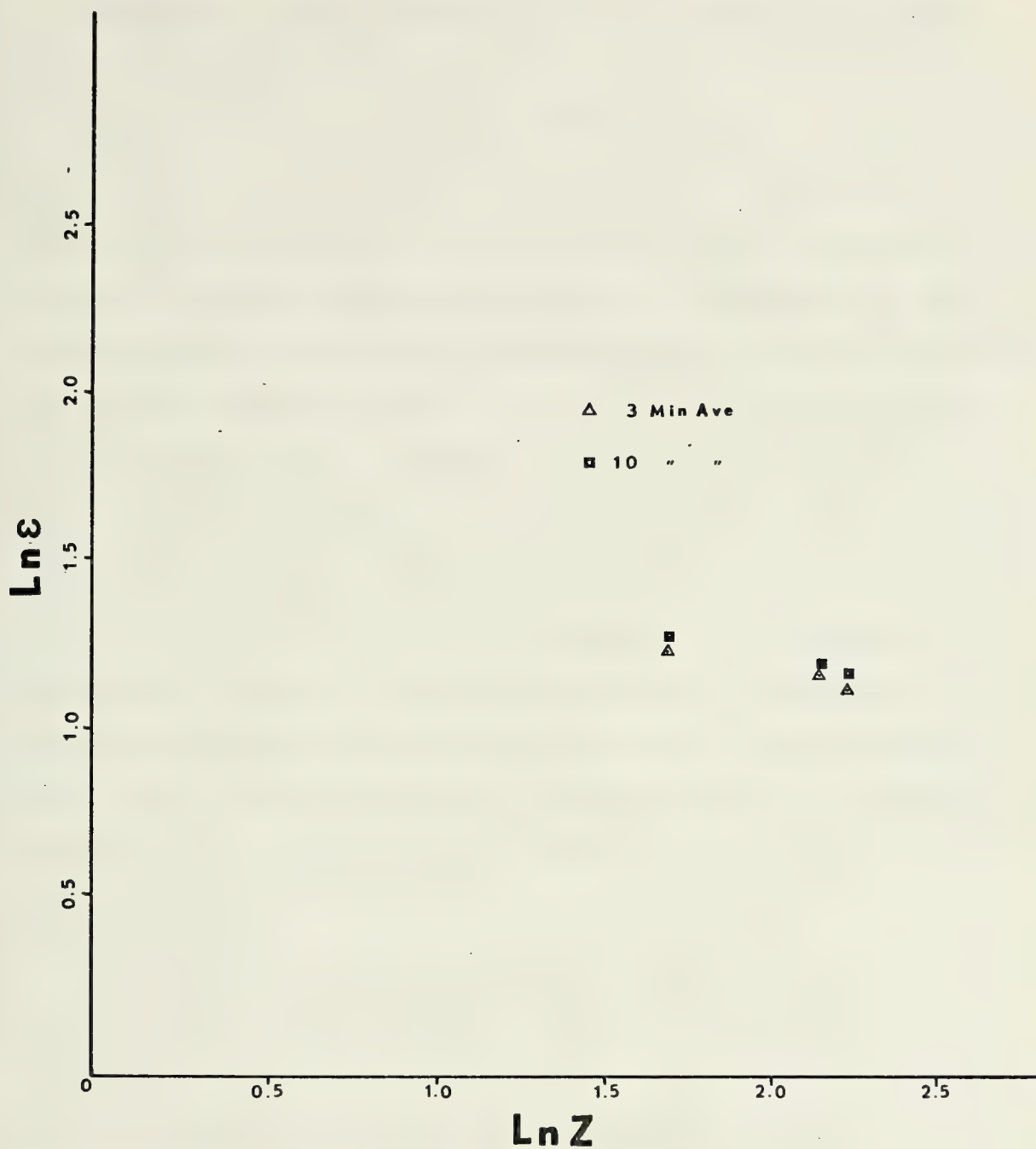


Figure 25. Measured Values of ϵ vs Height for 2323-2341 20 Sept 73. For Scaling Purposes a Factor of 5.0 and 1.4 were Subtracted from the X and Y Values, Respectively.

variation in slopes. Further support of this conclusion is provided by using Equation 11 as an independent method of determining the dissipation.

For the 2023-2053 20 Sept 73 data period, the spectra at all levels were similar to that shown in Figure 26, where scale separation between the pure inertial transfer and the viscous dissipation regions was discernable. The upper limits of the inertial subrange were determined from the spectra and Equation 11 was used to obtain an estimate of the dissipation. In Table XIII the values obtained by this method are compared to those obtained from spectral estimates. The inner scale computation is independent of sensor calibration since it is determined by frequency distributions and not on the spectral value. The apparent agreement between the two estimates is an in situ calibration which indicates the loss of sensitivity by individual sensors was not the cause for the deviation from the predicted slope.

The deviation from the predicted slope was also examined for possible influence of non-neutral stratifications or wind-wave coupling. Deacon (1951), from examinations of numerous vertical wind profiles, proposed the following expression for the wind shear

$$\frac{\partial \bar{u}}{\partial z} = \frac{u_*}{kz_0} \left(\frac{z}{z_0} \right)^{-\beta} \quad (15)$$

where β is a function of stability.



Figure 26. Twenty Minute Velocity Spectrum for 2023-2053
20 Sept 73.

TABLE XIII

A Comparison of Dissipation Obtained by Spectra (ϵ) and
Dissipation Obtained from the Inner Scale (ϵ_0)

Height (m)	ϵ (cm ² sec ⁻³)	ϵ_0 (cm ² sec ⁻³)	u_* (cm sec ⁻¹)
14.41	9.556	9.516	17.662
8.39	14.519	14.304	16.956
4.52	22.634	22.492	15.996

The variation of β as a function of Ri , proposed by Deacon, is shown in Figure 27. In Deacon's results, the variation of β may be described in terms of hydrostatic stability. For neutral conditions, $\beta = 1$ so Equation 15 then reduces to Equation 6 and the -1 slope on the $\ln \epsilon$ versus $\ln z$ plot is predicted.

For unstable conditions β is greater than 1 and for stable conditions β is less than 1. Deacon's results predict that the expected slope of a $\ln \epsilon$ versus $\ln z$ plot would deviate from the neutral case with slopes less than -1 for periods of stable stratifications and with slopes greater than -1 for unstable conditions. Examinations of Figures 22-24 indicate why such considerations are important in interpreting the shipboard results. Figures 22-23 correspond to periods of stable stratifications with the 2023-2053 20 September data period being the most stable. In both figures, slopes less than -1 occur, with the more stable of the two periods showing the greatest deviation from the -1 slope. The results are, therefore, consistent with arguments proposed by Deacon. Figure 24 corresponds to an unstable period and shows a slope greater than -1 as predicted by Equation 15.

The results were further examined with respect to predictions from the Monin-Obuhkov similarity theory. The theory states that in the boundary layer there exists a characteristic length determined by the stability and turbulence which can be used as a scaling parameter. For

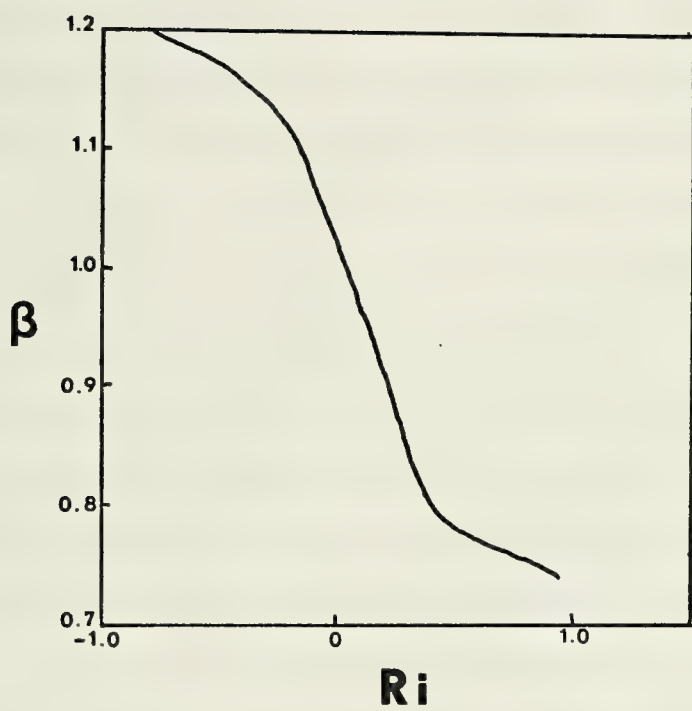


Figure 27. Variation of β with Ri (after Haltiner and Martin).



neutral conditions the appropriate characteristic length is the height above the marine boundary.

Equations 12 and 13 show the effect of non-neutral considerations in developing an expression describing the vertical variation of ϵ . Equation 12 indicates a relationship between the scaling parameters Ri and L . Such a relationship was described by Busch (1973) in a review of information available in the literature. As presented by Busch, the function $\phi_1(\frac{z}{L}) - \frac{z}{L}$ in Equation 12 has the form $(\phi_m - \frac{z}{L})$ where several flux-profile relationships have been suggested for ϕ_m . Table XIV includes the formulations which Busch used to describe ϕ_m along with constants estimated by Paulson (1970). Relationships between the Monin-Obuhkov length and the Richardson number were first used to obtain stability length (L) corrections for the shipboard results, since Richardson numbers were available from profile measurements described by Cavanaugh (1974). Values of L were then used to define $(\phi_m - \frac{z}{L})$ from relationships in Table XIV.

Figures 28 and 29 show the effects of stability corrections for the periods with stable stratifications listed in Tables IX and X, respectively. Comparisons of the corrected and uncorrected results indicate that adjustments were toward the predicted -1 slope. The fact that the stability correction produces a -1 slope supports the basic premise of the Monin-Obuhkov theory and the validity of the relationships in Table XIV.

TABLE XIV

Flux-Profile Relationships Describing the Stability Function, ϕ_m .

ϕ_m	Stability Condition
$1+7\frac{z}{L}$	$\frac{z}{L} \geq 0$
$(1-16\frac{z}{L})^{-1/4}$	$\frac{z}{L} \leq 0$
$(1-12Ri)^{-1/4}$	$Ri < -0.1$
$(1-3Ri)^{-1}$	$-0.1 \leq Ri \leq 0.036$
$0.88(1-6Ri)^{-1}$	$0.036 \leq Ri \leq 0.1$

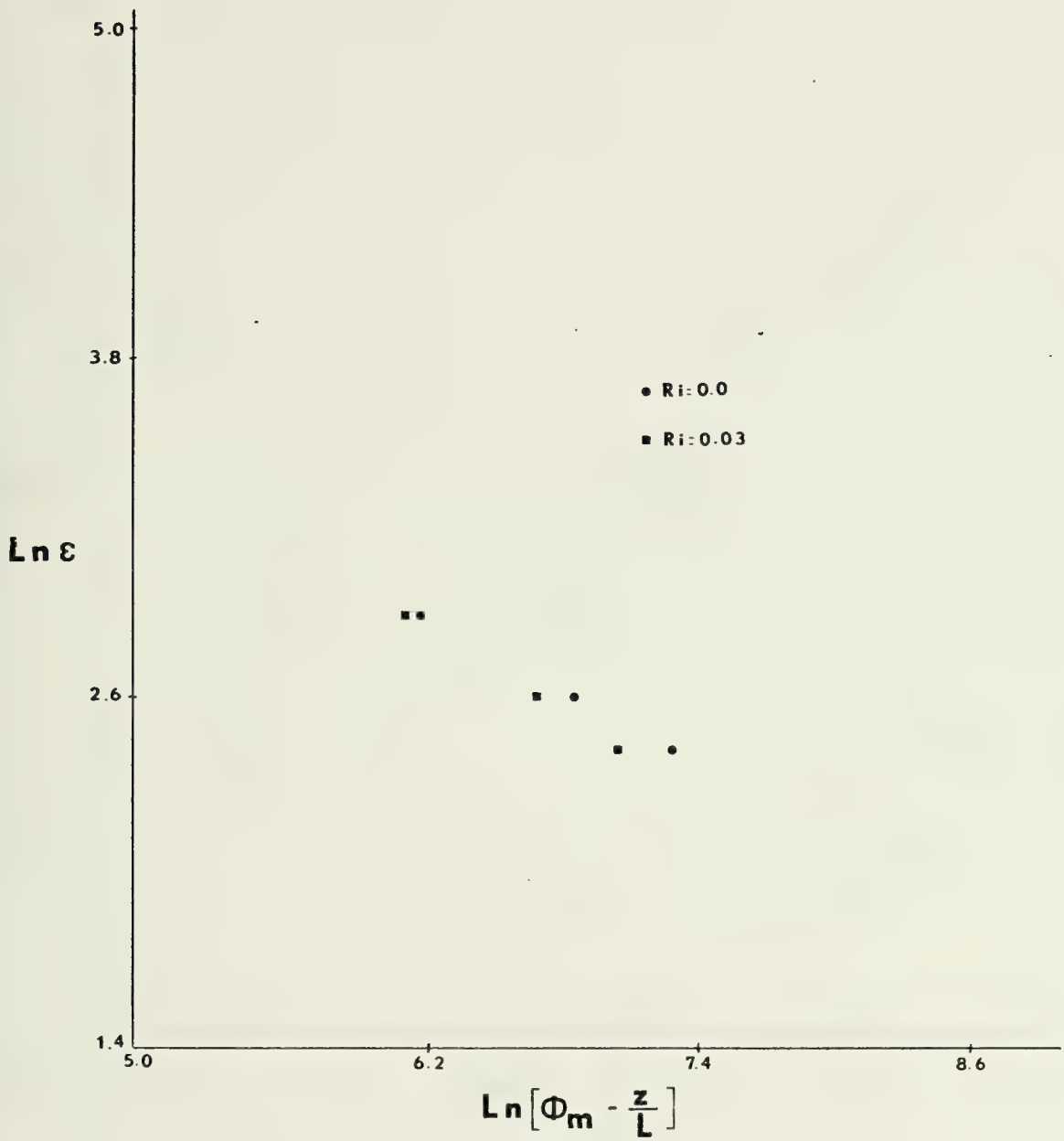


Figure 28. Effect of Stability Correction for 2008-2018
20 Sept 73.

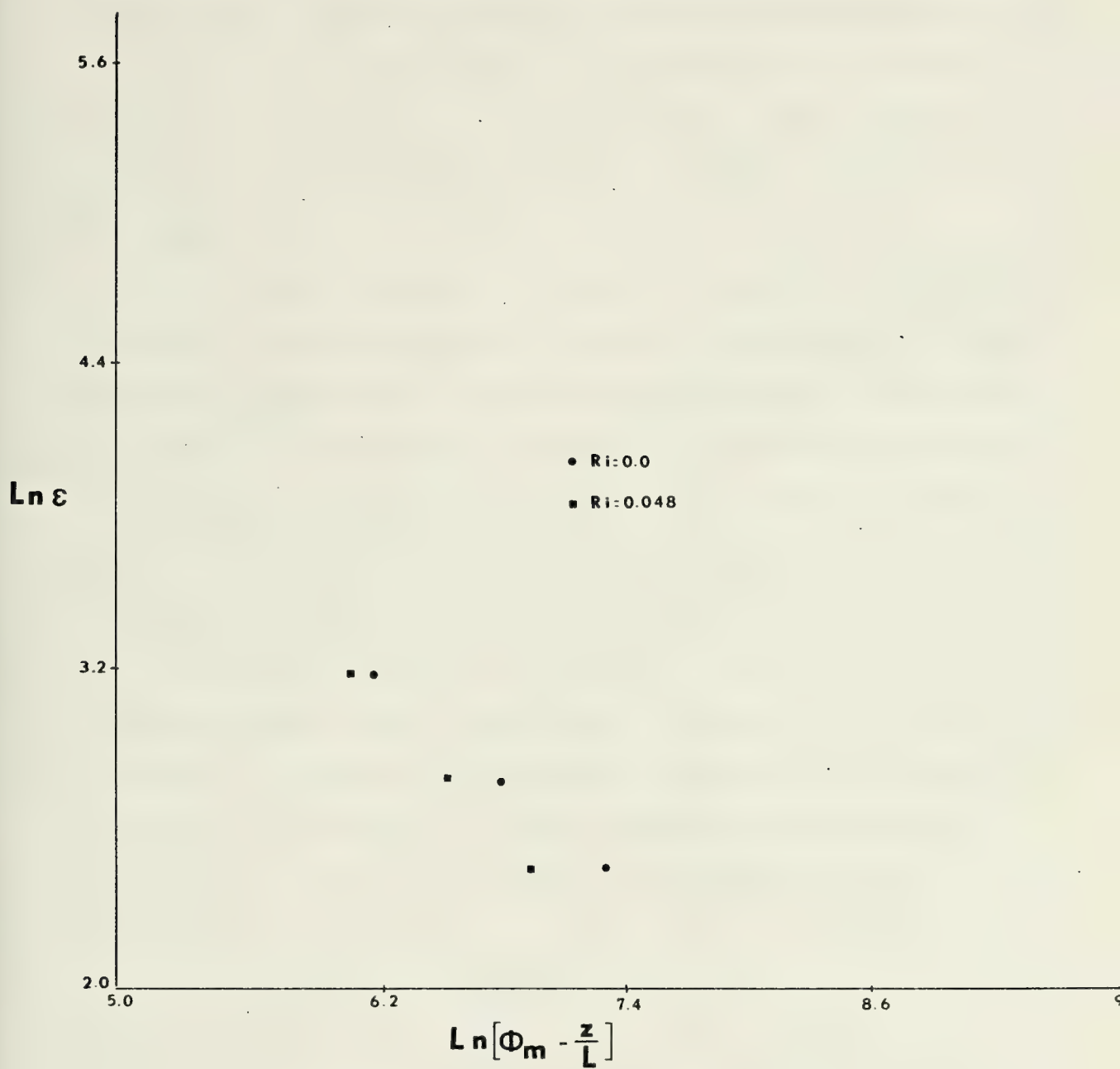


Figure 29. Effect of Stability Correction for 2023-2053
20 Sept 73.

The Monin-Obuhkov theory and the flux-profile relationships were also examined for the period with unstable stratification. Figure 30 shows the results of this examination. For $-0.05 \leq Ri \leq -0.15$ there is a tendency for adjustment toward the predicted -1 slope. However, further decreases in the Richardson number caused an unexpected reversal of the adjustment.

It is seen from Figure 30 that a value of -1.0 for the Richardson number results in a vertical variation of ε which deviates significantly from the predicted slope. The reason for this deviation can be explained by examining the function, $\phi_m \left(\frac{z}{L} - \frac{z}{L} \right)$. Figure 31, from Garratt (1972), shows a plot of this function using the expressions in Table XIV. To provide the correction necessary to obtain a -1 slope, $(\phi_m - \frac{z}{L})$ must decrease for decreasing values of $\frac{z}{L}$. It is apparent from Figure 31 that this criterion is not met. On the basis of these results there is some evidence that the expression $\phi_m (1 - 16 \frac{z}{L})^{-1/4}$ cannot provide the adjustment necessary to correct the plot for conditions of large instability.

The fact that the stability corrections did not completely restore the -1 slope, even in the stable case, leads to examinations of the possible effects of wind-wave coupling. Davidson and Frank (1971) observed wave-related velocity fluctuations and wave-related momentum transfer in spectral results obtained over natural waves. Davidson

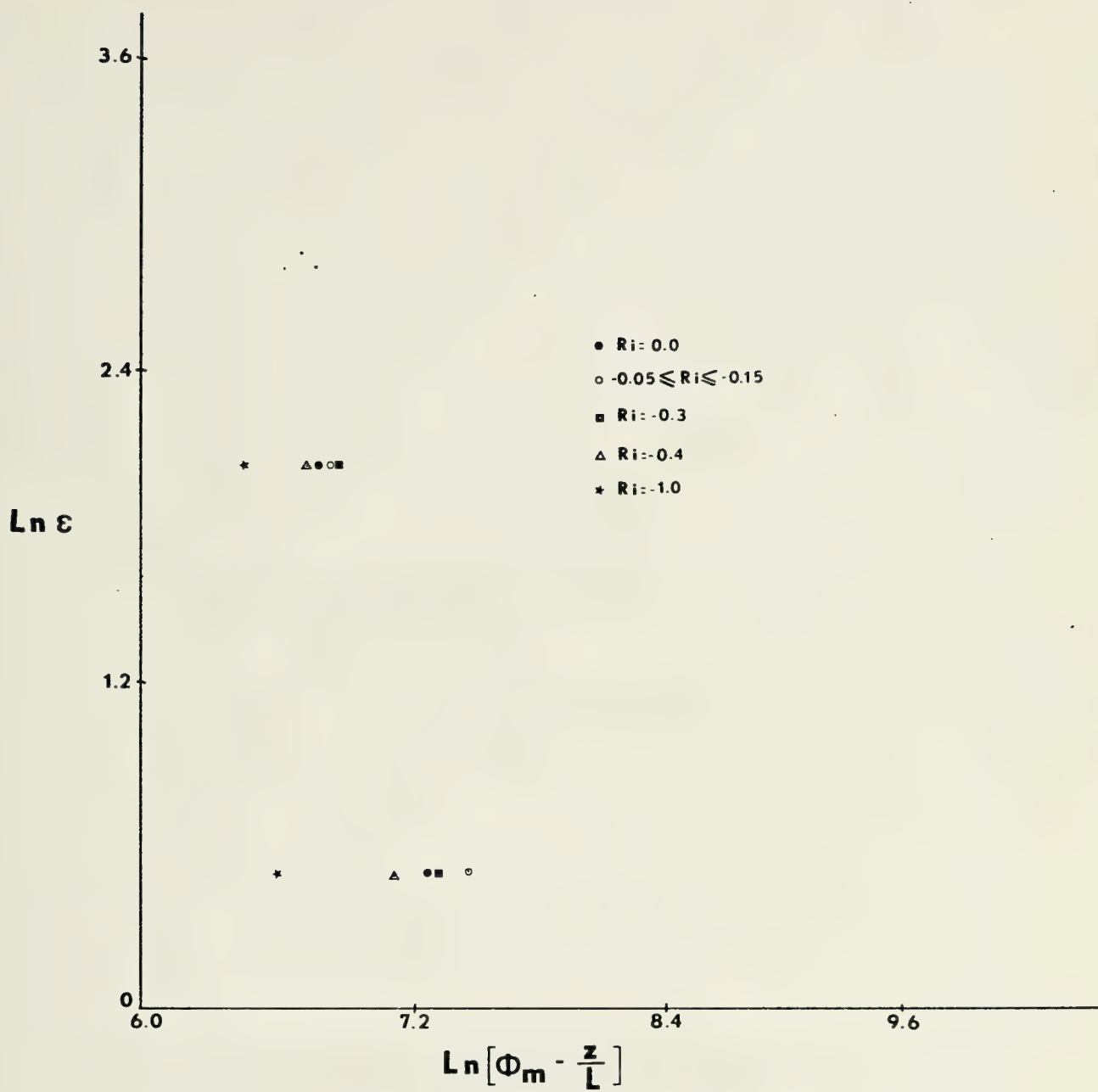


Figure 30. Effect of Stability Correction for 0637-0652
21 Sept 73.

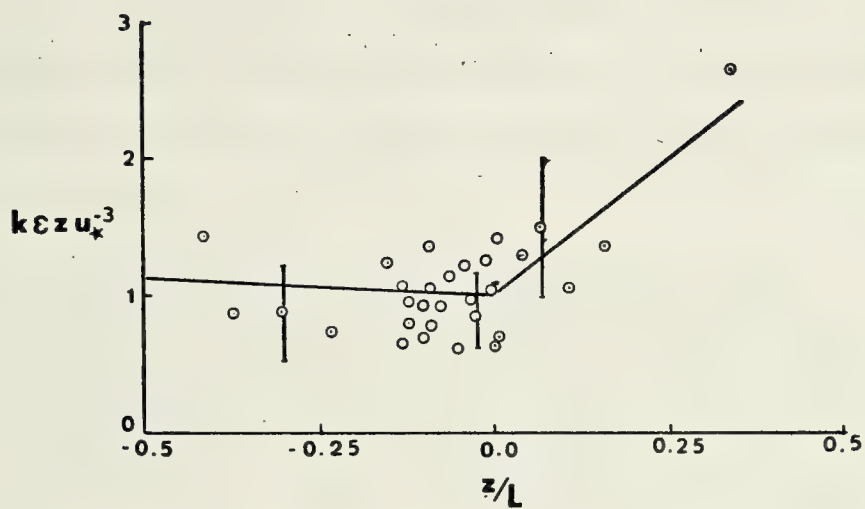


Figure 31. Non-dimensional Dissipation Rate as a Function of z/L (after Garratt).

(1974) described the influence of wind-wave coupling as having the same effect as would be due to the influence of stable stratification. The wave-related effect described by Davidson was a reduction in momentum transfer from that associated with neutral conditions. The results of the present study are consistent with Davidson's findings in that there is a decreased momentum transfer, u_* , as the surface is approached. If this were due to the influence of wind-wave coupling, it would yield the observed deviation from the neutral slope, shown in Figures 22 and 23.

F. VARIATION OF TEMPERATURE FLUCTUATIONS

Figure 32 represents the only temperature spectrum obtained from the five data periods which displayed the predicted $-5/3$ slope. Figure 33 is an example of the temperature spectra obtained from the majority of data runs. The paucity of temperature data precluded serious evaluations of the temperature fluctuation expressions.

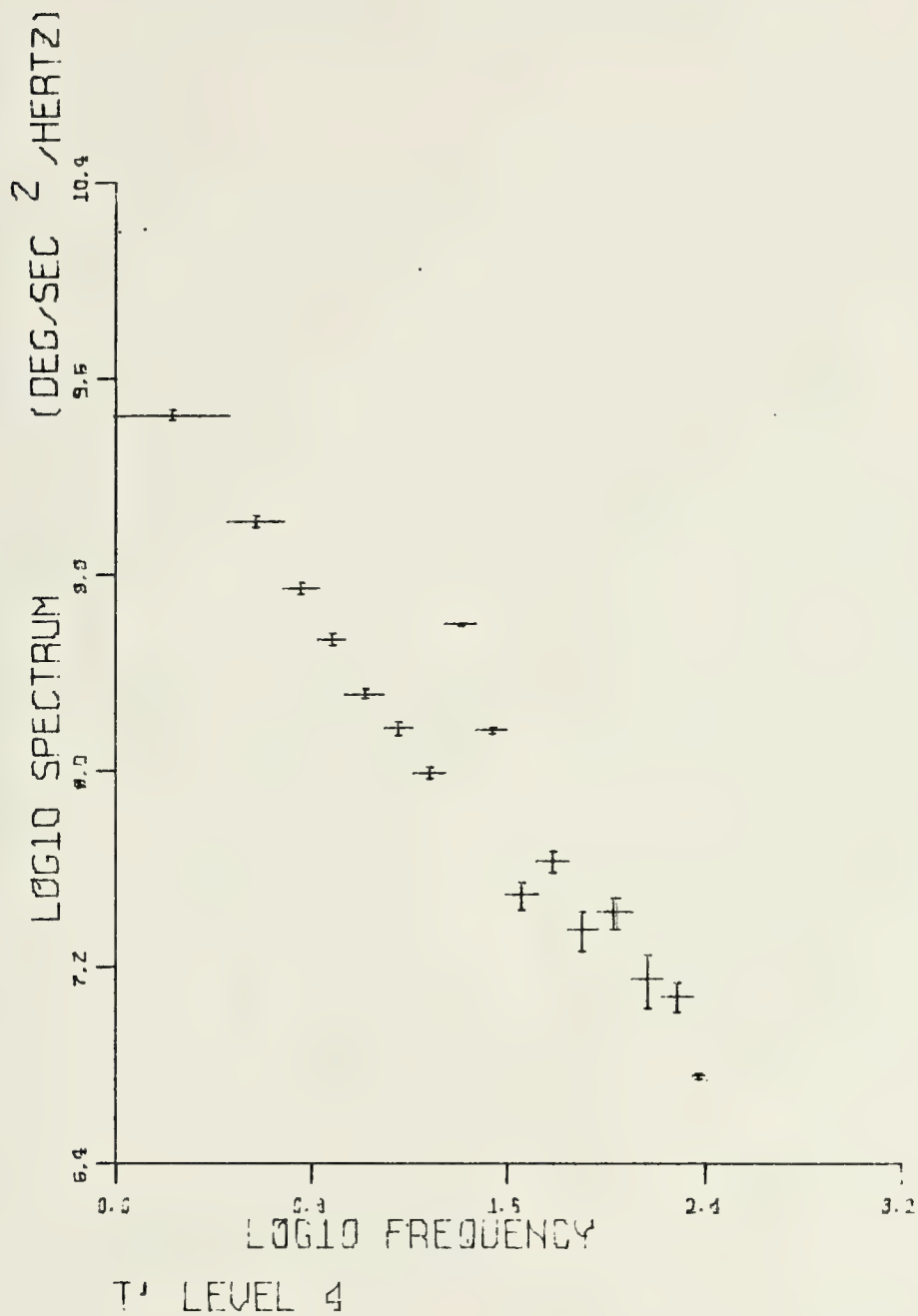


Figure 32. Ten Minute Temperature Spectrum for 2323-2341
20 Sept 73.

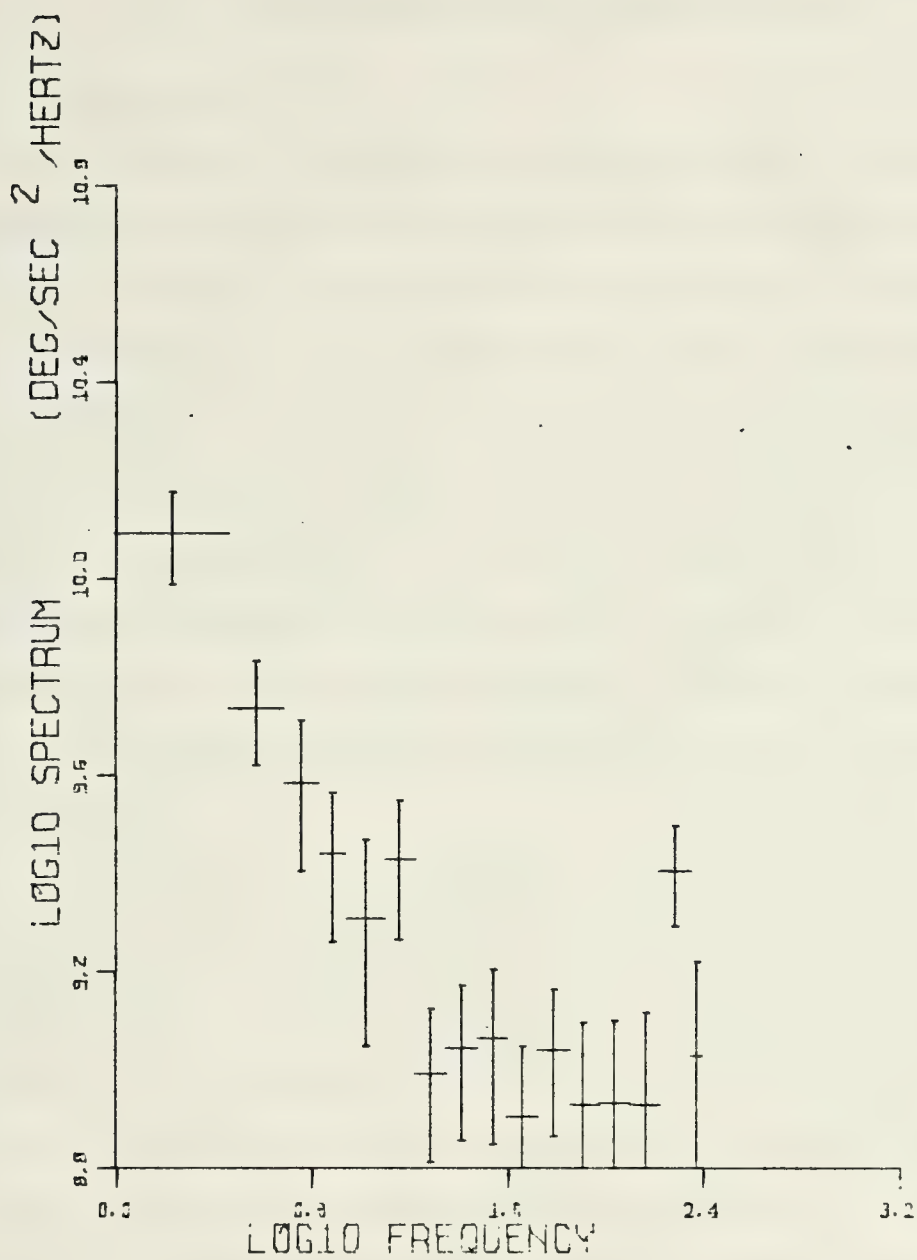


Figure 33. Ten Minute Temperature Spectrum for 2008-2018
20 Sept 73.

VI. CONCLUSIONS AND RECOMMENDATIONS

A. CONCLUSIONS

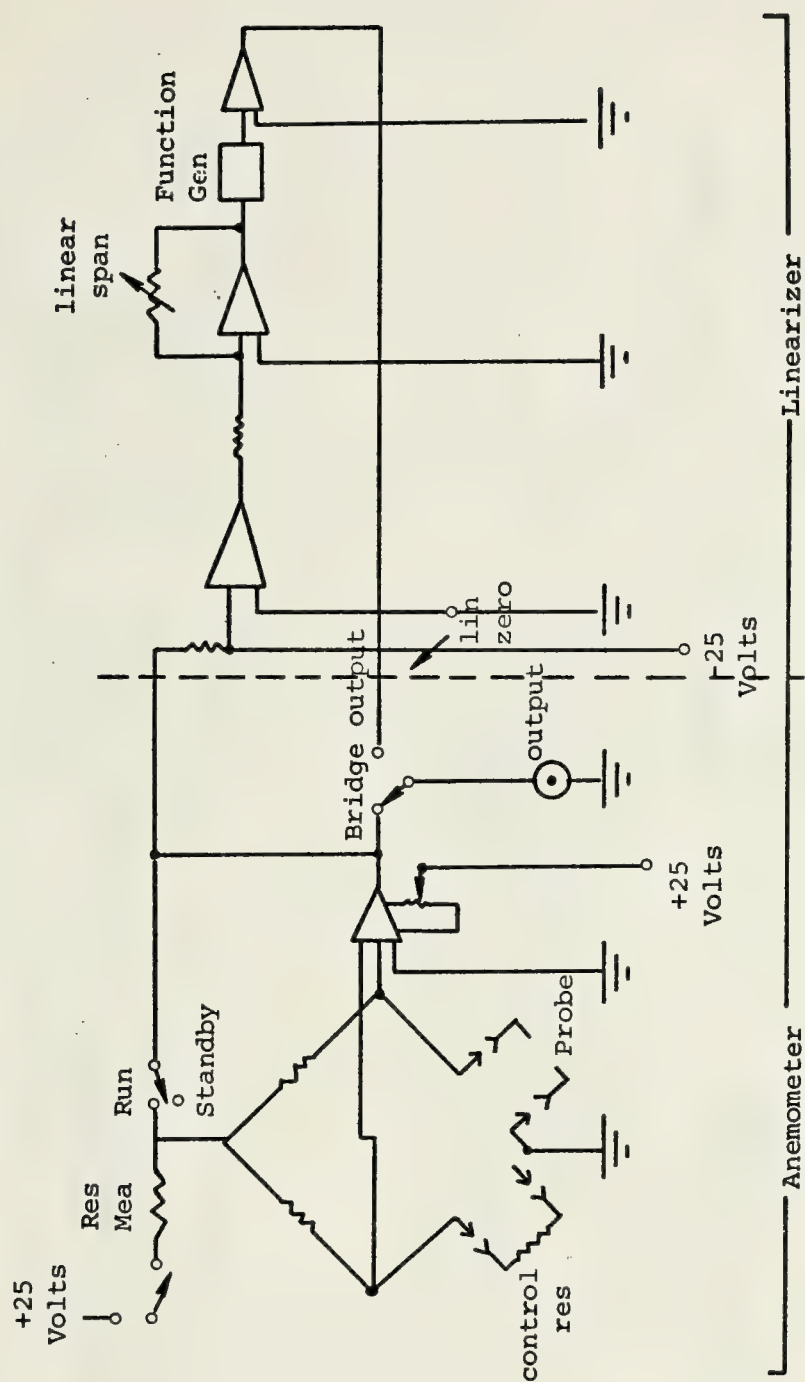
The results obtained from the one point spectral method are generally lower than those obtained by the intercept method. However, the simplicity of the one point spectral method would permit a more rapid determination of the dissipation and if a general estimate were all that was desired, this method would be acceptable. The results of the intercept method show excellent agreement among levels and with results from other studies. The longer time averages (~20 min.) appear to be necessary to avoid acceleration effects at the lower level.

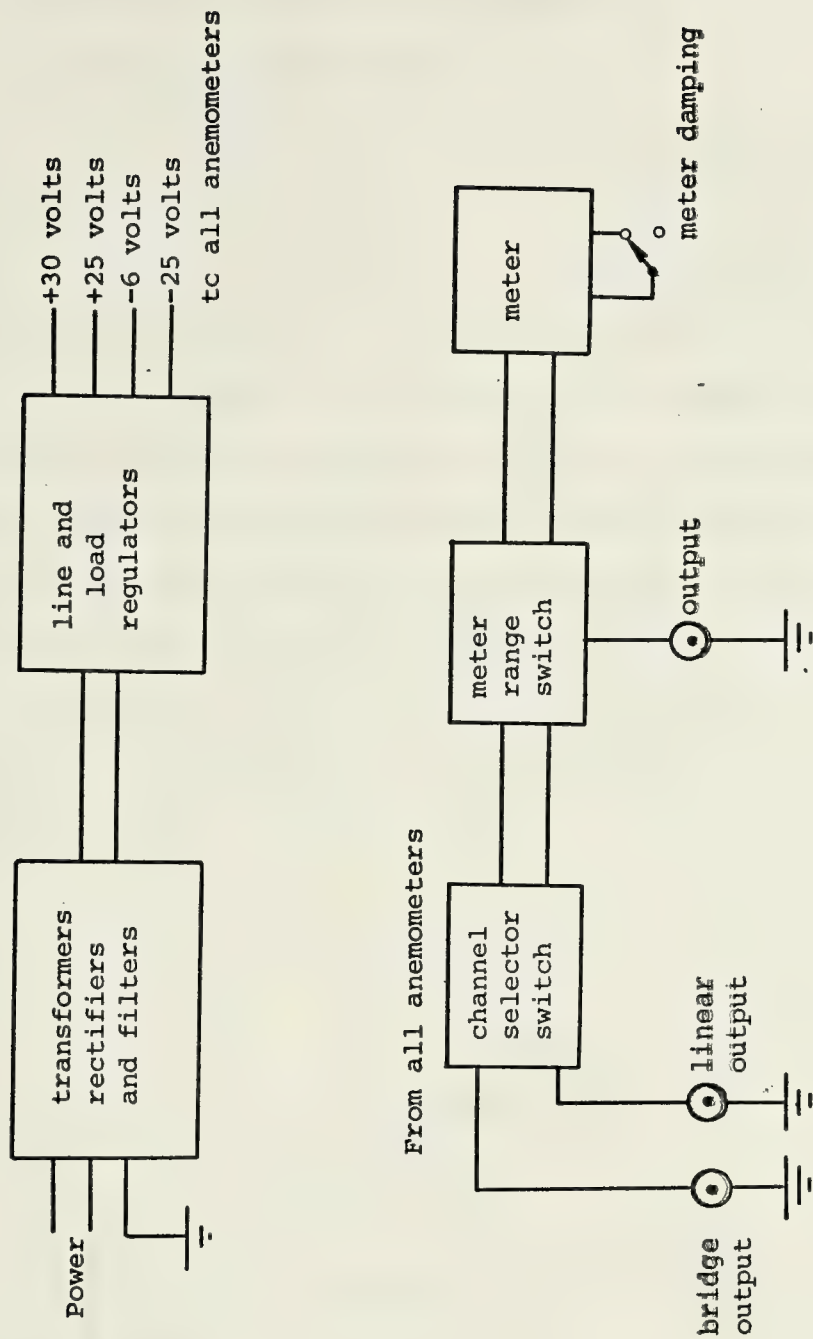
The close agreement between dissipation values derived from the spectral estimates and the inner scale calculations confirm the spectral estimates and also the choice of the constant, $\alpha = 0.48$. Results on the variation of ϵ with height also verified the formulations used in calculating the dissipation and flux. In addition, the sensitivity of the results to the varying conditions of hydrostatic stability and, perhaps, wind-wave coupling support the predictions proposed by Deacon and Davidson.

B. RECOMMENDATIONS FOR FUTURE EXPERIMENTS

It is strongly recommended that a real time spectrum analyzer be used in future observational experiments. In addition to the capability for instantaneous evaluation of spectral characteristics, the resulting spectral plots could be used for general estimates of the dissipation. If observational experiments are to be made on a more frequent basis, there is insufficient time to properly evaluate the data before the next experiment. The use of real time analysis techniques would preclude the need for digitization and tape manipulations and save valuable and costly computer time.

APPENDIX A





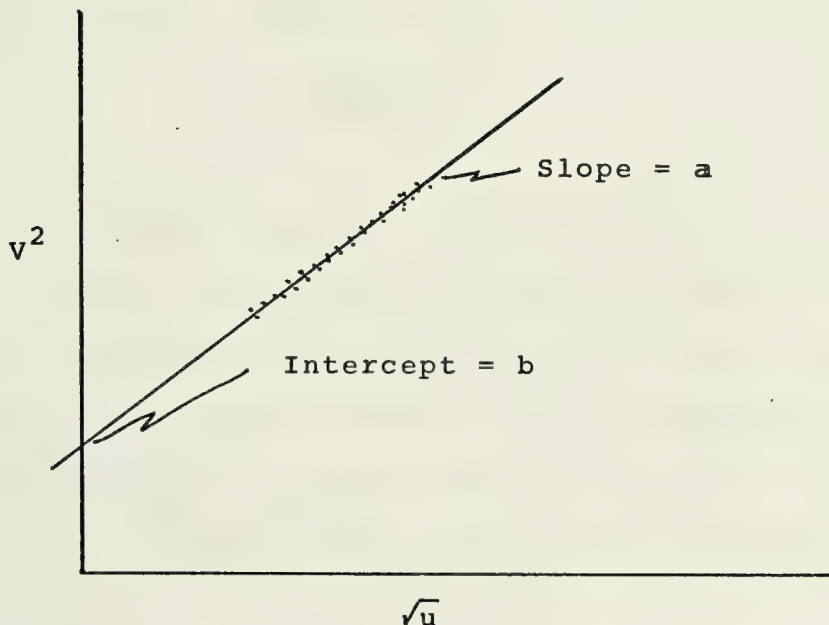
APPENDIX B

A. CALIBRATION AND SCALING PROCEDURES

1. Velocity Calibration

Calibration of the velocity sensors was accomplished using a manometer and a TSI Model 1125 Calibrator. The calibration procedure was to record voltage output versus manometer height over a certain range of velocities. The computer program included in this Appendix was utilized to generate the calibration curve for further use in establishing the calibration factor. This procedure was followed for each of the velocity systems and resulted in the calibration curves included in this Appendix.

The calibration curve obtained from this program resulted in a plot of V^2 versus \sqrt{u} where V is voltage and u is wind speed.



This curve describes a line

$$v^2 = a(u)^{1/2} + b \quad (1)$$

For use in data analysis it was necessary to obtain a scale such that

$$C \times e' = u'$$

where C = calibration factor; e' = voltage fluctuation and u' = velocity fluctuation. Differentiation of Equation (1) yields

$$2V dv = 1/2 au^{-1/2} du$$

or

$$\left[\frac{2 \times 2 V u^{1/2}}{a} \right] dv = du$$

or

$$\left[\frac{4Vu^{1/2}}{a} \right] e' = u'$$

The calibration factor is then

$$C = \left[\frac{4Vu^{1/2}}{a} \right]$$

where "C" scales between volts and cm/sec.

The procedures for actual calculation of this factor consisted of (1) obtaining the slope of the calibration curve (2) selecting a "u" value equal to that observed during the measurement period and (3) entering the curve with this "u" value to obtain the corresponding voltage.

2. Scaling Procedures for Estimation of Epsilon

In terms of the output of the spectral analyses programs the units associated with $f\phi(f)$ or $k\phi(k)$ were (volts)². An examination of Equation (1), Section II, shows that the units should be cm²/sec². Recalling that the calibration factor previously discussed scales between volts and cm/sec, it is necessary to multiply the ϵ value by

$$\left[\frac{(\text{cm}^2/\text{sec}^2)}{(\text{volts})^2} \right]^{3/2} = \left[\frac{\text{cm}/\text{sec}}{\text{volts}} \right]^3 = (C)^3$$

to obtain the value of ϵ in cm²/sec².

To obtain the correct value of ϵ it is also necessary to consider the gains used during the record and analog-to-digital conversion phases. In addition a scale factor is needed that scales between the analog voltage and the digital output. A 10 db gain was used when the raw signals were recorded and an additional 50 db gain was employed during the A-D process. The scaling between the voltage input and the corresponding digital output is obtained by considering that the maximum voltage input to the COMCOR Ci 5000 is 100 volts and this corresponds to a digital maximum of 2²³ on the XDX 9300.

The total gain and scaling for the observational data then becomes

$$V(\text{volts}) \times G1 \times G2 \times SC\left(\frac{\text{digital}}{\text{volts}}\right) = \text{Value obtained from IBM 360}$$

where V = signal from velocity unit

G_1 = amplification prior to record (10 db)

G_2 = amplification during A-D conversion (50 db)

SC = analog-to-digital scaling factor ($2^{23}/100$)

To obtain the value which corresponds to that which can be used with the calibration factor previously obtained

$$V = (\text{IBM 360 value} \times 1/SC \times 1/G_1 \times 1/G_2)$$

The final scaling then becomes

$$\left[[\text{Scale} \times \text{Gain}_1 \times \text{Gain}_2] \times C \right]^3$$

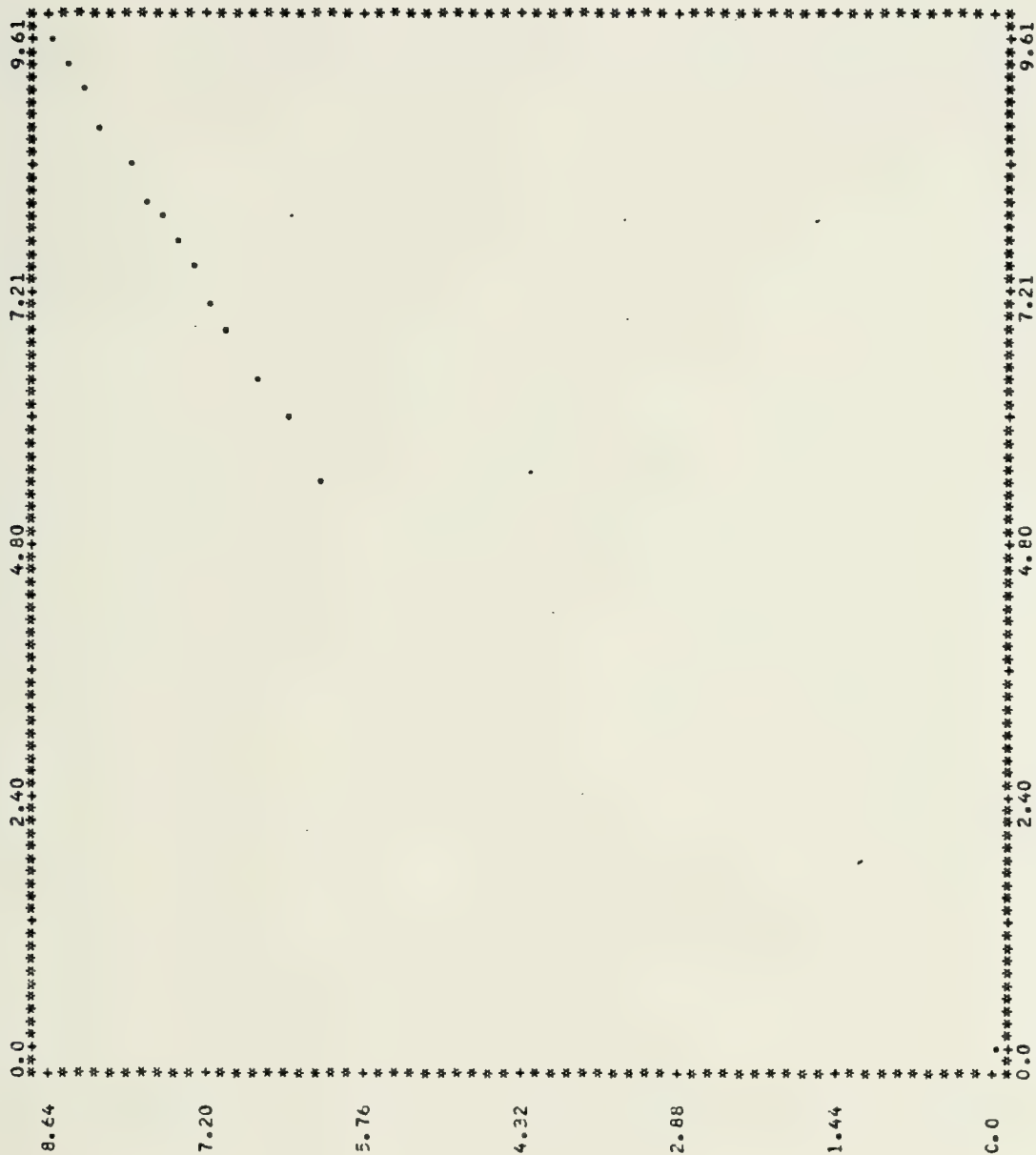
or in this instance

$$\left[[100/2^{23} \times 0.1 \times 0.02] \times C \right]^3$$


```

C*****
C*****
C*****
C***
C***
C*** THIS PROGRAM IS DESIGNED TO COMPUTE A CALIBRATION
C*** CONSTANT FOR USE IN THE SPECTRAL ANALYSES PACKAGE.
C*** THE INPUT PARAMETERS CONSIST OF THE MANOMETER HEIGHT
C*** AND THE CORRESPONDING VOLTAGE. THE PROGRAM WILL
C*** CALCULATE AND PRODUCE A PRINTER PLOT OF VOLTAGE
C*** VERSUS VELOCITY. A BEST FIT CURVE CAN THEN BE
C*** DRAWN THROUGH THE DATA POINTS TO OBTAIN THE
C*** CALIBRATION FACTOR.
C***
C***
C*** STATEMENT OF VARIABLES
C***
C*** H.....MANOMETER HEIGHT IN INCHES
C***
C*** V.....VOLTAGE
C***
C*** VSQRD.....VOLTAGE SQUARED(ORDINATE OF GRAPH)
C***
C*** U.....VELOCITY IN FEET PER SECOND
C***
C*** X.....SQUARE ROOT OF H
C***
C*** USQRT.....SQUARE ROOT OF U(ABCISSA OF GRAPG)
C***
C***
C*****
C*****
C*****
C*****
REAL*8 TITLE(10)
DIMENSION VSQRD(15),USQRT(15),U(15)
READ (5,20) TITLE
20 FORMAT (10A8)
WRITE (6,30)
30 FORMAT ('1',T9,'H',T18,'V',T28,'VSQRD',T39,'U',T47,'US
1QRT')
N=15
DO 60 I=1,N
READ (5,40) H,V
40 FORMAT (2F10.3)
X=SQRT(H)
VSQRD(I)=V**2
U(I)=65.3*X
USQRT(I)=SQRT(U(I))
WRITE (6,50) H,V,VSQRD(I),U(I),USQRT(I)
50 FORMAT ('0',5F10.3)
60 CONTINUE
WRITE (6,70)
70 FORMAT ('1')
CALL PLOTTP (USQRT,VSQRD,N,0)
WRITE (6,80) TITLE
80 FORMAT ('0',10A8)
STOP
END

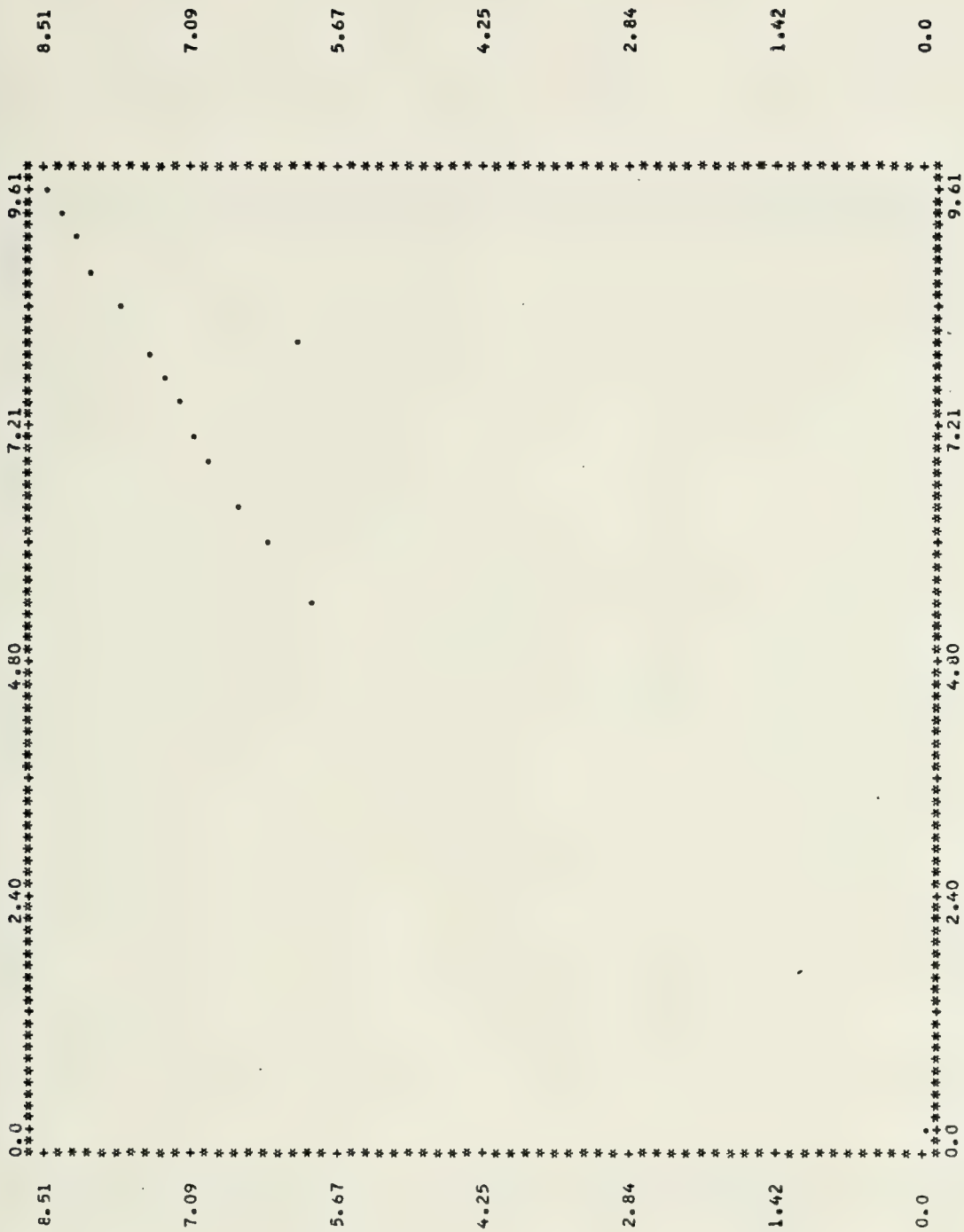
```

X-SCALE: "X"= 0.120E 00 UNITS

Y-SCALE: "Y"= 0.144E 00 UNITS

HOT WIRE PROBE NUMBER 18



X-SCALE: "X"= 0.120E 00 UNITS
Y-SCALE: "Y"= 0.142E 00 UNITS

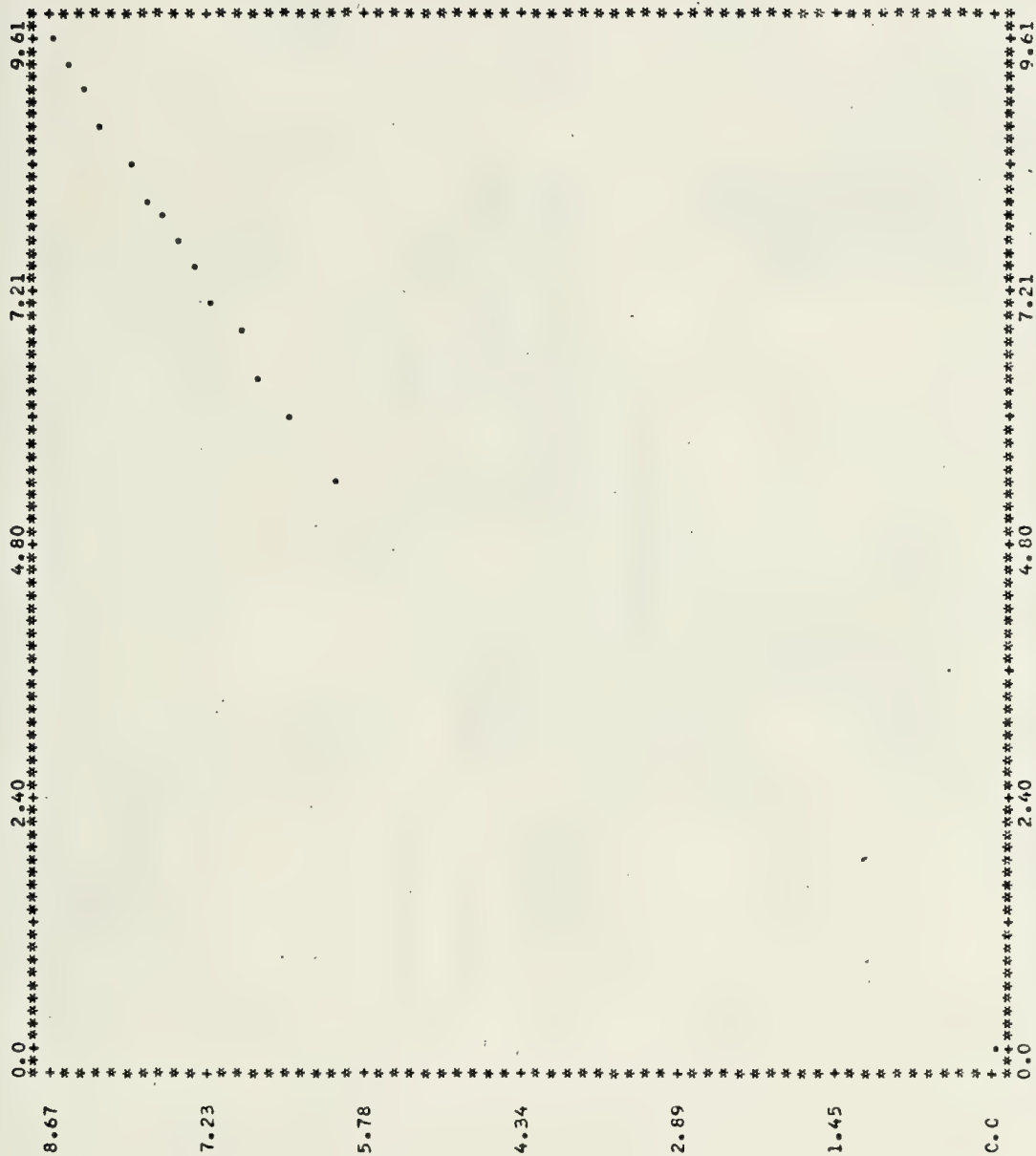
HOT WIRE PROBE NUMBER 38



X-SCALE: "*" = 0.120E 00 UNITS

Y-SCALE: "*" = 0.143E 00 UNITS

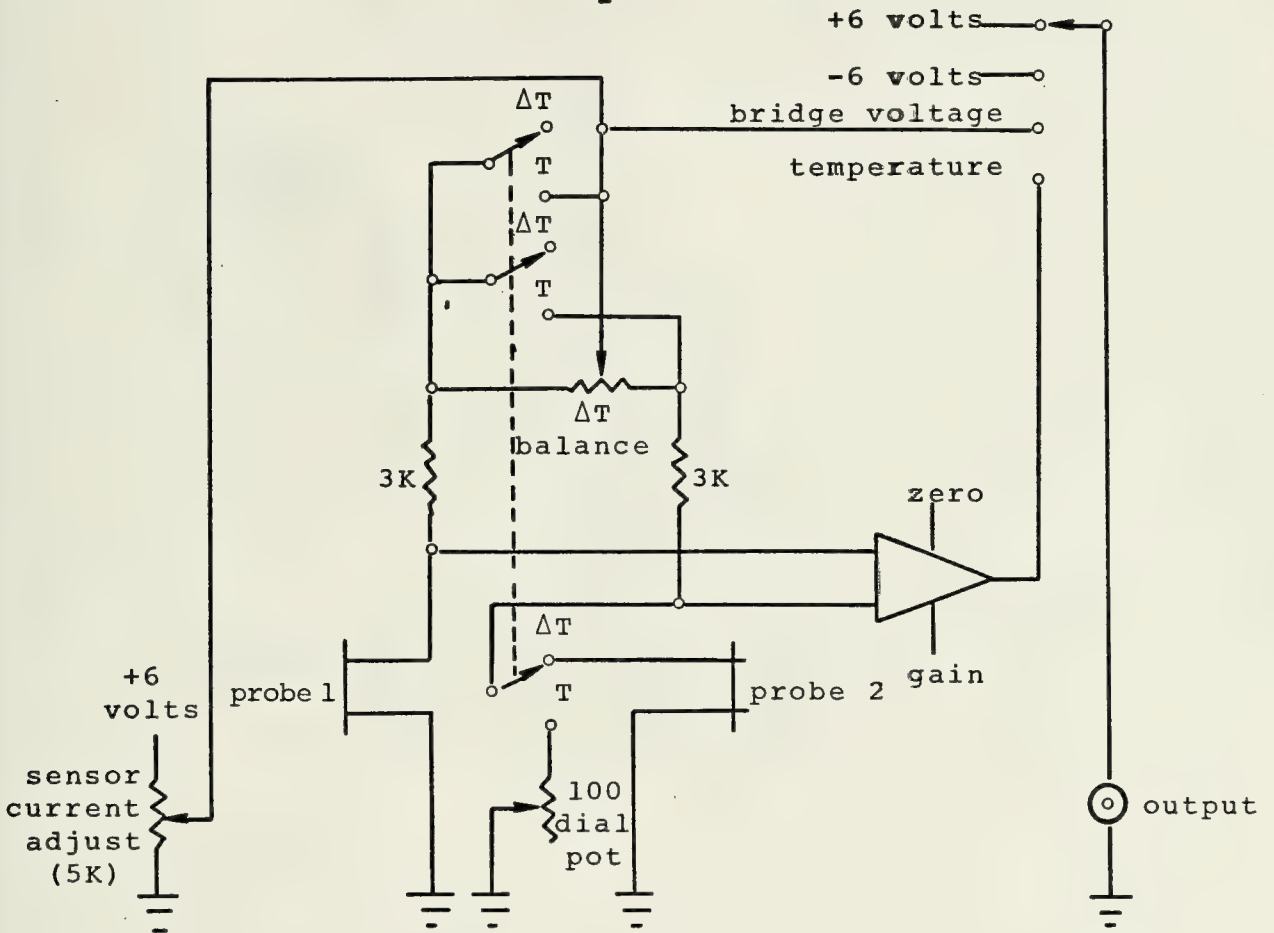
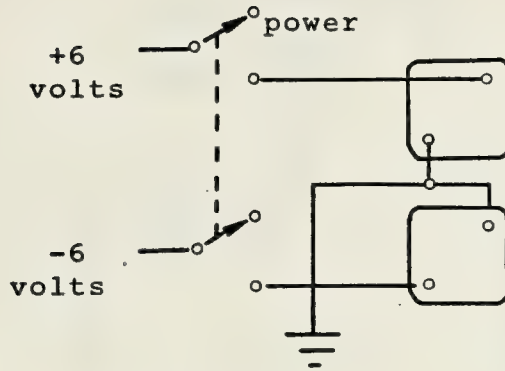
HOT WIRE PROBE NUMBER 28



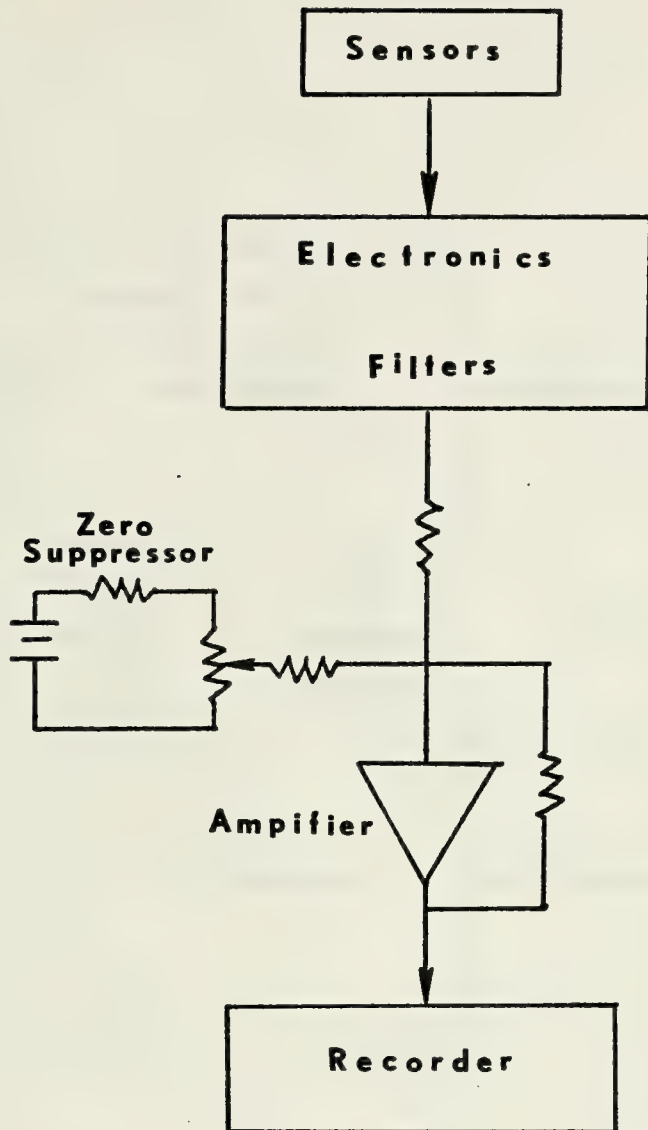
X-SCALE: "X"= 0.120E 00 UNITS
Y-SCALE: "Y"= 0.145E 00 UNITS

HDT WIPE PRIME NUMBER 4A

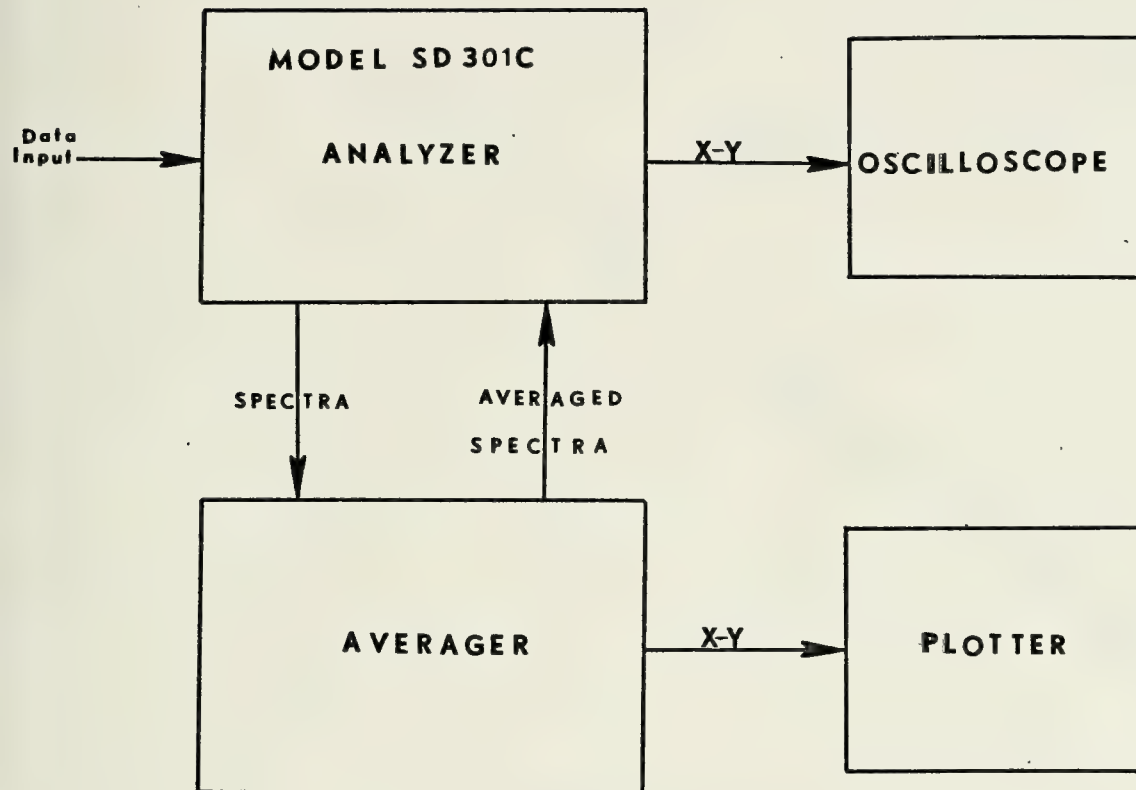
APPENDIX C



APPENDIX D



APPENDIX E



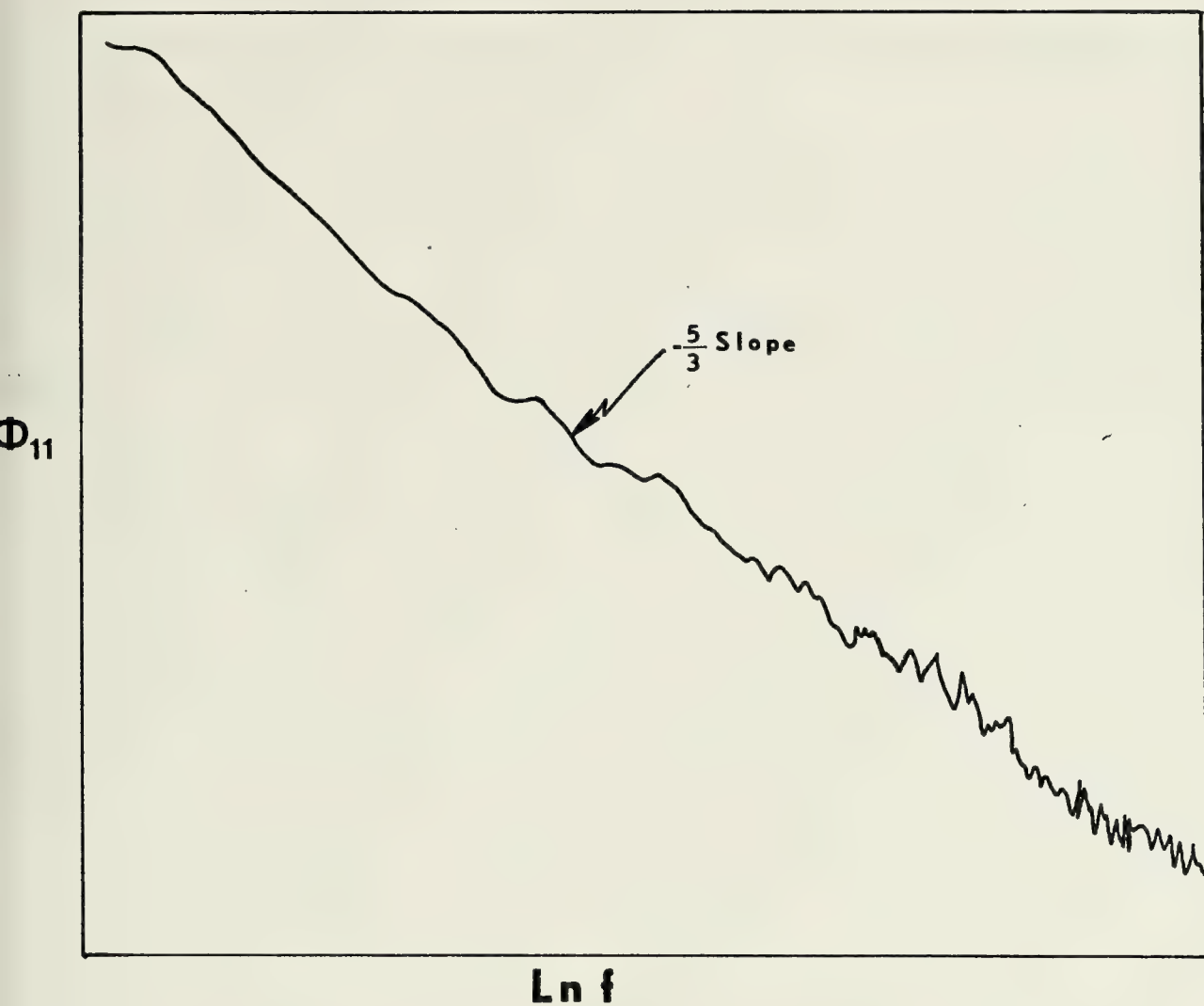


Figure E1. Real Time Spectral Analysis of Velocity Signal for 2008-2018 20 Sept 73.

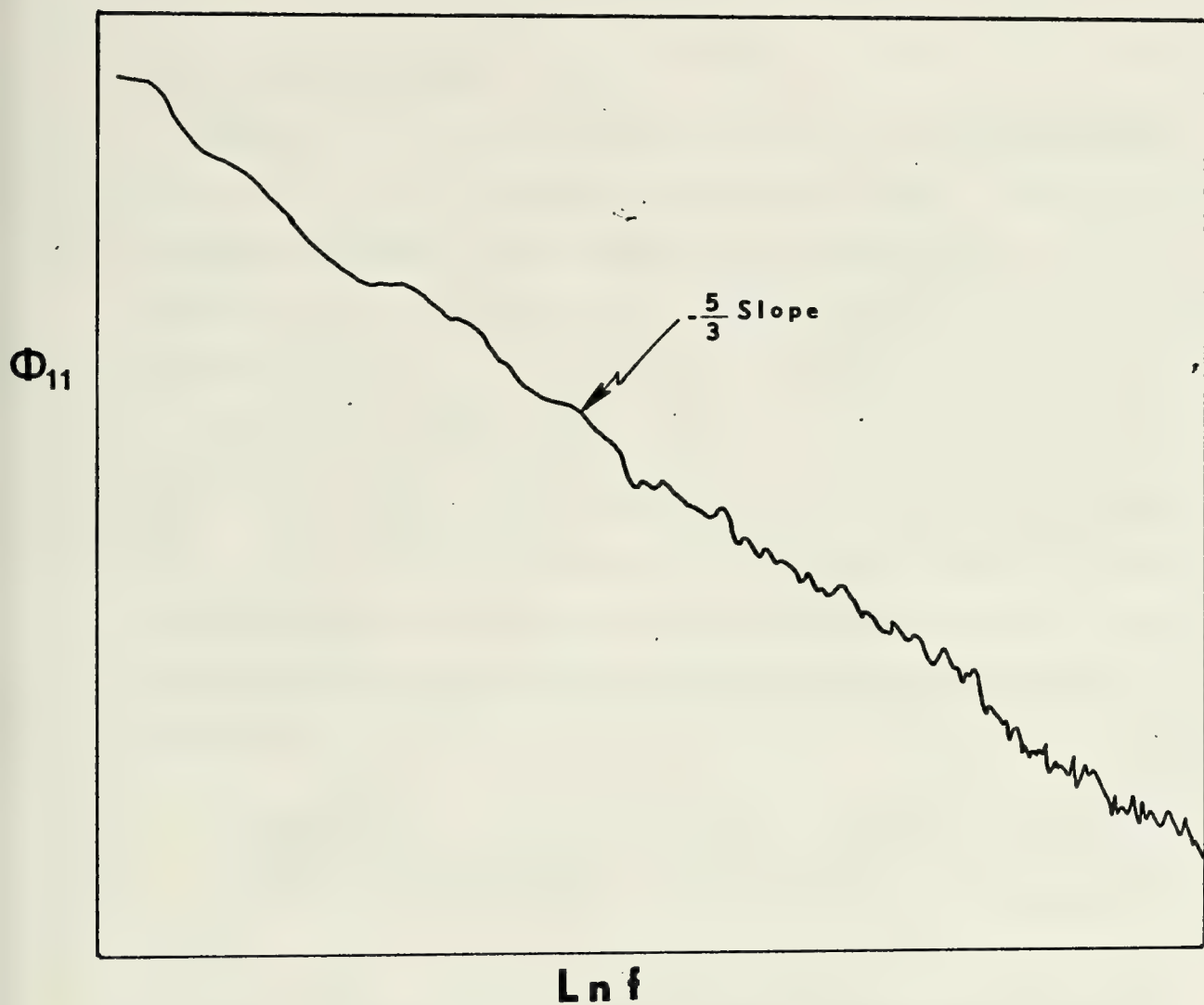


Figure E2. Real Time Spectral Analysis of Velocity Signal for 2023-2057 20 Sept 73.

APPENDIX F

A. TAPEOUT PROGRAM

TAPEOUT is a general purpose program used to determine the label and file contents of magnetic tapes. The program can take an otherwise unreadable tape and provide the user with sufficient information to permit access to the tape. TAPEOUT will print a file number, density, parity, length in bytes of the record and a dump of the record. In this study the two key outputs were the record length and record dump. These outputs permitted the user to obtain the block-size and ascertain the location of erroneous records. The following is an example of the TAPEOUT deck set-up used in this study.

```
//JOHNSTON JOB (2413,0392,XM24), 'JOHNSTON SMC 2561'  
//EXEC TAPEOUT, PARM='2.0,,2'  
//TAPEIN DD UNIT=2400-1,LABEL=(,BLP), VOL=SER=KARLYN  
/*
```

TAPEOUT is part of the IBM 360/67 subroutine library and a discussion of the parameters (PARM=) is available in the computer center consultant's office and also in Computer Center Technical Note No. 0211-08.

B. CONVERT PROGRAM

The seven-track octal tape is converted into nine-track hexadecimal data samples using the CONVERT program. The block characteristics of the data samples are still

maintained on the nine-track tape but two additional parameters are affixed to each block. These two parameters, NCHAN and KMAX, are affixed to the beginning of each block. NCHAN is the number of channels of analog data digitized on the seven-track tape. KMAX is a numerical value set equal to the maximum number of samples per block. The insertion of these numerical parameters at the beginning of each block and the change in the block format by the FORM subroutine will put the seven-track tape in the proper format for use in the UBCFTOR program. The CONVERT program used in this study along with sample JCL cards is given below.

```
//JOHNSTON JOB (2413,0392,XM24),'JOHNSTON SMC 2561'
//CONVERT EXEC FORTCLG,REGION.GO=100K
//FORT.SYSIN DD
    DIMENSION IDAT(1024), DAT(1024)
    FACTOR = 1.
    REWIND 2
    REWIND 4
    NCHAN = 8
    NRECL = 1024
    J = 0
10 READ (2,20,END=60,ERR=40) IDAT
20 FORMAT (20(50A4),24A4)
    J=J+1
    CALL FORM(IDAT,NRECL)
    DO 30 I=1,NRECL
    WRITE (4) NRECL,NCHAN,DAT
    GO TO 10
40 WRITE (6,50) J
50 FORMAT ('0',5X,'READ ERROR,RECORD NO.=' ,I4)
    GO TO 10
60 WRITE (6,70) J
70 FORMAT ('0',5X,'END OF TAPE,RECORD NO.=' ,I4)
    END FILE 4
    RETURN
    END
```

/*


```
//GO.FT02F001 DD UNIT=2400-1, VOL=SER=KARLYN,LABEL=(,NL),
//  DISP=OLD,DCB=(DEN=2,RECFM=VS,BLKSIZE=8192)
//GO.FT04F001 DD UNIT=2400, VOL=SER=NPS170, DSNAME=DEREK,
//  LABEL=(1,SL),DISP=(NEW,KEEP),DCB=(DEN=2,RECFM=VS,
//  BLKSIZE=8200)
```

It is noted that the user inputs to the program consist of the dimension of the arrays IDAT and DAT and the value of NRECL. IDAT and DAT should be dimensioned at least NSAMP x NCHAN thus signifying the need for recording the digitizing parameters. The argument NRECL must be assigned a value equal to NSAMP x NCHAN. The value of the scaling factor has been set equal to one in this study since it was found to be easier to perform all calibrations and scalings in one step following the use of the spectral analysis programs. Computer Center Technical Note No. 0211-08 provides additional information concerning the CONVERT program.

C. DIGITAL TAPE OPERATIONS

Unlike the Hybrid computer system, where all tape manipulations were performed by the user with technical assistance from the computer facility staff, the IBM 360 computer system manipulations were performed by the staff members. In order to have the tapes handled as desired, explicit instructions had to be given. These instructions were given in two ways. The first instruction consisted of a Job Request Form addressed to the computer center staff identifying the tapes to be utilized and whether they were to be read off of (RINGOUT) or written on (RINGIN). The second

instructional procedure was conducted using job control language (JCL) addressed to the computer and read as part of the submitted program.

1. Job Control Language

Job control language cards provide information to the computer about tape identification, tape disposition, tape data files, tape mount numbers and data format. The cards are appended to the program and read through the "hot card reader" as part of the program, whereas the Job Request Form is submitted "over the counter" to the computer center personnel. An example of a JCL card for tape processing would be:

```
//GO.FT08F001 DD UNIT=2400-1,VOL=SER=KARLYN,LABEL=(1,SL),  
//    DSNAME=DEREK,DISP=(NEW,KEEP), DCB=(DEN=2,RECFM=VS,  
//    BLKSIZE=8192)
```

While the majority of the JCL card remains unchanged, there are portions which are subject to change from tape to tape. These portions are discussed below.

FT08 - This group indicates the tape mount on which the tape is to be placed. The two digit number (08 in this case) must match the number provided in the program's "READ" or "WRITE" statement.

F001 - This group indicates the sequential number of passes through the tape which has occurred up to this point. In this case it is the first pass.

UNIT=2400-1 - This group specifies the tape as a seven-track tape. The nine-track designation is 2400.

VOL=SER=KARLYN - This group identifies the tape to be processed. In this case the name "KARLYN" signifies the tape is an "external" tape with the name "KARLYN" physically appearing on the tape. An "internal" tape would have a serial number such as NPS2111. These tapes are kept on file in the computer center and cannot be physically removed from the facility.

LABEL=(1,SL) - This group identifies the tape file to be processed and specifies that the tape has a standard label. "External" tapes may be processed as no label tapes (NL) but "internal" tapes will be given a standard label before the user gains access to them. This is accomplished by the computer center staff processing a "canned" program which places a standard label on the serialized tape.

DSNAME=DEREK - This group specifies the data set name (DSNAME) applicable to the specified LABEL group. The data set name may be a unique name limited to six alphanumeric characters. Once a file has been given a data set name access to the data file can only be obtained if this same DSNAME is used. This process can be circumvented by the use of by-pass label processing (BLP) but does provide protection against accidental erasures.

DISP=(NEW,KEEP) - This group specifies the tape disposition once it has been processed.

DCB=(DEN=2,RECFM=VS,BLKSIZE=8192) - This group is referred to as the data control block. The density (DEN=2),

tape record format (RECFM=VS) and block size (BLKSIZE=8192) are stipulated using this group. The density specifies the number of bytes per inch, in this case the number 2 denotes 556 bytes per inch. This corresponds to a manual setting of the DENSITY dial on the face of the seven-track tape unit. RECFM=VS specifies that the record format is variable spaced, the result of recording and digitizing on the seven track unit. The block size specifies the number of bytes per block of data. If 2048 words per block were used, four bytes per word would result in 8192 bytes per block.

APPENDIX G

A. GENERAL

All the UBC time series analysis programs (FTOR, SCOR, FC PLOT) were originally listed on faculty tape NPS216, file 1-3 respectively. The programs have since been placed on computer center disk, MARY, and are stored in machine language which disallows a listing of the program for user study. However, source decks for UBCFTOR and UBCSCOR have been retained by Dr. Kenneth Davidson of the Meteorology Department and by Dr. Noel Boston of the Oceanography Department. These source decks can be used to obtain a listing of the programs for individual study. The most recent computer center documentation on the use of the time series analysis package is given in the following memorandum written by Miss Sharon Raney of the computer center staff. This memorandum provides the information and JCL necessary for utilization of the disk-stored analysis programs.

B. FTOR

The preamble to the FTOR program is given following this discussion. It provides the user with the information needed to prepare the input data cards necessary for program execution. One of the most misleading parameters called for in the input values is the variable NBLOCK.

This value is provided by the user on the second data card with the value supposedly entered in columns 4-5. In actuality the value is read as a five digit integer thereby making the maximum value of NBLOCK 99999 vice 99 as implied by the program preface.

An important consideration involves the value of the variable MPRINT. This variable controls the computer printout of the FTOR program. If the user desires to suppress the printout the insertion of a specific value can save considerable paper and cut computer time significantly. In the unsuppressed mode, the output will follow the format shown in Figure 13, Section IV. The suppressed output will consist of one line outputs for each data block which will inform the user that "coefficients for block ____ have been written on the file ____ of the output tape." By using the suppressed output, computer turn-around time was significantly reduced.

C. SCOR

The preamble to the SCOR program also provides the user with the information necessary to compile the data input cards. The SCOR program requires the input of several variables whose values are determined during the A-D conversion process. One of the values on the first data card is the number of data blocks on which the spectral analysis will be performed. This value is set by the user and cannot exceed the number of data blocks processed by the FTOR

program. As was the case in the FTOR program the maximum number of blocks which can be handled is 99999 and not 99 as the preface would lead the user to believe.

As was discussed earlier in this thesis the output of the SCOR program consists of a computer printout and a graphic plot. The graphic plot consists of an output in which spectral density is plotted against frequency for all channels being processed. Since the original formulation of the SCOR program, the computer facility at the Naval Postgraduate School has installed a new plotting routine called NEWPLOT. This routine limits the user to 30 inches of plotting paper. The author found it necessary to submit a job request asking that plotting routine CALPLOT be used to prevent early termination of spectral plots consisting of four or more channels. The computer center staff has been alerted to this problem and any future user should consult with a staff member before using the SCOR program.

8 June 1973

MEMORANDUM

From: Sharon D. Raney

To: Users of UBC Time Series Analysis Package

Subj: New Operating Instructions for UBC Time Series Analysis Package

1. The new FTOR deck setup is given in Figure 1.

The dimension size of array DATA must correspond to the block size of the data on the input tape. This tape is generally the data as converted from the seven track XDS generated tape to the nine track IBM/360 tape.

Formerly, this array was dimensioned in subroutine OCEAN2 and had to be changed whenever the sample size changed. This meant the entire source deck for FTOR had to be used for each run.

FTOR is now compiled in FORTRAN IV (H) which generates a more efficient code and consequently speeds up execution time.

2. When the same dimension size is to be used repeatedly, Figure 2 shows how to obtain an object deck and how to execute FTOR with the object deck.
3. Figure 3 shows the deck setup for SCOR.
4. Notice the change in the format of the Job Control Language (JCL) to define the tape files. These changes enable more efficient processing by the operator. Note the use of the IN parameter in the LABEL parameter. This must be specified when the file is to be read only. OUT is used when the file is to be written only. All data sets are PASSED not KEEP. The UNIT-AFF is used on subsequent files of a tape as is the VOL=REF.
5. Any questions concerning these new operating instructions should be directed to Sharon Raney at X2631 or Ingersoll Hall Room 107.


```

//FTOR EXEC FORTHCD,REGION.FORT=150K
//FORT.SYSIN DD *
        DIMENSION DATA(3072)
        CALL FTOR(DATA)
        RETURN
        END

//FTOR EXEC LGO,REGION.GO=175K
//LINK.SYSLIB DD
//
//      DD
//      DD DSNNAME=F1178.TSLIB,UNIT=2314,VOL=SER=MARY,DISP=SHR
//LINK.SYSIN DD *

                                OBJECT DECK PUNCHED IN ABOVE JOB GOES HERE - MAKE SURE
                                THERE ARE NO BLANK CARDS ON FRONT OR BACK OF THIS DECK

//GO.FT08F001 DD UNIT=2400,VOL=SER=NPS290,DISP=(OLD,PASS),
//      DSN=DEREK,DCB=(DEN=2,RECFM=VS,BLKSIZE=6152),LABEL=(1,SL,IN)
//GO.FT08F002 DD UNIT=AFF=FT08F001,VOL=REF=*.GO.FT08F001,DSN=DEREK,
//      DISP=(OLD,PASS),LABEL=(2,SL,IN),DCB=(DEN=2,RECFM=VS,BLKSIZE=6152)
//GO.FT08F003 DD UNIT=AFF=FT08F001,VOL=REF=*.GO.FT08F001,DSN=DEREK,
//      DISP=(OLD,PASS),LABEL=(3,SL,IN),DCB=(DEN=2,RECFM=VS,BLKSIZE=6152)
//GO.FT03F001 DD UNIT=2400,VOL=SER=NP S133,DISP=(NEW,PASS),
//      DSN=COEFQ1,DCB=(DEN=2,RECFM=VS,BLKSIZE=12300),LABEL=(1,SL,OUT)
//GO.FT03F002 DD UNIT=AFF=FT03F001,VOL=REF=*.GO.FT03F001,DSN=COEFQ1,

```

Figure G2.


```
// DISP=(NEW,PASS),LABEL=(2,SL,,OUT),DCB=(DEN=2,RECFM=VS,BLKSIZE=12300)
//GO.FT C3F003 DD UNIT=AFF=FT03F001,VOL=REF=*.GO.FT03F001,DSN=COEFQ1,
// DISP=(NEW,PASS),LABEL=(3,SL,,OUT),DCB=(DEN=2,RECFM=VS,BLKSIZE=12300)
//GO.SYSIN DD *
```

FTOR DATA CARDS GO HERE


```

// EXEC PGM=UBCSCOR,REGION=150K
//STEPLIB DD UNIT=2314,VOL=SER=MARY,DSNAME=F1178.TSLIB,DISP=SHR
//FT06F001 DD SYSOUT=A
//SYSPLCT DD SYSOUT=B
//SYSPLOTS DD UNIT=SYSDA,SPACE=(TRK,(2,6))
//FT03F001 DD UNIT=2400,VOL=SER=NPS133,DISP=(OLD,PASS),
// LABEL=(1,SL,,IN),DSN=COEFQ1,DCB=(DEN=2,RECFM=VS,BLKSIZE=12300)
//FT03F002 DD UNIT=AFF=FT03F001,VOL=REF=*.FT03F001,DISP=(OLD,PASS),
// LABEL=(2,SL,,IN),DSN=COEFQ1,DCB=(DEN=2,RECFM=VS,BLKSIZE=12300)
//FT03F003 DD UNIT=AFF=FT03F001,VOL=REF=*.FT03F001,DISP=(OLD,PASS),
// LABEL=(3,SL,,IN),DSN=COEFQ1,DCB=(DEN=2,RECFM=VS,BLKSIZE=12300)
//FTC5F001 DD *

```

SCOR DATA CARDS GO HERE

Figure G3.

FOURIER TRANSFORM OF TIME SERIES DATA SUPPLIED THROUGH
'OCEAN' SUBROUTINES USING P-K FORT FAST FOURIER TRANSFORM
SUBROUTINE (SHARE SDA3465) IN THE IBM SYSTEM 360 MODEL 67.

LAST REVISION JANUARY 24,1969

JOHN GARRETT

NBLOCK BLOCKS OF 2**NPOW SAMPLES EACH ARE READ FOR KCHAN OF THE
NCHAN CHANNELS AVAILABLE TO THE 'OCEAN' SUBROUTINES. THE CONTENTS OF
ANY CHANNEL MAY BE REPLACED BY A LINEAR COMBINATION OF ITSELF WITH ANY
OTHER CHANNEL.

FOR EACH BLOCK 2** (NPOW-1) COMPLEX FOURIER COEFFICIENTS ARE
COMPUTED FOR EACH OF THE KCHAN CHANNELS. THESE ARE THEN WRITTEN ON THE
OUTPUT (TAPE) 03 IN THE FORMAT DESCRIBED BELOW. IN ADDITION THE
COEFFICIENTS MAY BE SUMMED IN GROUPS OF (2** (NPCW-1))/32 AND
PRINTED OUT.

ADDITIONAL OPTIONS ARE DESCRIBED UNDER THE RELEVANT CONTROL
PARAMETERS BELOW.

IT SHOULD BE NOTED THAT THE COEFFICIENTS PRODUCED ARE THOSE OF THE
FOURIER SERIES

$$Y(J) = \sum_{K=0}^{N/2} \text{OVER } K = 0, N/2 \text{ OF REAL PARTS OF}$$
$$(C(K) * \exp((2 * \pi * I / N) * J * K))$$

WITH $J = 0, N-1, Y(J) \text{ REAL, AND } I = \text{SQRT}(-1)$

THE FOLLOWING SUBROUTINES ARE REQUIRED

OCEAN1, OCEAN2, OCEAN3, RWUNLD
SKPFL
CONVOL
USCRMB
P-K FORT

THE FOLLOWING LOGICAL INPUT/OUTPUT DEVICES ARE USED IN THIS PROGRAM
2 = SCRATCH TAPE FOR TEMPORARY STORAGE OF COEFFICIENTS IF

3 = OUTPUT (TAPE) FOR COEFFICIENTS
5 = (CARD) INPUT FOR CONTROL PARAMETERS
6 = PRINTED OUTPUT
INUNIT = INPUT TAPE OF TIME SERIES DATA FOR 'OCEAN' SUBROUTINES

INPUT INFORMATION REQUIRED

***IMPORTANT NOTE. READ THE COMMENT CARDS IN THE OCEAN
SUB-ROUTINE. SOME FACTORS WILL HAVE TO BE CHANGED TO FIT BLKSIZE.
FIRST DATA CARD IN COLUMN NUMBER
1-9 IDUSER = USER IDENTIFICATION NUMBER (9-DIGIT INTEGER)
14-15 NCHAN = NUMBER OF CHANNELS DIGITIZED ON OCEAN TAPE
25 NTYPE = (NOT RELEVANT. SET TO ZERO.)


```

34-35 INFILE = FILE NUMBER OF DATA ON OCEAN TAPE
44-45 INUNIT = NUMBER OF UNIT ON WHICH INPUT TAPE IS MOUNTED
55 NSEARH = (NOT RELEVANT. SET TO ZERO.)
61-70 SAMFRQ = SAMPLING FREQUENCY OF DIGITIZING (SAMPLES/SECOND)
(MUST INCLUDE A DECIMAL POINT)

SECOND DATA CARD
4-5 NBLOCK = NUMBER OF BLOCKS DESIRED
14-15 NPOW- MAXIMUM NUMBERS OF SAMPLES PER BLOCK WILL BE 2**NPOW,
      MAX NPOW IS 13 (8192 SAMPLES/BLOCK) BUT NPOW WILL BE
      REDUCED UNTIL (2**NPOW)*KCHAN WILL FIT IN MEMORY. FOR
      KCHAN OF 10 THIS WILL GIVE NPOW = 10 (1024 SAMPLES/BLOCK).
24-25 MTAPE =+1 FOR NO OUTPUT TAPE TO BE WRITTEN
      =-1 FOR NO OUTPUT TAPE
34-35 NFILE = OUTPUT COEFFICIENTS WILL BE NFILE-TH FILE ON TAPE
43-45 MAXERR = (NOT RELEVANT. SET TO ZERO.)
54-55 MPRINT = -1 SUPPRESSES SUMMARY COEFFICIENTS PRINT OUT
      = 0 OR GREATER PERMITS PRINT OUT

THIRD DATA CARD
4-5 KCHAN = NUMBER OF CHANNELS TO BE TRANSFORMED (MAX 10)
15 LOFR = 2 IF COEFFICIENTS TO BE COMPUTED FROM DATA SMOOTHED
      AND SUBSAMPLED (DECIMATED) USING CONVOL SUBROUTINE.
      WEIGHTS USED IN SMOOTHING AND DECIMATING FACTOR ARE
      DETERMINED BY CHOICE OF CONVOL USED.
      = 1 IF ALTERNATE BLOCKS TO BE MADE UP OF SAMPLES FROM DATA
      SMOOTHED AND DECIMATED USING CONVOL SUBROUTINE.
      COEFFICIENTS WILL APPEAR ON OUTPUT TAPE IN FILE
      IMMEDIATELY FOLLOWING THAT CONTAINING RESULTS FROM
      UNSMOOTHED DATA
      = 0 IF DATA TO BE LEFT ALONE
25 IHANN = 1 IF FOURIER COEFFICIENTS TO BE HANNED AND
      = 0 IF NOT
      = 0 IF NORMALIZED (*SQRT(8/3))

```

```

NEXT KCHAN CARDS
1-5 NO. OF PRIMARY A TO D CHANNEL
6-10 NO. OF SECONDARY A TO D CHANNEL
11-20 CALIBRATION ASSOCIATED WITH THE PRIMARY A TO D CHANNEL
21-30 CALIBRATION ASSOCIATED WITH THE SECONDARY A TO D CHANNEL
31-66 ALPHAMERIC NAME OF RESULTING PRIMARY CHANNEL
71-78 8 CHARACTER NAME OF UNITS FOR RESULTING PRIMARY CHANNEL

```

THE DATA TRANSFORMED AS THE PRIMARY CHANNEL IS THEN
 CALIBRATION1 X VALUE OF PRIMARY + CALIBRATION2 X VALUE OF
 SECONDARY CHANNEL

A SECCND SET OF DATA CARDS WILL PRODUCE A SECCND ANALYSIS. A BLANK

C CARD TERMINATES THE RUN.

FORMAT OF OUTPUT TAPE FOR EACH BLOCK TRANSFORMED IS AS FOLLOWS
FIRST LOGICAL RECORD IS AN ARRAY OF 256 WORDS CALLED

ARTAPE
ARTAPE(1) = IDUSER
ARTAPE(2) = BLOCK NUMBER
ARTAPE(3) = NUMBER OF SAMPLES / BLOCK
ARTAPE(4) = NTAP (SEE BELOW)
ARTAPE(5) = NUMBER OF CHANNELS TRANSFORMED
ARTAPE(6) = SAMPLING FREQUENCY
ARTAPE(10) = IHANN
ARTAPE(10+K) = MCHAN(K)
ARTAPE(31+9(K-1)) = ACHNAM(K) (9A4)
ARTAPE(121+2(K-1)) = AUNITS(1,K) (2A4)
ARTAPE(140+K) = CAL(K)

NEXT NTAP LOGICAL RECORDS OF 256 WORDS EACH CALLED

TAPRAY AND CONSIST OF
1 WORD CONTAINING INTEGER HARMONIC NO (0 TO IBLOCK/2) FOLLOWED BY
2*KCHAN WORDS CONTAINING FOR EACH OF THE KCHAN CHANNELS THE
REAL PART OF THE FOURIER COEFF AT THIS HARMONIC (FIRST WORD)
FOLLOWED BY THE IMAGINARY PART (SECOND WORD).
ONLY COMPLETE SEQUENCES OF 1+(2*KCHAN) WORDS ARE INCLUDED IN A
TAPRAY SO THAT THE LAST FEW WORDS MAY CONTAIN ZEROS

AN END OF FILE IS WRITTEN ON THE OUTPUT TAPE AT THE END OF A SEQUENCE
OF BLOCKS

J.F. GARRETT
J.R. WILSON

INSTITUTE OF OCEANOGRAPHY
UNIVERSITY OF BRITISH COLUMBIA
VANCOUVER 8, CANADA

00010
00020
00030
00040
00050
00060
00070
00080
00090
00100
00110
00120
00130
00140
00150
00160
00170
00180
00190
00200
00210
00220
00230
00240
00250
00260
00270
00280
00290
00300
00310
00320
00330
00340
00350
00360
00370
00380
00390
00400
00410
00420
00430
00440
00450
00460
00470
00480

SPECTRUM AND CROSS SPECTRUM STATISTICS FROM FOURIER
COEFFICIENT TAPE PRODUCED BY 'FTOR' PROGRAM ON IBM
SYSTEM 360 MODEL 67

LAST REVISION JANUARY 27,1969 JOHN GARRETT

THIS PROGRAM READS FOURIER COEFFICIENTS FROM TAPE PRODUCED BY FTOR
PROGRAM, AND FROM THE APPROPRIATE SUMS OF THESE PRODUCE SPECTRA AND
COSPECTRA. THE SUMS USED MAY BE FIXED WITH FREQUENCY OR MAY GO IN HALF
OCTAVES FROM A SPECIFIED LOW FREQUENCY. AN AVERAGE, STANDARD DEVIATION
AND LINEAR COEFFICIENT OF REGRESSION OVER THE IBMAX BLOCKS USED (SEE
FTOR DESCRIPTION) ARE GIVEN FOR EACH VALUE OF SPECTRAL DENSITY.
AT EACH FREQUENCY, THE COSPECTRUM BETWEEN (1) AND (2) IS GIVEN BY
$$(R(1)*R(2) + I(1)*I(2))/2.0$$

A VARIETY OF PLOTTED INTERVALS IS AVAILABLE. IN ALL A HORIZONTAL BAR
INDICATES THE FREQUENCY INCLUDED IN THE ESTIMATE PLOTTED, AND
A VERTICAL BAR INDICATES THE EXPECTED STANDARD DEVIATION OF THE
SERIES (N) AT THAT FREQUENCY
AND THE QUADRATURE SPECTRUM BY
$$(R(2)*I(1) - R(1)*I(2))/2.0$$

WHERE $(R(N) + (I(N)*SQRT(-1)))$ IS THE COMPLEX FOURIER COEFFICIENT
ESTIMATE (= STD.DEV. OF BLOCKS AVERAGED TO GIVE ESTIMATE/ SQRT(NUMBER
OF BLOCKS))

THE FOLLOWING SUBROUTINES MUST BE SUPPLIED BY USER
PHASES
PLVAL,TIC,LABEL

THE FOLLOWING LOGICAL INPUT/OUTPUT UNITS ARE USED BY THIS PROGRAM
3= (TAPE) SUPPLYING COEFFICIENTS AND IDENTIFICATION AS
PRODUCED BY FTOR
5= (CARDS) CONTROL PARAMETERS
6= PRINTED OUTPUT

THE FOLLOWING INPUT IS REQUIRED

A CARD IS REQUIRED TO IDENTIFY YOUR GRAPHICAL OUTPUT FOR THE COMPUTING
CENTRE STAFF. IT MUST BE PRESENT WHETHER PLOTS ARE PRODUCED OR NOT.
THE FIRST 72 COLUMNS OF THIS CARD WILL BE REPRODUCED ON THE BEGINNING
OF YOUR PLOT. THIS CARD APPEARS ONLY ONCE IN THE JOB AND IS THE FIRST
DATA CARD. THE FOLLOWING SET OF CARDS IS PRESENT FOR EACH FILE OF
FOURIER COEFFICIENTS TO BE PROCESSED.

FIRST CARD, IN COLUMN
1-9 IUSER = USER IDENTIFICATION NUMBER FOR DATA DESIRED
14-15 ICMAX = NUMBER OF CHANNELS TO BE USED (MAX 10)

CC


```

24-25 IBMAX = NUMBER OF DATA BLOCKS FOR STATISTICS 00490
34-35 IBSTAR = STATISTICS START WITH BLOCK NC. IBSTAR 00500
44-45 NFILE = DATA IS IN NFILE-TH WITH FILE ON FOURIER COEFFICIENT TAPE 00510
54 IAXIS = 0 (BLANK) IF PLOT AXES TO BE SET BY PROGRAM 00520
      = 1 IF AXES TO BE SET BY USER 00530
55 IPLOT = 0 IF NO PLOTTED OUTPUT DESIRED 00540
      = 1 IF SPECTRAL DENSITY TO BE PLOTTED AGAINST FREQUENCY 00550
      = 2 IF LOG10 SPECTRAL DENSITY TO BE PLOTTED AGAINST FREQUENCY 00560
      = 3 IF LOG10 SPECTRAL DENSITY TO BE PLOTTED AGAINST LOG10 00570
        FREQUENCY 00580
      = 4 IF (FREQ*SPECTRAL DENSITY) TO BE PLOTTED 00590
        AGAINST LOG10 FREQUENCY 00600
      = 5 SAME AS IPLOT=1 EXCEPT COHERENCE AND PHASE PLOTTED 00610
        INSTEAD OF CO AND QUAD SPECTRA 00620
      = 6 SAME AS = 2 EXCEPT COHERENCE AND PHASE PLOTTED INSTEAD 00630
        OF CO AND QUAD 00640
      = 7 SAME AS 3 EXCEPT COHERENCE AND PHASE INSTEAD OF CO+QU 00650
        = 8 SAME AS 4 WITH COHERENCE AND PHASE INSTEAD OF CO + QU 00660
65 IPHASE = 0 FOR NO PHASE CORRECTIONS 00670
      = 1 FOR PHASES TO BE CORRECTED. 00680
      00690
      00700
      00710
      00720
      00730
      00740
      00750
      00760
      00770
      00780
      00790
      00800
      00810
      00820
      00830
      00840
      00850
      00860
      00870
      00880
      00890
      00900
      00910
      00920
      00930
      00940
      00950
      00960

CARD INSERTED ONLY IF IAXIS = 1
IN COLUMN
1-10 VALUE OF ORIGIN FOR SPECTRUM AND COSPECTRUM AXIS (F10:)
11-20 UNITS PER INCH FOR SPECTRUM AND COSPECTRUM AXIS (F10:)
      AXIS WILL BE 5.00 INCHES LONG
21-30 VALUE OF ORIGIN FOR QUAD SPECTRUM AXIS (F10.)
31-40 UNITS PER INCH FOR QUAD SPECTRUM AXIS (F10.)
      AXIS WILL BE 5.00 INCHES LONG. (COHERENCE AND PHASE WILL BE
      SCALED BY PROGRAM IF PLOTTED INSTEAD OF CO AND QUAD.)
41-50 VALUES OF ORIGIN FOR FREQUENCY AXIS (F10.)
51-60 UNITS PER INCH FOR FREQUENCY AXIS (F10.)
61-70 LENGTH OF FREQUENCY AXIS IN INCHES (F10.)
N.B. WHEN LOG10 PLOTS HAVE BEEN REQUESTED NUMBERS ABOVE MUST ALL
REFER TO LOG10, E.G. UNITS PER INCH = 1.00 MEANS 1 DECADE PER INCH

NEXT CARD, IN COLUMN
5 LINCOT = 0 FOR CONSTANT BANDWIDTH, GIVEN BY BANDW BELOW
      = 1 FOR EXPONENTIAL BANDWIDTHS (GIVES LOG10 FREQ.
      SCALE IN ALL PLOTS)
6-15 STRFRQ = APPROXIMATE CENTER FREQUENCY OF FIRST POINT OF
      SPECTRUM, IN HERTZ. (MUST INCLUDE A DECIMAL POINT)
      FIRST BAND WILL INCLUDE ZERO HARMONIC IF STRFRQ
      IS LESS THAN BANDW
16-25 BANDW = APPROX. BANDWIDTH FOR FIXED BANDWIDTH SPECTRA,
      IN HERTZ. (MUST INCLUDE A DECIMAL POINT)
30 INDOW = 1 IF FOURIER COEFFICIENTS TO BE HANNED BEFORE
      SPECTRA COMPUTED

```


00970
00980
00990
01000
01010
01020
01030
01040
01050
01060
01070
01080
01090
01100
01110
01120
01130
01140
01150
01160
01170
01180
01190
01200
01210
01220
01230
01240
01250
01260
01270
01280
01290
01300
01310
01320

SUBSEQUENT ICMAX CARDS = 0 IF NOT
4-5 CHANNEL NUMBER OF A CHANNEL FOR WHICH SPECTRA ARE WANTED
14-15, 19-20, 24-25, 29-30, 34-35, 39-40, 44-45, 49-50, 54-55, 59-60, 64-65, 69-70, 74-75, 79-80, 84-85, 89-90, 94-95, 99-100, 104-105, 109-110, 114-115, 119-120, 124-125, 129-130, 134-135, 139-140, 144-145, 149-150, 154-155, 159-160, 164-165, 169-170, 174-175, 179-180, 184-185, 189-190, 194-195, 199-200, 204-205, 209-210, 214-215, 219-220, 224-225, 229-230, 234-235, 239-240, 244-245, 249-250, 254-255, 259-260, 264-265, 269-270, 274-275, 279-280, 284-285, 289-290, 294-295, 299-300, 304-305, 309-310, 314-315, 319-320, 324-325, 329-330, 334-335, 339-340, 344-345, 349-350, 354-355, 359-360, 364-365, 369-370, 374-375, 379-380, 384-385, 389-390, 394-395, 399-400, 404-405, 409-410, 414-415, 419-420, 424-425, 429-430, 434-435, 439-440, 444-445, 449-450, 454-455, 459-460, 464-465, 469-470, 474-475, 479-480, 484-485, 489-490, 494-495, 499-500, 504-505, 509-510, 514-515, 519-520, 524-525, 529-530, 534-535, 539-540, 544-545, 549-550, 554-555, 559-560, 564-565, 569-570, 574-575, 579-580, 584-585, 589-590, 594-595, 599-600, 604-605, 609-610, 614-615, 619-620, 624-625, 629-630, 634-635, 639-640, 644-645, 649-650, 654-655, 659-660, 664-665, 669-670, 674-675, 679-680, 684-685, 689-690, 694-695, 699-700, 704-705, 709-710, 714-715, 719-720, 724-725, 729-730, 734-735, 739-740, 744-745, 749-750, 754-755, 759-760, 764-765, 769-770, 774-775, 779-780, 784-785, 789-790, 794-795, 799-800, 804-805, 809-810, 814-815, 819-820, 824-825, 829-830, 834-835, 839-840, 844-845, 849-850, 854-855, 859-860, 864-865, 869-870, 874-875, 879-880, 884-885, 889-890, 894-895, 899-900, 904-905, 909-910, 914-915, 919-920, 924-925, 929-930, 934-935, 939-940, 944-945, 949-950, 954-955, 959-960, 964-965, 969-970, 974-975, 979-980, 984-985, 989-990, 994-995, 999-1000, 1004-1005, 1009-1010, 1014-1015, 1019-1020, 1024-1025, 1029-1030, 1034-1035, 1039-1040, 1044-1045, 1049-1050, 1054-1055, 1059-1060, 1064-1065, 1069-1070, 1074-1075, 1079-1080, 1084-1085, 1089-1090, 1094-1095, 1099-1100, 1104-1105, 1109-1110, 1114-1115, 1119-1120, 1124-1125, 1129-1130, 1134-1135, 1139-1140, 1144-1145, 1149-1150, 1154-1155, 1159-1160, 1164-1165, 1169-1170, 1174-1175, 1179-1180, 1184-1185, 1189-1190, 1194-1195, 1199-1200, 1204-1205, 1209-1210, 1214-1215, 1219-1220, 1224-1225, 1229-1230, 1234-1235, 1239-1240, 1244-1245, 1249-1250, 1254-1255, 1259-1260, 1264-1265, 1269-1270, 1274-1275, 1279-1280, 1284-1285, 1289-1290, 1294-1295, 1299-1300, 1304-1305, 1309-1310, 1314-1315, 1319-1320, 1324-1325, 1329-1330, 1334-1335, 1339-1340, 1344-1345, 1349-1350, 1354-1355, 1359-1360, 1364-1365, 1369-1370, 1374-1375, 1379-1380, 1384-1385, 1389-1390, 1394-1395, 1399-1400, 1404-1405, 1409-1410, 1414-1415, 1419-1420, 1424-1425, 1429-1430, 1434-1435, 1439-1440, 1444-1445, 1449-1450, 1454-1455, 1459-1460, 1464-1465, 1469-1470, 1474-1475, 1479-1480, 1484-1485, 1489-1490, 1494-1495, 1499-1500, 1504-1505, 1509-1510, 1514-1515, 1519-1520, 1524-1525, 1529-1530, 1534-1535, 1539-1540, 1544-1545, 1549-1550, 1554-1555, 1559-1560, 1564-1565, 1569-1570, 1574-1575, 1579-1580, 1584-1585, 1589-1590, 1594-1595, 1599-1600, 1604-1605, 1609-1610, 1614-1615, 1619-1620, 1624-1625, 1629-1630, 1634-1635, 1639-1640, 1644-1645, 1649-1650, 1654-1655, 1659-1660, 1664-1665, 1669-1670, 1674-1675, 1679-1680, 1684-1685, 1689-1690, 1694-1695, 1699-1700, 1704-1705, 1709-1710, 1714-1715, 1719-1720, 1724-1725, 1729-1730, 1734-1735, 1739-1740, 1744-1745, 1749-1750, 1754-1755, 1759-1760, 1764-1765, 1769-1770, 1774-1775, 1779-1780, 1784-1785, 1789-1790, 1794-1795, 1799-1800, 1804-1805, 1809-1810, 1814-1815, 1819-1820, 1824-1825, 1829-1830, 1834-1835, 1839-1840, 1844-1845, 1849-1850, 1854-1855, 1859-1860, 1864-1865, 1869-1870, 1874-1875, 1879-1880, 1884-1885, 1889-1890, 1894-1895, 1899-1900, 1904-1905, 1909-1910, 1914-1915, 1919-1920, 1924-1925, 1929-1930, 1934-1935, 1939-1940, 1944-1945, 1949-1950, 1954-1955, 1959-1960, 1964-1965, 1969-1970, 1974-1975, 1979-1980, 1984-1985, 1989-1990, 1994-1995, 1999-2000, 2004-2005, 2009-2010, 2014-2015, 2019-2020, 2024-2025, 2029-2030, 2034-2035, 2039-2040, 2044-2045, 2049-2050, 2054-2055, 2059-2060, 2064-2065, 2069-2070, 2074-2075, 2079-2080, 2084-2085, 2089-2090, 2094-2095, 2099-2100, 2104-2105, 2109-2110, 2114-2115, 2119-2120, 2124-2125, 2129-2130, 2134-2135, 2139-2140, 2144-2145, 2149-2150, 2154-2155, 2159-2160, 2164-2165, 2169-2170, 2174-2175, 2179-2180, 2184-2185, 2189-2190, 2194-2195, 2199-2200, 2204-2205, 2209-2210, 2214-2215, 2219-2220, 2224-2225, 2229-2230, 2234-2235, 2239-2240, 2244-2245, 2249-2250, 2254-2255, 2259-2260, 2264-2265, 2269-2270, 2274-2275, 2279-2280, 2284-2285, 2289-2290, 2294-2295, 2299-2300, 2304-2305, 2309-2310, 2314-2315, 2319-2320, 2324-2325, 2329-2330, 2334-2335, 2339-2340, 2344-2345, 2349-2350, 2354-2355, 2359-2360, 2364-2365, 2369-2370, 2374-2375, 2379-2380, 2384-2385, 2389-2390, 2394-2395, 2399-2400, 2404-2405, 2409-2410, 2414-2415, 2419-2420, 2424-2425, 2429-2430, 2434-2435, 2439-2440, 2444-2445, 2449-2450, 2454-2455, 2459-2460, 2464-2465, 2469-2470, 2474-2475, 2479-2480, 2484-2485, 2489-2490, 2494-2495, 2499-2500, 2504-2505, 2509-2510, 2514-2515, 2519-2520, 2524-2525, 2529-2530, 2534-2535, 2539-2540, 2544-2545, 2549-2550, 2554-2555, 2559-2560, 2564-2565, 2569-2570, 2574-2575, 2579-2580, 2584-2585, 2589-2590, 2594-2595, 2599-2600, 2604-2605, 2609-2610, 2614-2615, 2619-2620, 2624-2625, 2629-2630, 2634-2635, 2639-2640, 2644-2645, 2649-2650, 2654-2655, 2659-2660, 2664-2665, 2669-2670, 2674-2675, 2679-2680, 2684-2685, 2689-2690, 2694-2695, 2699-2700, 2704-2705, 2709-2710, 2714-2715, 2719-2720, 2724-2725, 2729-2730, 2734-2735, 2739-2740, 2744-2745, 2749-2750, 2754-2755, 2759-2760, 2764-2765, 2769-2770, 2774-2775, 2779-2780, 2784-2785, 2789-2790, 2794-2795, 2799-2800, 2804-2805, 2809-2810, 2814-2815, 2819-2820, 2824-2825, 2829-2830, 2834-2835, 2839-2840, 2844-2845, 2849-2850, 2854-2855, 2859-2860, 2864-2865, 2869-2870, 2874-2875, 2879-2880, 2884-2885, 2889-2890, 2894-2895, 2899-2900, 2904-2905, 2909-2910, 2914-2915, 2919-2920, 2924-2925, 2929-2930, 2934-2935, 2939-2940, 2944-2945, 2949-2950, 2954-2955, 2959-2960, 2964-2965, 2969-2970, 2974-2975, 2979-2980, 2984-2985, 2989-2990, 2994-2995, 2999-3000, 3004-3005, 3009-3010, 3014-3015, 3019-3020, 3024-3025, 3029-3030, 3034-3035, 3039-3040, 3044-3045, 3049-3050, 3054-3055, 3059-3060, 3064-3065, 3069-3070, 3074-3075, 3079-3080, 3084-3085, 3089-3090, 3094-3095, 3099-3100, 3104-3105, 3109-3110, 3114-3115, 3119-3120, 3124-3125, 3129-3130, 3134-3135, 3139-3140, 3144-3145, 3149-3150, 3154-3155, 3159-3160, 3164-3165, 3169-3170, 3174-3175, 3179-3180, 3184-3185, 3189-3190, 3194-3195, 3199-3200, 3204-3205, 3209-3210, 3214-3215, 3219-3220, 3224-3225, 3229-3230, 3234-3235, 3239-3240, 3244-3245, 3249-3250, 3254-3255, 3259-3260, 3264-3265, 3269-3270, 3274-3275, 3279-3280, 3284-3285, 3289-3290, 3294-3295, 3299-3300, 3304-3305, 3309-3310, 3314-3315, 3319-3320, 3324-3325, 3329-3330, 3334-3335, 3339-3340, 3344-3345, 3349-3350, 3354-3355, 3359-3360, 3364-3365, 3369-3370, 3374-3375, 3379-3380, 3384-3385, 3389-3390, 3394-3395, 3399-3400, 3404-3405, 3409-3410, 3414-3415, 3419-3420, 3424-3425, 3429-3430, 3434-3435, 3439-3440, 3444-3445, 3449-3450, 3454-3455, 3459-3460, 3464-3465, 3469-3470, 3474-3475, 3479-3480, 3484-3485, 3489-3490, 3494-3495, 3499-3500, 3504-3505, 3509-3510, 3514-3515, 3519-3520, 3524-3525, 3529-3530, 3534-3535, 3539-3540, 3544-3545, 3549-3550, 3554-3555, 3559-3560, 3564-3565, 3569-3570, 3574-3575, 3579-3580, 3584-3585, 3589-3590, 3594-3595, 3599-3600, 3604-3605, 3609-3610, 3614-3615, 3619-3620, 3624-3625, 3629-3630, 3634-3635, 3639-3640, 3644-3645, 3649-3650, 3654-3655, 3659-3660, 3664-3665, 3669-3670, 3674-3675, 3679-3680, 3684-3685, 3689-3690, 3694-3695, 3699-3700, 3704-3705, 3709-3710, 3714-3715, 3719-3720, 3724-3725, 3729-3730, 3734-3735, 3739-3740, 3744-3745, 3749-3750, 3754-3755, 3759-3760, 3764-3765, 3769-3770, 3774-3775, 3779-3780, 3784-3785, 3789-3790, 3794-3795, 3799-3800, 3804-3805, 3809-3810, 3814-3815, 3819-3820, 3824-3825, 3829-3830, 3834-3835, 3839-3840, 3844-3845, 3849-3850, 3854-3855, 3859-3860, 3864-3865, 3869-3870, 3874-3875, 3879-3880, 3884-3885, 3889-3890, 3894-3895, 3899-3900, 3904-3905, 3909-3910, 3914-3915, 3919-3920, 3924-3925, 3929-3930, 3934-3935, 3939-3940, 3944-3945, 3949-3950, 3954-3955, 3959-3960, 3964-3965, 3969-3970, 3974-3975, 3979-3980, 3984-3985, 3989-3990, 3994-3995, 3999-4000, 4004-4005, 4009-4010, 4014-4015, 4019-4020, 4024-4025, 4029-4030, 4034-4035, 4039-4040, 4044-4045, 4049-4050, 4054-4055, 4059-4060, 4064-4065, 4069-4070, 4074-4075, 4079-4080, 4084-4085, 4089-4090, 4094-4095, 4099-4100, 4104-4105, 4109-4110, 4114-4115, 4119-4120, 4124-4125, 4129-4130, 4134-4135, 4139-4140, 4144-4145, 4149-4150, 4154-4155, 4159-4160, 4164-4165, 4169-4170, 4174-4175, 4179-4180, 4184-4185, 4189-4190, 4194-4195, 4199-4200, 4204-4205, 4209-4210, 4214-4215, 4219-4220, 4224-4225, 4229-4230, 4234-4235, 4239-4240, 4244-4245, 4249-4250, 4254-4255, 4259-4260, 4264-4265, 4269-4270, 4274-4275, 4279-4280, 4284-4285, 4289-4290, 4294-4295, 4299-4300, 4304-4305, 4309-4310, 4314-4315, 4319-4320, 4324-4325, 4329-4330, 4334-4335, 4339-4340, 4344-4345, 4349-4350, 4354-4355, 4359-4360, 4364-4365, 4369-4370, 4374-4375, 4379-4380, 4384-4385, 4389-4390, 4394-4395, 4399-4400, 4404-4405, 4409-4410, 4414-4415, 4419-4420, 4424-4425, 4429-4430, 4434-4435, 4439-4440, 4444-4445, 4449-4450, 4454-4455, 4459-4460, 4464-4465, 4469-4470, 4474-4475, 4479-4480, 4484-4485, 4489-4490, 4494-4495, 4499-4500, 4504-4505, 4509-4510, 4514-4515, 4519-4520, 4524-4525, 4529-4530, 4534-4535, 4539-4540, 4544-4545, 4549-4550, 4554-4555, 4559-4560, 4564-4565, 4569-4570, 4574-4575, 4579-4580, 4584-4585, 4589-4590, 4594-4595, 4599-4600, 4604-4605, 4609-4610, 4614-4615, 4619-4620, 4624-4625, 4629-4630, 4634-4635, 4639-4640, 4644-4645, 4649-4650, 4654-4655, 4659-4660, 4664-4665, 4669-4670, 4674-4675, 4679-4680, 4684-4685, 4689-4690, 4694-4695, 4699-4700, 4704-4705, 4709-4710, 4714-4715, 4719-4720, 4724-4725, 4729-4730, 4734-4735, 4739-4740, 4744-4745, 4749-4750, 4754-4755, 4759-4760, 4764-4765, 4769-4770, 4774-4775, 4779-4780, 4784-4785, 4789-4790, 4794-4795, 4799-4800, 4804-4805, 4809-4810, 4814-4815, 4819-4820, 4824-4825, 4829-4830, 4834-4835, 4839-4840, 4844-4845, 4849-4850, 4854-4855, 4859-4860, 4864-4865, 4869-4870, 4874-4875, 4879-4880, 4884-4885, 4889-4890, 4894-4895, 4899-4900, 4904-4905, 4909-4910, 4914-4915, 4919-4920, 4924-4925, 4929-4930, 4934-4935, 4939-4940, 4944-4945, 4949-4950, 4954-4955, 4959-4960, 4964-4965, 4969-4970, 4974-4975, 4979-4980, 4984-4985, 4989-4990, 4994-4995, 4999-5000, 5004-5005, 5009-5010, 5014-5015, 5019-5020, 5024-5025, 5029-5030, 5034-5035, 5039-5040, 5044-5045, 5049-5050, 5054-5055, 5059-5060, 5064-5065, 5069-5070, 5074-5075, 5079-5080, 5084-5085, 5089-5090, 5094-5095, 5099-5100, 5104-5105, 5109-5110, 5114-5115, 5119-5120, 5124-5125, 5129-5130, 5134-5135, 5139-5140, 5144-5145, 5149-5150, 5154-5155, 5159-5160, 5164-5165, 5169-5170, 5174-5175, 5179-5180, 5184-5185, 5189-5190, 5194-5195, 5199-5200, 5204-5205, 5209-5210, 5214-5215, 5219-5220, 5224-5225, 5229-5230, 5234-5235, 5239-5240, 5244-5245, 5249-5250, 5254-5255, 5259-5260, 5264-5265, 5269-5270, 5274-5275, 5279-5280, 5284-5285, 5289-5290, 5294-5295, 5299-5300, 5304-5305, 5309-5310, 5314-5315, 5319-5320, 5324-5325, 5329-5330, 5334-5335, 5339-5340, 5344-5345, 5349-5350, 5354-5355, 5359-5360, 5364-5365, 5369-5370, 5374-5375, 5379-5380, 5384-5385, 5389-5390, 5394-5395, 5399-5400, 5404-5405, 5409-5410, 5414-5415, 5419-5420, 5424-5425, 5429-5430, 5434-5435, 5439-5440, 5444-5445, 5449-5450, 5454-5455, 5459-5460, 5464-5465, 5469-5470, 5474-5475, 5479-5480, 5484-5485, 5489-5490, 5494-5495, 5499-5500, 5504-5505, 5509-5510, 5514-5515, 5519-5520, 5524-5525, 5529-5530, 5534-5535, 5539-5540, 5544-5545, 5549-5550, 5554-5555, 5559-5560, 5564-5565, 5569-5570, 5574-5575, 5579-5580, 5584-5585, 5589-5590, 5594-5595, 5599-5600, 5604-5605, 5609-5610, 5614-5615, 5619-5620, 5624-5625, 5629-5630, 5634-5635, 5639-5640, 5644-5645, 5649-5650, 5654-5655, 5659-5660, 5664-56

'./,TITLE(10),TITLED(12)

124

LIST OF REFERENCES

1. Busch, N. E., 1973: The surface boundary layer. Bndy-Layer Meteor., 4, 213-240.
2. Cavanaugh, M. P., 1974: Examination of shipboard measurements of the vertical profiles of mean temperature, humidity and wind speed. M.S. Thesis, U. S. Naval Postgraduate School, Monterey, California.
3. Davidson, K. L., 1970: An investigation of the influence of water waves on the adjacent airflow. Ph.D. Dissertation, University of Michigan, 259 pp.
4. Davidson, K. L., 1974: Observational results on the influence of stability and wind-wave coupling on momentum transfer and turbulent fluctuations over ocean waves. Bndy-Layer Meteor., (in press), 5, 123-145.
5. Davidson, K. L. and Frank, A. J., 1973: Wave-related fluctuations in the airflow above natural waves. J. Phys. Oceanogr., 3(1), 102-119.
6. Garratt, J. R., 1972: Studies of turbulence in the surface layer over water (Lough Neagh). Part II. Production and dissipation of velocity and temperature fluctuations. Quart. J., Roy. Meteor. Soc., 98, 642-657.
7. Haltiner, G. J. and Martin, F. L., 1957: Dynamical and Physical Meteorology, McGraw-Hill Book Company, (New York), 470 pp.
8. Kaimal, J. C., Wyngaard, J. C., Izumi, Y., and Cote, O. R., 1972: Spectral characteristics of surface-layer turbulence. Quart. J., Roy. Meteor. Soc., 98, 563-589.
9. Kraus, E. B., 1972: Atmosphere-Ocean Interaction, Clarendon Press, (Oxford), 275 pp.
10. Lumley, J. L., and Panofsky, H. A., 1964: The Structure of Atmospheric Turbulence, Interscience, (New York), 239 pp.

11. McKendrick, J. M., 1972: An investigation of digital spectral analysis programs and computer methods utilized at the Naval Postgraduate School in the analysis of high frequency random signals. M.S. Thesis, U. S. Naval Postgraduate School, Monterey, California, 147 pp.
12. Paulson, C. A., 1970: The mathematical representation of wind and temperature profiles in the unstable surface layer. J. Appl. Meteorol., 9, 857-861.
13. Pond, S., Smith, S. D., Hamblin, P. F. and Burling, R. W., 1966: Spectra of velocity and temperature fluctuations in the atmospheric boundary layer over the sea. J. Atmospheric Sci., 23(4), 376-386.
14. Stegen, G. R., Gibson, C. H., and Friehe, C. A., 1973: Measurements of momentum and sensible heat fluxes over the open ocean. J. Phys. Oceanog., 3(1), 86-92.
15. Taylor, G. I., 1938: The spectrum of turbulence. Proc. Roy. Soc., A164, 476.
16. Welsh, P. T., 1974: An investigation of ship related motions on turbulent measurements. M.S. Thesis, U. S. Naval Postgraduate School, Monterey, California.

INITIAL DISTRIBUTION LIST

	No. Copies
1. Defense Documentation Center Cameron Station Alexandria, Virginia 22314	2
2. Library (Code 0212) Naval Postgraduate School Monterey, California 93940	2
3. Naval Oceanographic Office Library (Code 3330) Washington, D. C. 20373	1
4. Commander, Naval Weather Service Command Naval Weather Service Headquarters Washington Navy Yard Washington, D. C. 20390	1
5. Professor Kenneth L. Davidson, Code 51Ds Department of Meteorology Naval Postgraduate School Monterey, California 93940	20
6. Professor Thomas M. Houlihan, Code 59Hm Department of Mechanical Engineering Naval Postgraduate School Monterey, California 93940	3
7. Mr. P. Vial, Code 048 Naval Ordnance Laboratory White Oak Silver Spring, Maryland 20910	1
8. Mr. E. Boudreaux, Code 048 Naval Ordnance Laboratory White Oak Silver Spring, Maryland 20910	1
9. Dr. P. Livingston Applied Optics Branch, Bldg. 30 Naval Research Laboratory Washington, D. C. 20390	1
10. LT William E. Johnston c/o Mr. Lou Hanna 33 East Bond Street Corry, Pennsylvania 16407	3

11. Mr. Steve Rinard 1
Department of Meteorology
Naval Postgraduate School
Monterey, California 93940
12. Mr. Robert Smith 1
Department of Research, Code 023
Naval Postgraduate School
Monterey, California 93940
13. Ms. Sharon Raney 1
Computer Center, Code 0211
Naval Postgraduate School
Monterey, California 93940
14. Mr. Robert Limes 1
Code 72Ec
Naval Postgraduate School
Monterey, California 93940
15. Professor Dale F. Leipper 1
Chairman, Department of Oceanography
Naval Postgraduate School
Monterey, California 93940
16. LT Michael P. Cavanaugh 1
c/o Mr. James A. Cavanaugh
3607 Husted Drive
Chevy Chase, Maryland 20015
17. LT Patrick T. Welsh 1
Student, Naval Destroyer School
Naval Station
Newport, Rhode Island 08240
18. R/V ACANIA 1
Department of Oceanography
Naval Postgraduate School
Monterey, California 93940

REPORT DOCUMENTATION PAGE		READ INSTRUCTIONS BEFORE COMPLETING FORM
1. REPORT NUMBER	2. GOVT ACCESSION NO.	3. RECIPIENT'S CATALOG NUMBER
4. TITLE (and Subtitle) Estimating Boundary Layer Fluxes from Shipboard Measurements of Dissipations of Turbulent Kinetic Energy and Temperature Variance		5. TYPE OF REPORT & PERIOD COVERED M.S. Thesis March 1974
7. AUTHOR(s) William Edward Johnston		6. PERFORMING ORG. REPORT NUMBER
9. PERFORMING ORGANIZATION NAME AND ADDRESS Naval Postgraduate School Monterey, California 93940		8. CONTRACT OR GRANT NUMBER(s)
11. CONTROLLING OFFICE NAME AND ADDRESS Naval Postgraduate School Monterey, California 93940		10. PROGRAM ELEMENT, PROJECT, TASK AREA & WORK UNIT NUMBERS
14. MONITORING AGENCY NAME & ADDRESS (if different from Controlling Office) Naval Postgraduate School Monterey, California 93940		12. REPORT DATE March 1974
		13. NUMBER OF PAGES 132
		15. SECURITY CLASS. (of this report) Unclassified
16. DISTRIBUTION STATEMENT (of this Report) Approved for public release; distribution unlimited.		15a. DECLASSIFICATION/DOWNGRADING SCHEDULE
17. DISTRIBUTION STATEMENT (of the abstract entered in Block 20, if different from Report)		
18. SUPPLEMENTARY NOTES		
19. KEY WORDS (Continue on reverse side if necessary and identify by block number) Turbulence Marine Boundary Layer Dissipation of Turbulent Kinetic Energy Momentum Flux Friction Velocity		
20. ABSTRACT (Continue on reverse side if necessary and identify by block number) Velocity and temperature fluctuation measurements were made over the open ocean from instruments mounted on the R/V ACANIA. These data were examined to determine the validity of present formulations and prediction techniques. Values of momentum flux, u_*^2 , were inferred from the rate of dissipation of turbulent kinetic energy, ϵ . Dissipation values were obtained from spectral estimates and inner scale estimates. Values of u_* were examined for representativeness on the basis of the constant-flux assumption and by comparisons		

with other studies. The vertical variation of the dissipation rate was examined for possible effects of stability and wind-wave coupling.

The momentum flux, computed from spectra, supported the constant-flux assumption for neutral conditions. For periods of instability, the stability corrections applied to the vertical variation of ϵ resulted in the proper adjustments toward the predicted slope. The reductions in momentum transfer during periods of stable stratifications were consistent with wind-wave coupling effects described by Davidson. The shape of a spectrum of temperature fluctuations was in agreement with predictions.

23 SEP 74

21107

Thesis

J675

Johnston

c.1

Estimating boundary
layer fluxes from ship-
board measurements of
dissipations of turbu-
lent kinetic energy and
temperature variance.

148566

23 SEP 74

21107

Thesis

J675

Johnston

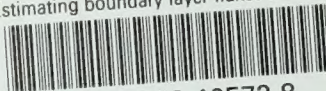
c.1

Estimating boundary
layer fluxes from ship-
board measurements of
dissipations of turbu-
lent kinetic energy and
temperature variance.

148566

thes.J675

Estimating boundary layer fluxes from sh



3 2768 002 10572 8

DUDLEY KNOX LIBRARY